Master of Science Thesis

Automatic exposure control in CT:

an investigation between different manufacturers considering radiation dose and image quality

Marcus Söderberg

Supervisor: Mikael Gunnarsson, PhD

This work has been performed at the
Department of Radiation Physics
Malmö University Hospital

Medical Radiation Physics
Clinical Sciences, Lund
Lund University, 2008

Abstract

Background: Data from 1998 showed that CT represents about 10% of all the diagnostic X-ray examinations and almost 70% of the total radiation dose from medical diagnostic examinations in Sweden. Because of this there is a strong need to minimize the radiation dose and adapt the dose to each patient's examination area and anatomy. Today practically all-modern CT systems are delivered with automatic exposure control (AEC) systems that perform tube current modulation in 3D.

Aim: The purpose of this work is to investigate the potential of dose reduction and the possibility to maintain adequate image quality using the AEC systems from four different manufacturers: Siemens Medical Solutions, Philips Medical Systems, General Electric (GE) Healthcare and Toshiba Medical Corporation.

Material and methods: A general scanning protocol was created for each examination where as many as possible of the scanning parameters were set equal. The dynamic of each AEC system has been investigated by scanning an anthropomorphic thorax phantom and an anthropomorphic head phantom on 16- and 64-slice CT scanners for each manufacturer with the AEC system activated and non-activated. The image quality in the thorax phantom has been evaluated by measuring the image noise (standard deviation) by insert regions of interests.

Results and discussion: The result for each AEC system is strongly dependent on the selected image quality parameters. Each system has different solutions of defining the image quality level; consequently it is not possible to make direct comparison between the manufacturers. The dynamic of the tube current modulation is rather similar between the manufactures AEC system and there is large potential for dose reductions (thorax ~50%). A common result is that the image noise increases, especially in regions where the tube current is greatly decreased by the AEC systems, e.g. in the lung region.

Conclusion: There are large possibilities to attain large dose reductions. The AEC systems cause a general increase in the image noise but the noise becomes more consistent between different anatomic regions.

Summary for the general public in Swedish

Individanpassa stråldosen vid CT – Gör det någon skillnad?

Med dagens dosregleringssystem kan strålningen anpassas efter varje patients anatomi och undersökningsområde i 3 dimensioner. Detta gör det möjligt att halvera stråldosen till patienten.

Inom radiologin har användningen av datortomografi eller CT som står för *Computed Tomography*, även kallad skiktröntgen, kraftigt ökat under de senaste åren. Med tekniken kan mycket tydliga tvärsnittsbilder av kroppens innandöme återges. Patienten ligger på en brits som långsamt rör sig fram genom datortomografens runda hål. Där sänds röntgenstrålning från ett roterande röntgenrör genom ett tunt skikt av patienten i taget. De motstående likaså roterande detektorerna registrerar strålarnas styrka och sänder vidare informationen till en dator. Beroende på vilken vävnad strålarna passerar på sin väg genom kroppen försvagas de olika mycket. Det är skillnaden i *attenuering* (försvagning) som är förutsättningen för att en bild skall kunna skapas. I datorn sker bearbetning av informationen och en tvärsnittsbild av det undersökta området rekonstrueras.

Datortomografi är förknippat med betydligt högre stråldoser än andra strålningsbaserade medicinska undersökningar, såsom konventionell röntgen och nukleärmedicinska studier. Stråldosen för en generell CT-undersökning av *thorax* (bröstkorg) motsvarar ungefär fem gånger den naturliga bakgrundsstrålning en människa utsätts för under ett år. Det är alltså av stor vikt att minimera stråldoserna. Idag har alla tillverkare utvecklat automatiska dosregleringssystem. Varje system fungerar på olika sätt men grundprincipen är att användaren specificerar en bildkvalitetsnivå. *Rörströmmen*, d.v.s. intensiteten på strålningen anpassas sedan efter varje patients form, storlek och attenuering så att den valda bildkvalitetsnivån uppnås med ökad strålningseffektivitet. Rörström är proportionellt mot stråldos, d.v.s. en halvering av rörströmmen medför en halvering av stråldosen till patienten.

Syftet med arbetet är att undersöka potentialen till dosreduktion samt erhållen bildkvalitet då ett automatiskt dosregleringssystem från fyra olika tillverkare används; Siemens, Philips, General Electric samt Toshiba. Mätningar har utförts på två människoliknande *fantom* (dockor) i form av en skalle och en bröstkorg.

Resultatet av studien visar att de fyra dosregleringssystemen anpassar rörströmmen likartat efter anatomin i respektive fantom. T.ex. för mindre täta objekt såsom de luftfyllda lungorna som inte attenuerar strålningen fullt så mycket som axelpartiet med mycket ben, finns det möjlighet att sänka rörströmmen och därmed stråldosen. Studien visar att det finns goda möjligheter till att erhålla kraftiga dosreduktioner, omkring 50 % för en CT thorax undersökning. Ett gemensamt resultat är att bruset i bilderna ökar men brusnivån blir mer jämn mellan olika anatomiska regioner.

Det är av stor vikt att radiologer och fysiker är väl medvetna om hur bildkvaliteten påverkas av ett dosregleringssystem. Framtida studier kan vara att undersöka hur den diagnostiska informationen påverkas av brusökningen.

Table of contents

1. INTRODUCTION **5**

1.1 AIM 6

2. BACKGROUND **6**

2.1 BASIC PRINCIPLES OF CT 6
2.2 DOSIMETRY 7
2.2.1 Computed Tomography Dose Index *7*
2.2.2 Dose Length Product *8*
2.2.3 Effective dose *8*
2.3 RADIATION RISKS 8
2.4 PARAMETERS THAT AFFECT IMAGE QUALITY AND PATIENT RADIATION DOSE 9
2.4.1 Scanner model and manufacturer *9*
2.4.2 Tube current and tube load *9*
2.4.3 Tube voltage *9*
2.4.4 X-ray filtration *9*
2.4.5 Reconstruction filter *9*
2.4.6 Slice thickness *10*
2.4.7 Pitch *10*
2.4.8 Reconstruction matrix *10*
2.4.9 Summary *10*
2.5 AUTOMATIC EXPOSURE CONTROL 11
2.5.1 Angular modulation *12*
2.5.2 Longitudinal modulation *13*
2.5.3 Combined modulation *13*
2.5.4 Methods to select the required image quality level *14*
2.5.5 Benefits of an AEC system *15*
2.5.6 Limitations of an AEC system *15*
2.5.7 Summary *15*
2.6 THE MAJOR CT SCANNER MANUFACTURES AEC SYSTEMS 16
2.6.1 Siemens - CARE Dose 4D *16*
2.6.2 Philips - DoseRight *18*
2.6.3 General Electric - AutomA 3D *19*
2.6.4 Toshiba - SureExposure 3D *20*
2.6.5 Summary *20*

3. MATERIALS AND METHODS **21**

3.1 CT SCANNERS COVERED IN THIS REPORT 21
3.1.1 Siemens *21*
3.1.2 Philips *21*
3.1.3 GE *21*
3.1.4 Toshiba *21*
3.2 PHANTOMS USED IN THIS STUDY 22
3.2.1 Thorax phantom (Chest Phantom PBU-X-21, Kyoto Kagaku CO, Ltd, Kyoto, Japan) *22*
3.2.2 Head phantom (SK 150, The Phantom Laboratory, Salem, NY, USA) *22*
3.3 TESTING APPROACH 22
3.4 DETERMINATION OF DOSE REDUCTION 23
3.5 EVALUATION OF IMAGE QUALITY 24
3.5.1 Thorax phantom *24*
3.5.2 Head phantom *25*
3.5.3 Uncertainties *25*

4. RESULTS **26**

4.1 SIEMENS 26
4.1.1 Determination of dose reduction and dynamic of the AEC system for the thorax phantom *26*
4.1.2 Determination of dose reduction and dynamic of the AEC system for the head phantom *28*

4.1.3 Evaluation of image quality for the thorax phantom *29*
4.2 PHILIPS 30
4.2.1 Determination of dose reduction and dynamic of the AEC system for the thorax phantom *31*
4.2.2 Determination of dose reduction and dynamic of the AEC system for the head phantom *33*
4.2.3 Evaluation of image quality for the thorax phantom *34*
4.3 GE 35
4.3.1 Determination of dose reduction and dynamic of the AEC system for the thorax phantom *36*
4.3.2 Determination of dose reduction and dynamic of the AEC system for the head phantom *37*
4.3.3 Evaluation of image quality for the thorax phantom *39*
4.4 TOSHIBA 40
4.4.1 Determination of dose reduction and dynamic of the AEC system for the thorax phantom *40*
4.4.2 Determination of dose reduction and dynamic of the AEC system for the head phantom *42*
4.4.3 Evaluation of image quality for the thorax phantom *43*
4.5 UNCERTAINTIES IN ROI POSITION 45
4.6 SUMMARY OF THE RESULTS 45
4.6.1 Thorax phantom *46*
4.6.2 Head phantom *50*

5. DISCUSSION 51

5.1 SIEMENS 51
5.2 PHILIPS 52
5.3 GE 53
5.4 TOSHIBA 54
5.5 GENERAL DISCUSSION 55

6. CONCLUSIONS 58

7. ACKNOWLEDGEMENTS 59

8. REFERENCES 59

1. Introduction

There has been a continuously growing of computed tomography (CT) scanning since its introduction in the early 1970s. The use of CT imaging has increased tremendously in recent years resulted from improved technology, such as the introduction of modern multidetector-array CT scanners and parallel increases in clinical applications of CT scanning. Several studies have suggested that, although CT is not the most common radiological examination, it is responsible for the largest radiation dose. According to the United Nations Scientific Committee on the Effects of Atomic Radiation (UNSCEAR), CT constitutes only about 5% of all radiological examinations in the world, but contributes about 34% of the collective radiation dose to the population (period 1991-1996) (1). Data from 1998 showed that CT represents about 10% of all the diagnostic X-ray examinations and almost 70% of the total radiation dose from medical diagnostic examinations in Sweden (Fig. 1) (2). CT scanning is associated with significantly higher radiation exposure compared with other radiation-based medical examinations, including conventional radiography and nuclear medicine studies (3). Because of this, there is a strong need to minimize the radiation dose according to the ALARA (As Low As Reasonably Achievable) principle.

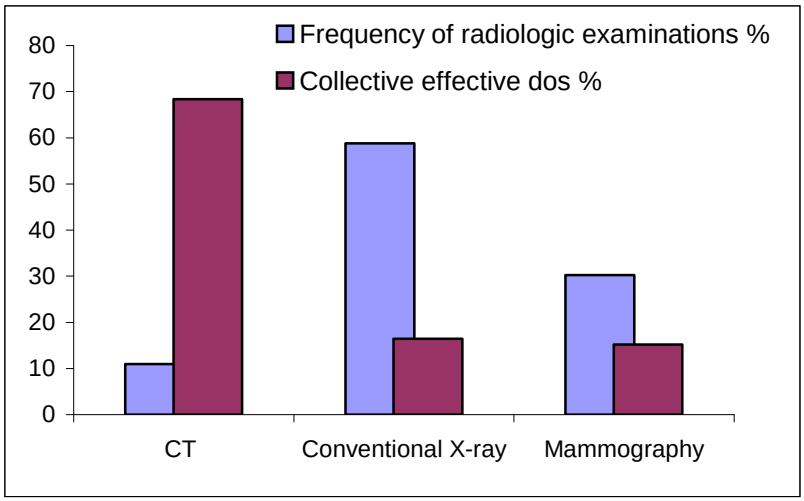

Figure 1. Although CT examinations only contribute with a relatively low percentage of the total number of X-ray examinations, CT contributes with a high proportion of the collective effective dose from medical diagnostic examinations. The figure refers to data from 1998 in Sweden (2).

Over the past years automatic exposure control (AEC) systems on CT scanners have been a subject of great interest (4-7). Today practically all-modern CT systems are delivered with AEC systems operating with tube current modulation in 3D. Each of these systems has different implementation and works to some extent on different basis. Their main principle however is to manage the required image quality and radiation dose in a repeatable and expected way by modulate the tube current to the patients shape, size and attenuation. If the AEC system is used properly and optimised it can reduce the dose of about 20-40% to the patient and still produce the image quality necessary for confident diagnosis (8). AEC systems have a number of benefits; consistency of image quality, better control of patient radiation dose, reduction of certain image artefacts and reduced load of the X-ray tube which will lead to extended scan runs (4). Few studies have however investigate AEC systems in 3D in terms of dose reduction versus image quality (4, 9-12). The challenge to the radiologists and the physicists is to establish adequate image quality with lowest amount of radiation exposure to the patient, in agreement with the ALARA principle.

1.1 Aim

The purpose of this work is to investigate the potential of dose reduction and the possibility to maintain adequate image quality using the automatic exposure control systems from four different manufacturers: Siemens Medical Solutions, Philips Medical Systems, General Electric (GE) Healthcare and Toshiba Medical Corporation.

2. Background

2.1 Basic principles of CT

CT is a diagnostic imaging method, which generate cross-section pictures of the internals of a body by using X-ray absorption measurements from multiple directions around the region of interest. CT scanning has since G.N. Hounsfield and J. Ambrose introduced the method in the early 1970s, been a technology that increasingly has been developed to give more detailed information about the examined area in a shorter examination time. One of the main benefits of CT imaging is the extremely good ability to visualize structures with low contrast, which makes it possible to detect very small changes in tissue types. CT images give accurate diagnostic information about the anatomic distribution in the body (13, 14).

A modern CT scanner consists of an X-ray tube that rotates around the patient, emitting X-ray beams that pass through a cross section of the body (Fig. 2). The arcs of detectors that are placed opposite to the X-ray tube collect the image raw data (attenuation profiles). Actually the average linear attenuation coefficient is measured which describes how the X-ray intensity is reduced by the materia. The measurements are today commonly performed in fan-beam geometry over an angular range of 360°. After sampling of the raw data, X-ray beam projections from multiple directions around the region of interest are generated and a CT reconstruction algorithm is then used to reconstruct the images. Today the convolution-backprojection procedure is the most common reconstruction method (13, 14).

The measured attenuation coefficient μ is presented as CT number (value) relative to the attenuation of water. CT numbers is given in Hounsfield Units (HU) and is for a random tissue with attenuation coefficient μ_{tissue}, defined as:

$$\text{CT number} = \frac{\mu_{tissue} - \mu_{water}}{\mu_{water}} \cdot 1000 \text{ HU} \qquad \text{(Eq. 1)}$$

The Hounsfield scale has no upper boundary but in medical use the scale reaches from -1024 HU to +3071 HU. Water corresponds to a CT number of 0 HU and air to a CT number of -1000 HU. As the CT numbers of water and air is independent of the energy of the photons they corresponds to fixed numbers. Tissues with lower attenuation than water are thus defined with negative CT numbers (e.g. lungs) while tissues with higher attenuation are defined with positive CT numbers (e.g. bone) (13).

The region from -1024 HU to +3071 HU, i.e. 4096 gray levels, can not be visualized on a monitor since human observers can only distinguish about 60 to 80 grey levels. Through using so-called windowing techniques, parts of measured values can be presented as a greyscale between black and white. Also the center of the window can be chosen randomly with this technology. The center is selected analogous approximately to mean CT number of the interesting structures and the window width establish the contrast in the image (13).

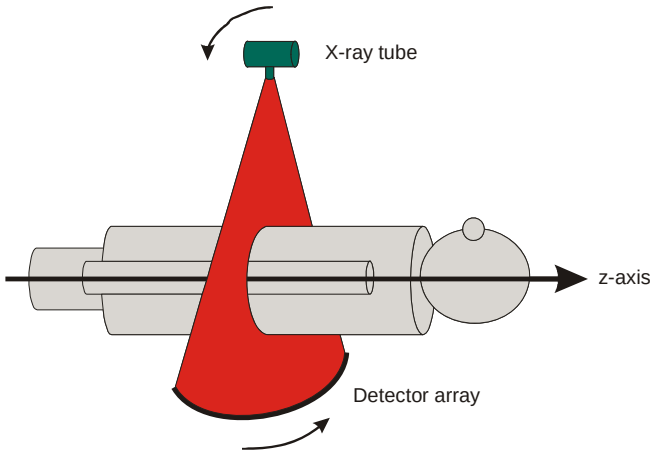

Figure 2. Schematic representation of a modern CT scanner; the X-ray tube and detector system rotate together around the patient.

2.2 Dosimetry

Absorbed radiation dose (D) is the expectation value of energy imparted by the X-ray beam at a given point in an exposed material and is measured in gray [Gy]. Absorbed dose is dependent on the energy absorption factors of the material and on the X-ray exposure. Exposure describes the ability of X-rays to ionize air (15). The absorbed dose is proportional to the exposure, which increases with increasing tube current [mA], tube voltage [kV] and scan time. As it is not possible to distinguish the specific dose received by individual patients, dose indices are used. Dose index values can be usable to compare CT systems and protocols, as well as help for the operator to select suitable scanning parameters (16).

2.2.1 Computed Tomography Dose Index

During a CT scan, the radiation energy deposition in tissue is not only limited to the scanned volume. Adjacent slices also are exposed to radiation because of scattered radiation, divergence of the beam and restricted efficiency of the collimator. The primary dose measurement concept in CT is the Computed Tomography Dose Index (CTDI), which is measured in Gy. CTDI is the integrated dose profile along the z-axis, delivered both within and beyond the scan volume, for a single slice, normalized to the nominal slice thickness (represents the average absorbed dose) (17). The mathematical definition of CTDI describes the summation of the dose contribution along a line parallel to the axis of rotation for the scanner (z-axis):

$$CTDI = \frac{1}{nt}\int_{-\infty}^{\infty} D(z)\cdot dz \qquad \text{(Eq. 2)}$$

Where n is the number of slices per rotation, t is the nominal slice thickness and $D(z)$ represents the radiation dose profile along the z-axis (18). CTDI can be acquired either in free air ($CTDI_{air}$) or in a polymethylmethacrylate (PMMA) phantom (called weighted CTDI or $CTDI_w$), using a 100 mm pencil ion chamber. $CTDI_w$ is the average dose in a slice of the PMMA phantom at different positions (19):

$$CTDI_w = \frac{1}{3}\cdot CTDI_{100,\,\text{center}} + \frac{2}{3}\cdot CTDI_{100,\,\text{periphery}} \qquad \text{(Eq. 3)}$$

To take into account axial scan spacing, another CTDI parameter is introduced, $CTDI_{vol}$ (20):

$$CTDI_{vol} = \frac{1}{\text{pitch}} \cdot CTDI_{w} \qquad \text{(Eq. 4)}$$

Pitch is defined as the table transportation per rotation to the total nominal beam width. The principal of CTDI is that it gives a measure of the scanner radiation output for a given examination and characterizes the local exposure of the patient. On modern CT scanners $CTDI_{vol}$ is displayed on the operator's console. However, to get the opportunity to fully estimate the radiological risk of an examination, further dose parameters have to be introduced (21).

2.2.2 Dose Length Product

The Dose Length Product (DLP) is the mean absorbed dose for the whole scanned volume and is measured in [Gy*cm]:

$$DLP = CTDI_{vol} \cdot \text{scan length} \qquad \text{(Eq. 5)}$$

DLP reflects the total number of photons absorbed in the patient and is correlated to the effective dose. In some modern CT systems the DLP is displayed to the operator. DLP takes no account of the radiation sensitivity of the irradiated tissues; consequently it is not in itself a satisfactory risk indicator (22).

2.2.3 Effective dose

Effective dose [Sv] reflects the biological effects from radiation. It is possible to make an estimation of effective dose from DLP by multiplying DLP by conversion factors (k) that are age-, scanned region-, and CT geometry-specific:

$$\text{Effective dose} = k \cdot DLP \qquad \text{(Eq. 6)}$$

The effective dose factors are achieved by Monte Carlo simulations and expressed in mSv/mGy*cm (20).

2.3 Radiation risks

Risks related to radiation exposure can be divided into two main categories: deterministic effects and stochastic effects. Deterministic effects are due to cell death and are quantified in terms of the radiation dose to a particular region. These effects have a threshold level and are not expected to be seen after a CT examination, because radiation doses do not typically reach the threshold level (23). The major risks are due to stochastic effects, where the probability of incidence depends on amount of absorbed dose. Stochastic effects may result in cancer and genetic effects in the offspring of the irradiated person (20). On statistical bases, the radiation exposure from CT examinations may increase the risks of certain cancers, particularly in children (24).

The manufacturers of the CT-equipment have an important role in decreasing the radiation doses. Each modern manufacturer is conscious of the problem with high radiation doses and has developed automatic exposure control techniques. However, there is still much work to do, both by users and producers concerning defining the acceptable reference image quality for different diagnostic subjects. The work of finding the optimal examination protocol comprises balancing the advantage of improved image quality with higher radiation doses (7).

2.4 Parameters that affect image quality and patient radiation dose

There are an amount of scanning parameters that influence the radiation dose and the image quality. The operator can monitor most of these parameters and modify them to obtain the desired image quality with minimum radiation dose to the patient. Image quality and radiation dose are always connected to each other, which means that a modification of image quality has an effect on radiation dose and vice versa.

2.4.1 Scanner model and manufacturer

There is a considerable difference between scanning geometry from one scanner model/manufacturer to another. The distance between the focal spot of the X-ray tube and the centre of rotation (isocenter) depends on the geometry. The intensity of the radiation beam varies between the source and the patient according to the inverse of the squared distance. A CT model with short-geometry will produce more interaction of the radiation and therefore higher dose to the patient and lower image noise than a long-geometry scanner. There are also differences in filtration of the X-ray beams, efficiency of detection systems, reconstruction algorithms and noise levels in data acquisition electronics. Consequently, the image quality obtained at a given tube load, tube voltage and image width on a CT model may be different to another (17, 23).

2.4.2 Tube current and tube load

There is a simple relationship between the tube load (25) (the product of tube current and the exposure time per rotation) and the radiation dose to the patient. Whatever dose quantity considered, the measured dose is direct proportional to the tube load. A 50% reduction in tube load will halve the dose (17). Unfortunately, this will cause an increase in the image noise because of fewer photons contribute with information to the image, since the tube load is proportional to the photon fluence. The image noise is inversely proportional to the square root of the mAs, i.e. the noise level will increase by a factor of $\sqrt{2}$ when the dose is reduced by 50% (18).

2.4.3 Tube voltage

The tube voltage [kV] determines the energy of the photons emitted from the X-ray tube; increased tube voltage will generate photons with higher energy. A variation in tube voltage will result in a change in radiation dose and image quality. The relationship between tube voltage and image quality is complex, since it influences both image noise and contrast. The variation in dose is approximately proportional to the square of the tube voltage change (i.e. square of the ratio final and initial peak voltage). The noise change is approximately inversely proportional to the change in tube voltage, i.e. a decrease in kV causes an increase in noise (23).

2.4.4 X-ray filtration

The manufacturer usually fixes this parameter and it is a very effective way to reduce the radiation exposure to the patient. The filter is absorbing the photons that do not have enough energy to penetrate the body and reach the detectors (23). This X-rays would not contribute with any information to the image, but only cause unnecessary high radiation exposure to the patient. Bow-tie filters or beam shaping filters reduce the surface radiation dose and minimize the radiation exposure in the thinner parts of the patient (17). This provides better noise uniformity within the image and reduces the beam hardening artefacts (18).

2.4.5 Reconstruction filter

To reconstruct each cross-sectional CT image, X-ray beam projections from multiple directions around the region of interest are used. In convolution-backprojection procedure the beam projections is mathematically filtered before being back-projected into an image. The filtration is done to avoid unsharpening and to emphasize the signal from diagnostic relevant structures in the image (13). The noise in the reconstructed image will depend on which type of filter is used.

A low-pass filter will reduce image noise, but thereby spatial resolution is decreased as well. Using an edge-enhancing filter the spatial resolution will be improved, but also the noise will be enhanced. When correct filter is used one gives the opportunity for dose reduction (18).

2.4.6 Slice thickness

It is a balance between resolution ability and noise since they counteracts each other when choosing slice thickness. A reduced slice thickness leads to an increase in z-axis resolution and a reduction in partial volume effects. The disadvantage is that the noise in the image increases since the amount of photons at the detector is less. In the opposite way, an increase in slice thickness leads to an improved noise level and reduced spatial resolution (18).

2.4.7 Pitch

Pitch is defined as the ratio of table feed per gantry rotation to the nominal collimator width of the X-ray beam. The definition expresses the degree of overlap of the radiation beam: a pitch of 1 state contiguous radiation beams, a pitch less than 1 states overlap of the radiation beams, and a pitch greater than 1 state gap between the radiation beams. If the pitch is increased the duration of radiation exposure to the patient is decreased, hence the patient dose. The three parameters: beam collimation, table speed and pitch are connected to each other and affect the image quality. Increased table speed for a specified collimation gives rise to a higher pitch value, associated with a reduced radiation dose because of shorter exposure time. If the collimation is made narrower with slow table speed, this will result in longer exposure time and hence higher radiation dose to the patient. This is not correct for all CT scanners, e.g. Siemens use effective mAs (mAs/pitch) setting and maintain a constant radiation dose for effective mAs value. For these scanners the effective mAs value is constant irrespective of the pitch value. Hence, the radiation dose does not vary with any change in pitch value (17, 23). Likewise Philips report tube load as the average mAs per unit length along the longitudinal axis (mAs/slice) and is in fact calculated as mAs/pitch (7).

2.4.8 Reconstruction matrix

Different matrix sizes are available, for example 512 x 512 and 256 x 256. When the matrix is reduced, the spatial resolution will be worse. But at the same time, the noise will be reduced. If the matrix is halved, the noise level will be halved. It is then possible to reduce the radiation dose with a factor 4 (the noise is inverse proportional to the square root of the dose) (26).

2.4.9 Summary

Table 1 lists how CT scanning parameters influence the radiation dose to the patient and the image noise.

Table 1. Parameters that affect patient dose and image noise.

Parameter	Affect on patient dose	Affect on image noise
Scanner geometry	Higher for short-geometry	Lower noise for short-geometry
Tube load	Linear increase in dose with mAs value	Inversely proportional to the square root of the mAs
Tube voltage	Approximately proportional to the square of the ratio final and initial peak voltage	Approximately inversely proportional to the ratio final and initial voltage
Filtration	Higher degree of filtration is advantageous	Better noise uniformity
Reconstruction filter	Opportunity for dose reduction	Low-pass filter will reduce image noise
Slice thickness	Approximately linear increase in dose with slice thickness	Improved noise level with increased slice thickness
Pitch	Decrease for higher pitch (not for Siemens and Philips)	More noise for higher pitch (not for Siemens and Philips)
Matrix	Opportunity for dose reduction with reduced size	Proportional to the matrix size

2.5 Automatic exposure control

Automatic exposure control could be defined as a CT technique that performs automatic modulation of tube current in the x, y plane (angular modulation), or along the scanning direction, z-axis, (longitudinal modulation), or both (combined modulation) (Fig. 3). The modification is done according to each patient's size, shape and attenuation of body parts being scanned. The operator must select a required image quality level and then the system can adjust the tube current to obtain the predetermined image quality with improved radiation efficiency (6). AEC system (angular modulation) can in most cases reduce radiation dose by typically between 10-50%, without any deterioration of the image quality. In the shoulder region is even more than 50% dose reduction possible, because of big differences in attenuation (13). However, for large patients the radiation dose can increase to preserve the specified image quality (6).

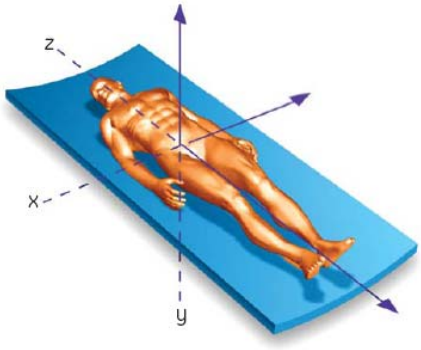

Figure 3. Orientation of the three-dimensional coordinate system. Illustration courtesy of GE (27).

Throughout a CT scan, the X-ray tube rotates around the patient and emitting x-rays that pass through a cross section of the body. At the detectors these X-ray beams give rise to attenuation profiles (image raw data). To reconstruct each cross-sectional CT image, X-ray beam projections from multiple directions around the region of interest are used. The accuracy of the attenuation measurements made by the detectors depends on the beam intensity. If few photons are detected, the accuracy of the measurement is poor and the reconstructed images from this data will be nosier. The photon fluence (number of photons) emitted by the X-ray tube is due on tube current, whereas the tube potential determine the incident beam energy. A reduction in the tube current when other scanning parameters are constant will result in a decreased radiation dose and an increased image noise that is proportionately with the reduction. Likewise an increase in the tube current will lead to an increase in radiation exposure, whereas image noise decrease (28, 29).

AEC technique is based on the fact that projection with the most noise primarily determines noise of the final image, because the noise in the reconstructed image is related to the square root of the sum of the squares of the individual projection noises (Fig. 4) (18). The image noise is mainly attributable to the projections, which correspond to the most attenuating paths through the patient, and therefore the greatest quantum noise occurs. For that reason it is possible to reduce dose for other projections without increasing the noise in the final image, with the assumption that image noise is attributable to the quantum noise in the X-ray beam projections (30). For example, greater beam attenuation in a particular projection will cause greater noise and will require higher tube current than needed by a beam undergoing less attenuation in another projection. Another way to do is reduce the dose for projections that are of limited interest. For example, the AEC technique can reduce the dose for a cardiac CT examination about 50%, by decreasing the tube current through systole (5).

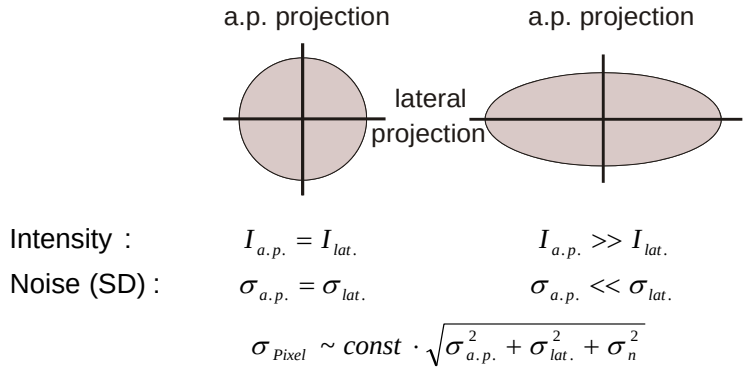

Figure 4. The basic idea behind AEC (angular). For cross-sections that deviate significantly from circular form it is possible to reduce the radiation intensity in projections with less attenuation, without any significant effect on the noise. In the figure n stands for the remaining individual projection noises (13).

2.5.1 Angular modulation

With a fixed tube current technique, the X-ray tube rotates around the patient continuously emitting X-rays with constant fluence. In angular (rotational) modulation technique the tube current is adjusted for each projection angle to the size, shape and attenuation of the patient in order to minimize X-rays in beam projection angles (in the x- and y-axes) that are associated with less beam attenuation and consequently contribute less to the overall image noise (Fig. 5a). For example in anatomy that is highly asymmetric such as the shoulders and pelvis, the X-ray beams are much less attenuated in the anterior-posterior direction compared with the lateral direction and hence is associated with less noise (Fig. 5b). For that reason, angular modulation technique reduces unneeded radiation in the anterior-posterior projection without any obvious degradation of the image quality (6, 28). In regions where the patient is more circular and homogenous, such as the head, less modulation will occur (4).

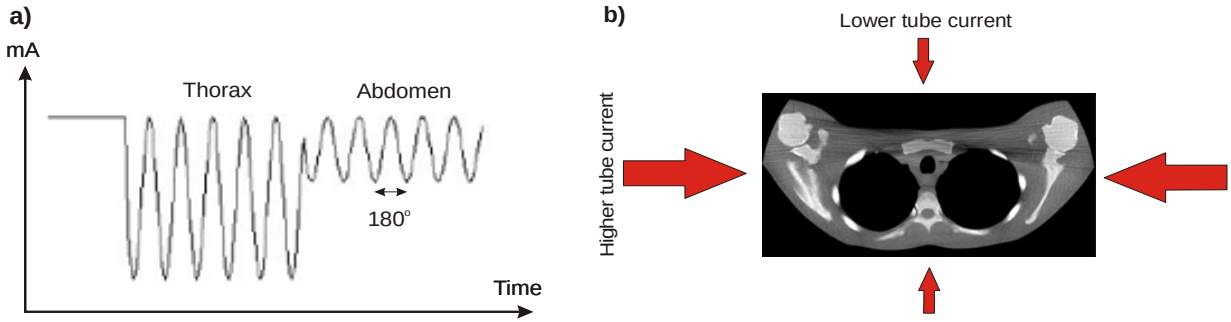

Figure 5. a) Illustration of angular modulation technique; the tube current (vertical axis) is varied as the X-ray tube rotates around the patient (horizontal axis). In thorax region there is greater variation since more asymmetry than in abdomen. **b)** Principle of angular modulation technique; in the shoulder region it is possible to reduce the tube current in the anterior-posterior direction compared with the lateral direction, which is the thickest cross section and has an amount of bony material that attenuates the X-rays.

In asymmetric regions of the body, e.g. the shoulders, where the lateral scan range goes through the thickest cross section and has a higher than usual amount of bony material, starvation (streaking) artefacts can arise. This artefact is due to insufficient of photons in the attenuation measurements, in the lateral direction. Angular modulation tries to diminish the variation in uncertainty of attenuation measurements by increasing the tube current in lateral projection angles and reducing where the attenuation is lower. This has the effect that the noise is more uniform across the image and starvation artefacts will be reduced (4).

The method for angular modulation technique is different between various manufactures. Some use the pattern of the attenuation profile across the patient at each z-axis position to estimate the patient's asymmetry. Another possibility is to use feedback from online measurements during the CT scan. It is practicable to make use of the shape of the attenuation profile at each angle during each rotation to adjust the tube current during the next rotation, since the patient's asymmetry generally changes gradually along the scanning direction. A predefined function (e.g. a sine wave) could be applied to adjust the tube current to the variation of attenuation with the projection angle (4).

2.5.2 Longitudinal modulation

When a fixed tube current technique is used images are acquired at a constant tube current value along the scanning direction (z-axis), independent of patient size or local attenuation. With longitudinal modulation technique, the tube current is adjusted along the scanning direction (z-axis) of the patient, grounded on the size, shape and attenuation of the anatomic region being scanned (e.g. shoulders versus the abdomen versus the pelvis) (Fig. 6). The purpose of longitudinal modulation technique is to produce similar noise in all images independent of patient size and anatomy. The aim is also to reduce the variation in image quality from patient to patient. Consequently, the operator must select a required level of image quality as an input to the AEC algorithm. The methods used for this are different between various manufacturers. But irrespective of type, the longitudinal modulation technique uses a single localizer radiograph to determine the tube current required to produce images with required level of image noise (6, 28).

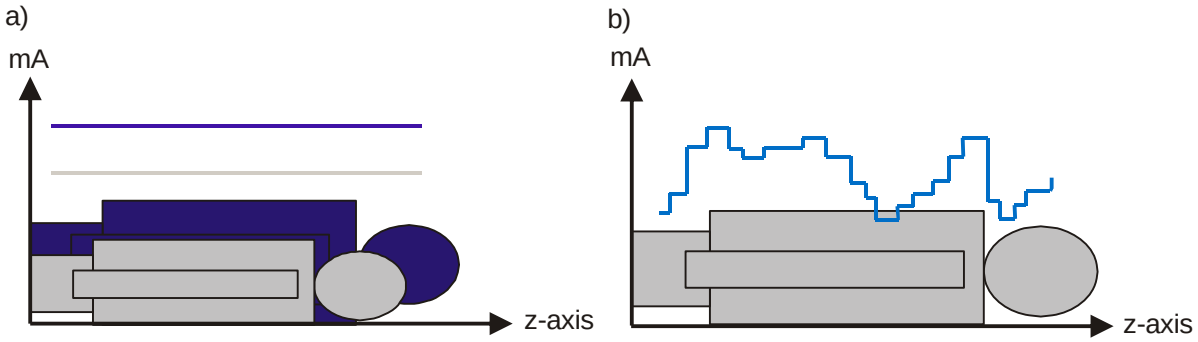

Figure 6. Illustrations of longitudinal modulation. **a)** Lower mA is used for a smaller patient. **b)** Lower mA is used where the attenuation is low along the scanning direction, e.g. the lung region.

2.5.3 Combined modulation

Combined modulation technique is a simultaneous combination of angular and longitudinal (x-, y-, and z-axis) tube current modulation, i.e. this technique modulates the tube current both during each gantry rotation and for each slice position (Fig. 7). As mentioned earlier, the operator must still specify the required level of image quality. Combined modulation technique is the most extensive approach to CT dose reduction, since the X-ray dose is adjusted in accordance with the patient attenuation in three dimensions (5).

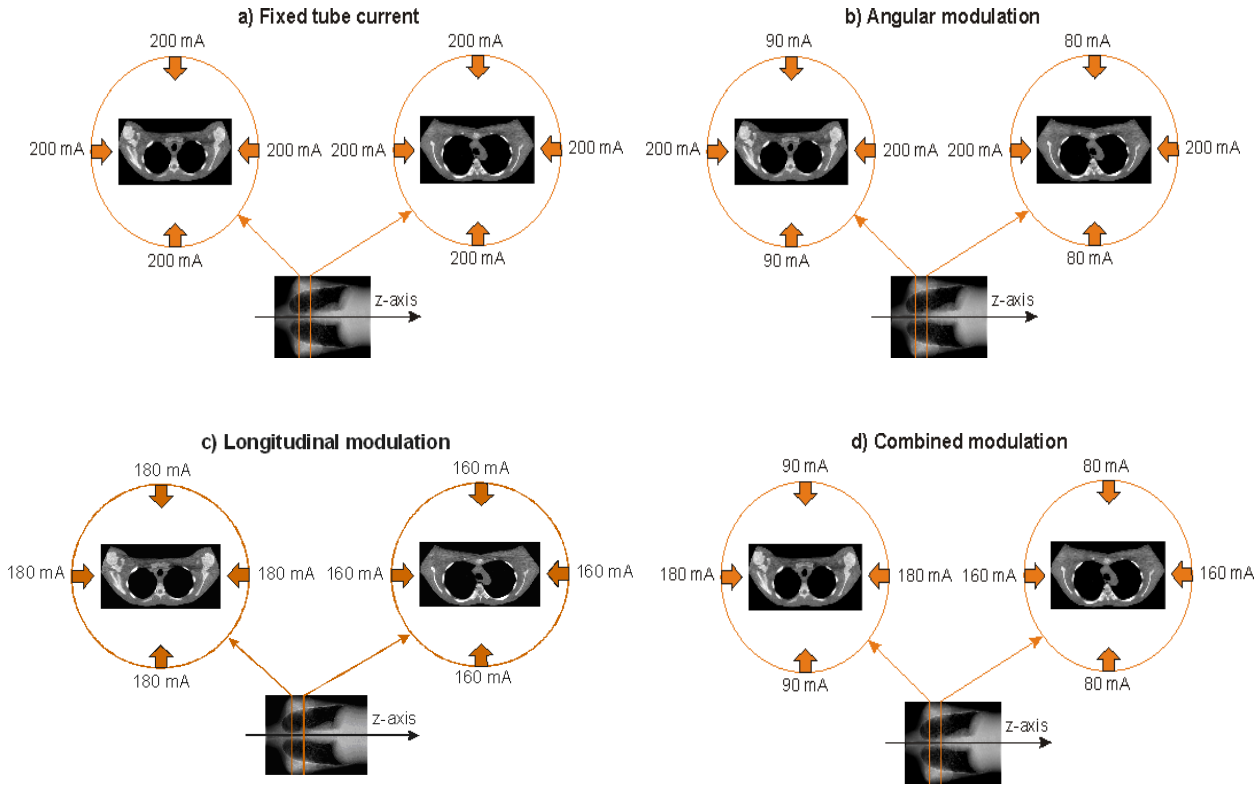

Figure 7. Schematic representation of AEC techniques. **a)** Fixed tube current: same tube current is used at all projection angles and slice positions. **b)** Angular modulation: the tube current is adjusted during each gantry rotation (in the x, y plane) according to the size, shape and attenuation of body region being scanned. **c)** Longitudinal modulation: the tube current is adjusted along the scanning direction (z-axis) of the patient, grounded on the attenuation of the anatomic region being scanned and the predetermined image quality. **d)** Combined modulation: CT scanning is performed with different tube currents for different slice positions in the scanning direction (z-axis) and for different projection angles during the gantry rotation.

2.5.4 Methods to select the required image quality level

The manufactures have figured out different solutions of defining the image quality level. Each method has its own benefits and drawbacks. Image quality is a non-specific and subjective measure of the legibility of an image and must be established by a trained viewer. But objective measures, for instance image noise or contrast-to-noise ratio can be measured. It is complex to determine optimal image quality for a clinical diagnose, since both quantitative measurements and the observer's perception are accountable. It is important to remember that nice-looking pictures are not necessary for all diagnostic tasks. The selection of low noise or low dose shall always be performed depending on type of diagnose (5).

A method is to specify the image quality in terms of the resultant *standard deviation* (SD) of pixel values. The tube current is adjusted to attain the operator selected SD on an image-by-image basis, i.e. the specified SD (noise level) will represent the SD in the reconstructed images of a water phantom. Selecting a high SD value will result in an image with higher noise than if a lower SD value is chosen. This technique has a benefit; it is easier to compare image quality resulting from protocols from different CT scanners (4).

Another method is to set a *reference mAs* value for each scanner protocol. This value would represent an averaged sized patient (standard patient). The AEC system determines the size of the patient's cross-section and then adapts the tube current relative to the reference mAs value. This technique allows the tube current modulation to be more adaptable to the circumstances

than an AEC system based on SD. With SD based AEC systems is the AEC response to different patient sizes predefined, since the goal is to always produce images with a constant noise level. The systems based on the reference mAs have the opportunity to vary the response due to image quality requirements (4). For instance, normally smaller patients require better image quality than larger patients (31). It is therefore possible to obtain images of small patients with lesser noise than in images of the standard patient. A drawback is that it is not simple to compare reference mAs protocols since the tube current that is used for a standard patient is due on scanner design, e.g. beam filtration and scanner geometry, also the definition of the standard patient (4).

A further method to use is a *reference image* concept. Then each patient is matched to a reference image that earlier has been collected and judged to have suitable quality for a particular examination. The system tries to adapt the tube current so that same level of image noise in the reference image will be obtained. This technique has one main benefit; the required image quality is based on a real clinical image, not on an abstract SD value. A possible disadvantage is that it is easy to choose a reference image with too low noise rather than one that is appropriate for the clinical task. This will lead to unnecessary high radiation exposure to the patient. Further, it is also complicated to compare scan protocols since there is no related value with the image quality in the reference image (4).

2.5.5 Benefits of an AEC system

There are a number of benefits when an AEC system is used. First of all, the potential for *dose reduction* through optimised modulation of the tube current according to patient attenuation in all three planes. Using a too high tube current for smaller patients is avoided with AEC technique, since a required image quality level has been determined before. With longitudinal modulation overcomes the problem that some body regions will either get higher then necessary radiation dose or too high image noise. Angular modulation makes it possible to reduce the tube current for projections with low attenuation without significant increase the image noise. With an AEC system could even more *consistent image quality* obtains. There should be more similar noise in all produced images and the variation in image quality from patient to patient will be diminished. If the tube current is reduced, the heating of the X-ray tube is also reduced. Consequently *extended scans* (examinations) could be done. A further benefit is the potential for *reduction of photon starvation artefacts* (streak artefacts), explained earlier in section 2.5.1 Angular modulation (x, y) (4).

2.5.6 Limitations of an AEC system

There are a number of limitations with AEC systems. Each manufacturer has come up with different solutions of AEC techniques and this makes it very difficult to do universal standardization for different scanning protocols. For example, it is difficult to convert a reference mAs value into a SD value when defining the image quality level. The optimal image quality level for different techniques is undefined. Some AEC systems need modification in small patients to avoid too much tube current reduction; otherwise it will result in noisier images. To avoid this problem some systems offers a restriction of minimum tube current. There are some studies that have shown that AEC technique can increase the radiation dose to larger patients. This is desirable if the selected image quality should be preserved (6, 28). Results from a recent study found in some cases that the AEC system can lead to an increase of the dose if the maximum tube current is not properly set (11). The AEC systems have a special demand upon the scanner hardware; the X-ray output must be rapidly and predictably varied (21).

2.5.7 Summary

Table 2 summarize the principle of three different levels of AEC.

Table 2. AEC techniques available in modern CT systems.

AEC modulation	Angular	Longitudinal	Combined
Principle	The tube current is adjusted during each gantry rotation, according to the size, shape and attenuation of body region being scanned.	The tube current is adjusted along the scanning direction of the patient, according to the size and attenuation of the anatomic region being scanned and the predetermined image quality.	The tube current is adjusted both during each gantry rotation and for each slice position.
Modulation plane	x, y	z	x, y, z

2.6 The major CT scanner manufactures AEC systems

Each manufacturer of CT systems has developed different AEC techniques and use proprietary nomenclature. The AEC systems have different capabilities and work as described earlier in a variety of ways, but their main purpose is to adapt the tube current to compensate for changing patient attenuation of the X-ray beam.

2.6.1 Siemens - CARE Dose 4D

Siemens use a combined tube current modulation system called CARE Dose 4D. The system works with automatic tube current modulation of the patient's size and shape together with real-time, online, controlled tube current modulation during each tube rotation (32).

Based on a single CT localizer radiograph, "topogram", anterior-posterior or lateral attenuation profile (size, anatomic shape and attenuation at each position) along the patient's long axis (z-axis) is measured in the direction of the projection and estimated for the perpendicular direction with a mathematical algorithm (Fig. 8). From the estimation of these attenuation profiles, axial tube current values are determined. The correlation between attenuation profile and tube current is defined by an analytical function for slice position in the z-axis and adjust the tube current to the patient size and attenuation changes (longitudinal modulation). Modulation of tube current with CARE Dose 4D is grounded on the operator selected *image quality reference mAs* and intend to preserve required image quality along the scanning direction (6, 28).

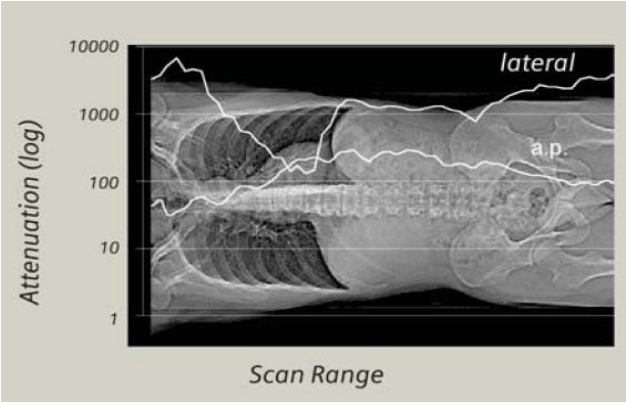

Figure 8. Example of an anterior-posterior topogram where anterior-posterior and lateral attenuation profile is estimated. Illustration courtesy of Siemens (32).

Based on the axial tube current profiles (anterior-posterior and lateral), the system performs online tube current modulation during each tube rotation (angular modulation). The system use feedback from the previous rotation to set the tube current according to the patients angular attenuation profile at different projection angles (Fig. 9) (4, 28).

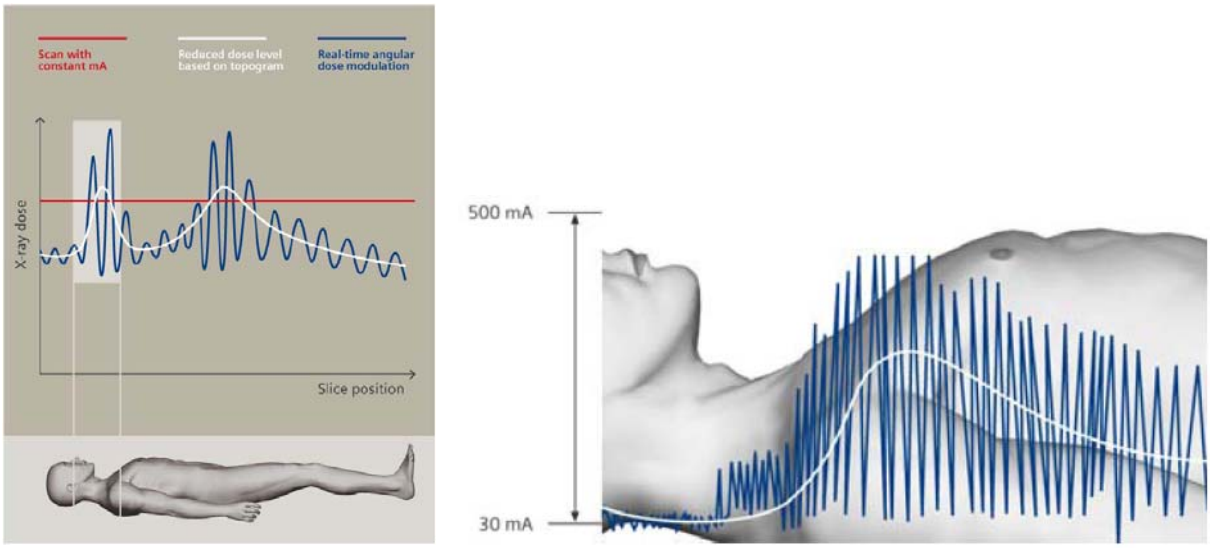

Figure 9. Illustration of automatic current modulation by CARE Dose 4D for a helical scan from shoulder to pelvis (very high table feed for demonstration). In shoulder and pelvis are high mA and strong modulation performed. In abdomen and thorax are lower mA and low modulation performed. Illustration courtesy of Siemens (32).

The quality reference mAs value, which is selected by the operator, should be based on the diagnostic requirements of a given protocol and the individual preference of the department. For each type of examination (i.e. protocol), quality reference mAs indicate the mean effective mAs (tube current-time product/pitch). The operator selects a typical value represented a reference patient, which is defined as an adult with a weight of approximately 70 to 80 kg. For pediatric protocols, the effective mAs should be selected for a typical child with a weight of 20 kg (5, 6). Thus, CARE Dose 4 D adjusts the tube current for each rotation. Depending on the patient attenuation at z-axis position relative to the reference patient size, a value that is higher or lower than the quality reference mAs is set (4). For adult head protocols the tube current is only modified to the variation along the patients scanning direction (longitudinal modulation) and consequently no angular modulation is performed (32).

The quality reference mAs value is not altered for patients of various sizes. If a modification to image quality or radiation dose is desirable, it is possible to change the quality reference mAs or strength of tube current modulation. For each type of protocol a typical X-ray attenuation of a standard sized patient is internally stored and the quality reference mAs value is related to this reference X-ray attenuation. The system determines whether the patient/region is small "slim" or large "obese" from the localizer radiograph. The degree of change in tube current decides according to the modulation strength specified by the operator. For slim patients/regions, weak, average or strong modulation settings will result in weak, average or strong decrease in radiation dose, respectively (Tab. 3). As well for obese patients/regions, weak, average or strong modulation settings will result in weak, average or strong increase in radiation dose, respectively (6, 28). Studies with CARE Dose 4D have shown that compared with constant tube current, a 20-60% dose reduction due to anatomical region and patient shape, with improved image quality (28).

Table 3. Modulation strength settings for CARE Dose 4D (6).

Patient/region size	Weak modulation	Average modulation	Strong modulation
Slim	Weak decrease in tube current	Moderate decrease in tube current	Strong decrease in tube current
Obese	Weak increase in tube current	Moderate increase in tube current	Strong increase in tube current

2.6.2 Philips - DoseRight

Philips AEC system, DoseRight has three elements: Automatic Current Selection (ACS) that provides patient based AEC, D-DOM that provides angular AEC and Z-DOM that provides longitudinal AEC. It is not currently possible to use all three dose modulation tools together, but you can apply ACS together with Z-DOM or D-DOM (33).

To set the required image quality level Philips uses a *reference image* concept. The manufacturer call this method ACS and the process are like the user selects a suitable patient examination and the system saves the image data including the raw CT projection data and the CT projection radiograph, "surview". The data is saved as a reference case for comparison with CT projection radiograph and data obtained from other patients in examinations for the same diagnostic issue (5). The pre-defined reference values are respected to be for a standard patient size, which is 33 centimetres in diameter. The standard patient size is used as a baseline for ACS when it proposes specific mAs values for each patient, performed of a proprietary algorithm (33). The suggested mAs values are in order to achieve a constant image noise level (34).

ACS works by the patient's absorption coefficient acquired from the surview is matched to the absorption coefficient from the reference sets surview (Fig. 10). Whether the patient is larger than the reference set (standard patient), an increase in mAs will follow. In the corresponding way, if the patient is smaller than the standard patient, the system will suggest a decrease in the mAs value. It is then possible for the operator to change the proposed mAs value by the ACS to an appropriate mAs value (Fig. 11). The system will "learn" the users preference mAs settings interactively. If the proposed tube load is increased, the system will "learn" to increase mAs values for patients of that size. In the corresponding way, the system will learn to decrease mAs values if the suggested mAs value was decreased for a patient of that size (33).

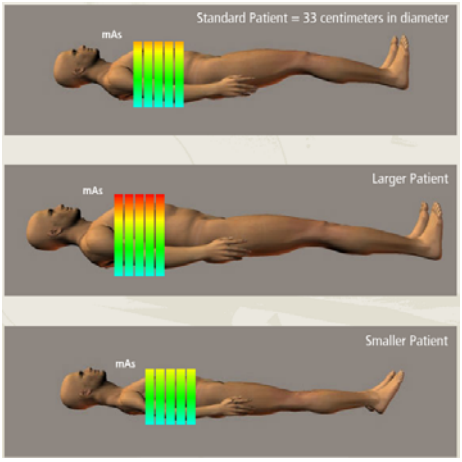

Figure 10. For a patient that is larger than the standard patient the system will suggest a higher mAs value and for a patient that is smaller than the standard patient the system will suggest a lower mAs value. Illustration courtesy of Philips (33).

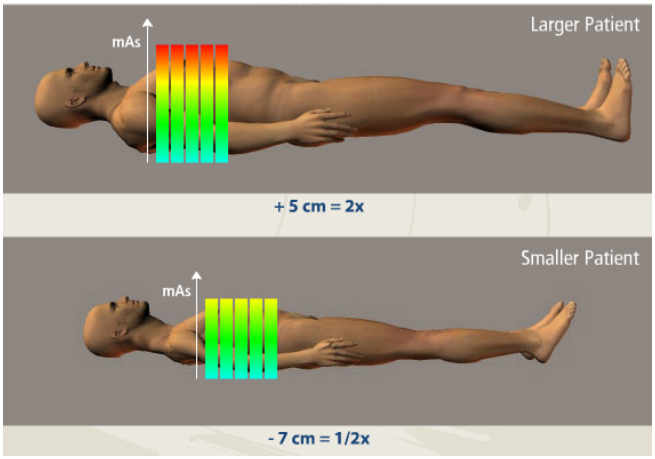

Figure 11. The tube load is doubled for every 5 cm the patient is above the reference size. For every 7 cm the patient is below the reference size, the mAs value is halved. Illustration courtesy of Philips (33).

There are a number of CT parameters that if they were changed will disable or turn off the ACS. These CT parameters are: tilt, resolution, collimation, thickness, tube voltage, tube load and filter. All these parameters if they are changed have a great influence of the image noise. Even though ACS is disabling it still continues to "learn", grounded on the operators input. It will take approximately 20 patients before the ACS software have learned the users dose preference (33).

D-DOM is the name of Philips angular modulation system and accordingly is the tube current modulation based on the patients symmetry change in the rotational direction of the gantry (x- and y-axis). The modulation is calculated online in real-time during each rotation of the gantry around the patient by using data of the previous rotation to calculate the next rotation modulation. D-DOM makes use of the detector dose and determines which part of the rotation can advantage from a reduced dose, without lost in image quality (4, 33).

Z-DOM can be referred as longitudinal modulation and consequently is the tube current modulated according to changes in the body attenuation along the longitudinal axis of the patient (z-axis). Based on a single CT localizer radiograph, surview, the mAs values are calculated to the real scanning of the patient to achieve same image quality in all slices. As the scanning process advance, the Z-DOM mAs values change and the modification is based on absorption changes in the scanning direction instead of adjustment grounded on the patients anatomic shape (33).

2.6.3 General Electric - AutomA 3D

General Electric (GE) uses a combined tube current modulation system called AutomA 3D. The system consists of two elements: AutomA that provides longitudinal AEC and SmartmA that provides rotation AEC. It is possible to use AutomA individual and together with SmartmA.

AutomA make use of a single localizer radiograph, "scout", to determine patient size, anatomic shape and attenuation characteristics to adjust tube current for each slice position along the patient's long axis. With SmartmA the tube current is for different projection angles within each x-ray tube rotation adjusted (6, 28). For each rotation (4 times/turn), the system calculates each x and y mA-value from the relation between the patient's long and short axis, based on the scout image (35).

To use AutomA 3D the operator must specify a *noise index* value, minimum and maximum mA limits (28). The noise index allows the user to set a required image quality and it is referenced to the image noise (the SD of pixel values in the central region of an image of a uniform water phantom) (29). A lookup table maps the patient's attenuation values measured on the scout image into mA values for each gantry rotation according to a proprietary algorithm. The algorithm is intentionally to preserve the same image noise level as the attenuation values change from one rotation to the next (Fig. 12). For different patient sizes and study indications the noise index may be changed (5). The selected minimum and maximum tube current limits define the range of where the tube current modulation is desired. Studies have reported that up to 60% dose reduction with use of AutomA 3D technique in abdominal/pelvic CT examinations (28).

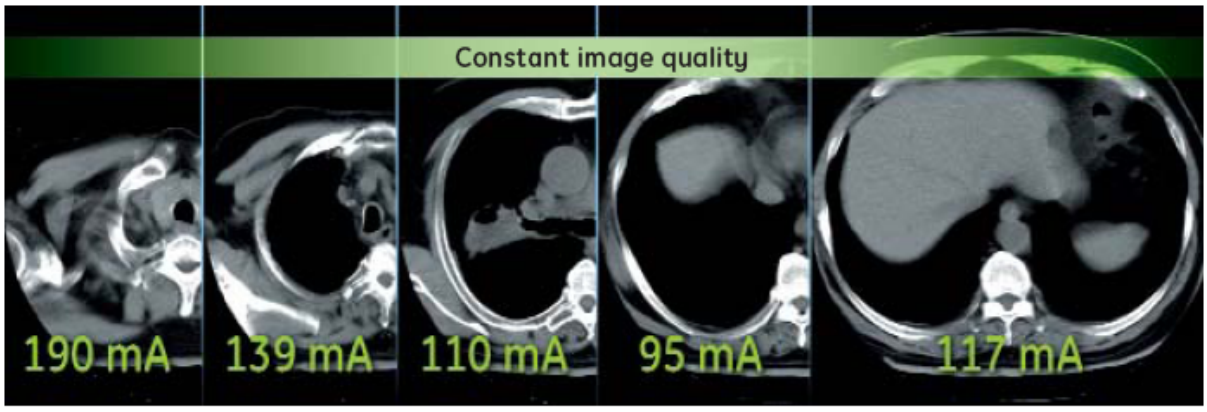

Figure 12. The system aims to achieve the same level of noise in each image. Illustration courtesy of GE (27).

If the user measures the noise (SD) by inserting a region of interest (ROI) in the image, it will sometimes be different from the operator selected noise index. This wills due to that the noise index only adjust the tube current (i.e. quantum noise in the projection data), however image noise depends also on other factors, shown in table 1. When very large patients are scanned, electronic noise can become the dominant image noise source because of insufficient detector signal. This will also result in differences between the selected noise index and the standard deviation (16).

2.6.4 Toshiba - SureExposure 3D

Toshiba uses a combined modulation system called SureExposure 3D. The technique offers the operator two methods of setting the required image quality: *standard deviation* of CT numbers or *image quality level*. Both methods are based on measurements of SD of pixel values measured in a patient-equivalent water phantom (5).

The operator starts to specify the SD value for the HU image noise and also minimum and maximum tube current. A too low tube current can bring intense image noise and very poor image quality. Very high tube currents cause only high radiation exposure and reduce hardly nothing of the noise (36). The process will follow with acquiring one frontal and one lateral CT localizer radiograph, "scanogram", of the patient (Fig. 13). Information from the scanograms is then used to map the selected image quality to tube current values. The system makes use of the frontal and lateral diameters and the detector intensities to account for the oscillating tube current modulation during each gantry rotation. Table 5 list a number of parameters that affect SureExposure 3D. Studies with Toshibas AEC system have shown that, compared with constant tube current, up to 40% dose reduction due to anatomical region and patient shape (37).

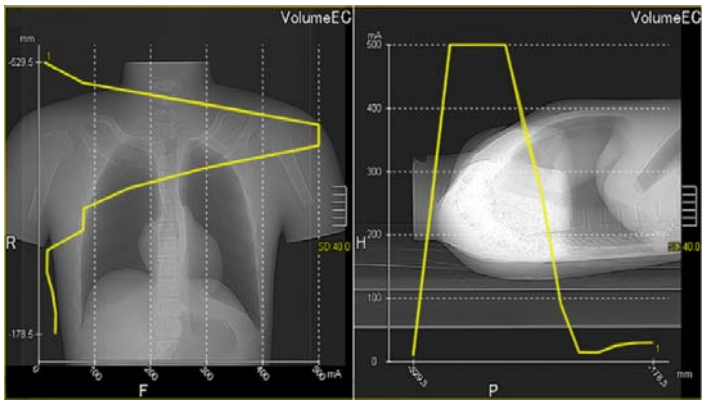

Figure 13. Frontal and lateral scanogram are used to map the selected SD to tube current values. Illustration courtesy of Toshiba (38).

2.6.5 Summary

Table 4 lists the AEC systems from the manufacturers of the CT equipment. Each system has different solutions of defining the image quality level.

Table 4. The AEC systems from the manufacturers included in this study.

Manufacturer	AEC system	Method to set level of image quality
Siemens	CARE Dose 4D	Quality reference mAs
Philips	DoseRight	Reference image
GE	AutomA 3D	Noise index
Toshiba	SureExposure 3D	Image quality level/standard deviation

The response of different AEC systems when scan and reconstruction parameters are varied has been reported by ImPACT (4). Table 5 shows when a cell is marked with "X", a modification in that parameter will result in a change in the tube current by the AEC system.

Table 5. Response of the AEC systems to variation of parameters, from ImPACT (4).

AEC system	Tube voltage	Rotation time	Pitch	Slice thickness	Reconstruction kernel
CARE Dose 4D	*	X	X		
DoseRight	X	X	X	X	
AutomA 3D	X	X	X	X	
SureExposure 3D	X	X	X	X	X

* For new versions of CARE Dose 4D, a change in the tube voltage will result in a change in the tube current by the AEC.

3. Materials and methods

3.1 CT scanners covered in this report

CT equipment from four manufactures, mentioned above, was used in this study. Measurements were performed on 16 and 64 slices CT-scanners for each manufacturer.

3.1.1 Siemens

Measurements were performed on Siemens *SOMATOM Sensation 16* and *SOMATOM Sensation 64* which are situated at Malmö University Hospital, Diagnostic Center. The Somatom Sensation 64 is equipped with a new X-ray tube (Straton). This x-ray tube utilizes two alternating focal spots, which result that double X-ray projections reach each detector element (Double z-Sampling). The technique involves that the slice width can be reduced and Siemens claims that this remove so called windmill artefacts (32). The SOMATOM Sensation 16 is equipped with an X-ray tube named Akron. This X-ray tube is somewhat slower in the tube current modulation compared to the smaller and faster X-ray tube Straton.

3.1.2 Philips

Philips AEC system, DoseRight was investigated on a GEMINI PET/CT that consists of a *Brilliance CT 16* and is located at Malmö University Hospital, Diagnostic Center. Measurements were also performed on a *Brilliance CT 64 Power*, which is located at Lund University hospital at the neuro-section of the radiology department.

3.1.3 GE

Used CT scanners from GE are *LightSpeed*[16] that is situated at Simrishamn hospital at the radiology department and a *LightSpeed VCT* that is placed at Halmstad county hospital at the radiology department. GE LightSpeed VCT has compared to LightSpeed[16] a better data acquisition system, which GE claims may have potential to result in better image quality. It is therefore possible to accept a higher noise index for LightSpeed VCT (39). Both scanners offer two choices how the algorithm should use the information for the dynamic of the tube current modulation and thus for the image reconstruction. In full mode is the information based on a 360° X-ray tube rotation and in plus mode on 360° plus 45° X-ray tube rotation (11).

3.1.4 Toshiba

Measurements on Toshibas AEC system has been performed on an *Aquilion 16* and *Aquilion 64*, both located at Toshibas training center in Zoetermeer, Netherlands. Both CT scanners offer a Quantum Denoising System (QDS) filter process. QDS is a three-stage mathematical filter algorithm, which mix a smoothing- and enhancement filter. Toshiba claims that with QDS activated; the image quality will be improved for less tube load and the image noise will be reduced while maintaining both spatial and low contrast resolution. QDS is clinically used by routine (40).

3.2 Phantoms used in this study

The automatic exposure control system of each manufacturer has been investigated by using two kinds of phantoms, an anthropomorphic thorax phantom and an anthropomorphic head phantom.

3.2.1 Thorax phantom (Chest Phantom PBU-X-21, Kyoto Kagaku CO, Ltd, Kyoto, Japan)

The thorax phantom is an anthropomorphic phantom that closely resembles a real human chest (Fig. 14). The skeleton consists of epoxy resins, calcium hydroxyapatite and other substances to achieve changes in contrast in the phantom images as in an actual human body. To provide accurate evaluation and analysis the phantom is made of material that resemble soft tissue such as body tissue, which is made of urethane. The phantom also contains material that resembles blood vessels, including pulmonary capillaries (41).

During CT acquisitions the phantom was centred according to a clinical routine CT examination, i.e. supine position, sagittal midline, and midthickness of the phantom at the isocenter of the gantry. This position was to ensure proper image quality and minimal dose. The scanning direction was chosen according to the recommendations of the manufacturer and varies.

3.2.2 Head phantom (SK 150, The Phantom Laboratory, Salem, NY, USA)

Head phantom SK 150 is an anthropomorphic phantom, constructed around natural human bone (Fig. 15). The feature consists of RANDO® material, a specially formulated urethane that accurately resembles the density of human tissue. The skull and upper cervical vertebrae are cast into the phantom. To represent the oral, pharynx and trachea anatomy an internal air cavity have been incorporated (42).

The head phantom was centred in supine position, sagittal midline, and midthickness of the phantom at the isocenter of the gantry. The scanning direction was chosen according to the recommendations of the manufacturer and varies.

Figur 14. Thorax phantom.

Figur 15. Head phantom.

3.3 Testing approach

Each manufacturer of CT systems has developed different AEC techniques, which differ in method of adjusting the tube current. Consequently it was not practical to use a common standard protocol for all manufacturers. The manufactures CT systems also differ between 16 and 64 slices, so instead a general protocol was created for each examination (Tab. 6 and Tab. 7). The procedure was to modify an already existing standard clinical thorax respective head protocol for each CT-scanner. As many as possible of the scanning parameters was set equal for all examinations.

Table 6. General scanning parameters for thorax and head protocol.

Settings	Thorax protocol	Head protocol
Tube voltage [kV]	120	120
Rotation time [s]	0.5	1
Slice width [mm]	5	5
Increment [mm]	5	5
Filter	Standard	Standard
Reconstruction kernel	Standard	Standard
FOV [mm]	400	250*
Matrix	512 x 512	512 x 512

*For Toshiba was 240 mm used.

Table 7. Individual scanning parameters for thorax/head protocol.

Manufacturer	Model	Collimation [mm]	Pitch	Reconstruction kernel
Siemens	SOMATOM Sensation 16	16 x 0.75	1	B31f/H31s
	SOMATOM Sensation 64	64 x 0.6	1	B31f/H31s
Philips	Brilliance CT 16	16 x 0.75	1.063/1.058	Standard B
	Brilliance CT 64 Power	64 x 0.75	1.078	Standard B
GE	LightSpeed[16]	16 x 0.625	0.938	Standard
	LightSpeed VCT	64 x 0.625	0.984	Standard
Toshiba	Aquilion 16	16 x 0.5	0.938/0.934	FC10/FC23
	Aquilion 64	64 x 0.5	0.828/0.844	FC10/FC23

All tests were performed in helical scan mode with AEC activated and non-activated. If the AEC system offers different modulation techniques, the effect of each element was individually examined.

3.4 Determination of dose reduction

Details of the radiation dose were obtained for each CT scan from the DICOM image information. From the DLP values it was possible to estimate the variation in radiation dose by calculate the difference of the DLP values in percent relative to the DLP values for the constant tube current scan (Eq. 7). The DLP values were compared with national diagnostic reference levels (DRL) from SSI FS 2002:2 (Tab. 8).

$$\text{Dose reduction} = \frac{DLP_{\text{Fix mA}} - DLP_{\text{AEC}}}{DLP_{\text{Fix mA}}} \cdot 100\,\% \qquad \text{(Eq. 7)}$$

Table 8. Recommended DRL from SSI (43).

Examination	$CTDI_{vol}$ [mGy]	DLP [mGy*cm]
Thorax	20	600
Abdomen	25	*
Head	75	1200

* These examinations include a lot of different issues, which affect the size of the investigated anatomic region. Therefore no DRL of DLP have been established.

The mean mAs used in each slice image was showed on the CT console. To study the characterization, i.e. the dynamic of the tube current modulation of each AEC system the mean mAs used for each image slice have been plotted against the image slices. This makes it possible to study how the tube current is varied along the z-axis of the anthropomorphic thorax and head phantom.

3.5 Evaluation of image quality

CT image quality may be determined by: contrast, noise, spatial resolution and artefacts. A radiation dose reduction is limited by worse image quality, e.g. an increase in image noise. Image noise can potentially obscure lesions otherwise visible on a higher dose CT protocol. It is therefore considerable important to investigate whether AEC systems affect the image quality or not.

To evaluate whether AEC systems affects image quality, the image noise was compared in images obtained from scans performed with fixed mA and with AEC activated. The comparison was performed in different ways. CT image noise (quantum mottle) is related to the number of X-rays contributing to each detector measurement. Image noise can be estimated by insert regions of interest (ROIs) and receive a magnitude (SD) of the fluctuations in CT-numbers. The random fluctuations are related to image noise. The higher SD value, the more image noise is present. The evaluation of image quality for images from Siemens, Philips and GE were performed on a Syngo MultiModality Workplace, earlier known as LEONARDO. Images from Toshiba were analysed in Sante DICOM Viewer Pro 2.1.

3.5.1 Thorax phantom

In some specific slices where the tube current modulation was pronounced (shoulder-, thorax- and abdomen region) the image noise was evaluated as 1 standard deviation of Hounsfield unit values of a ROI (Fig. 16). In each investigated slice 5 ROIs were placed at identical anatomic positions in different rather uniform areas. The sizes of the ROIs were made as big as possible but not too big to hazard the homogeneity (1-2 cm^2). The larger used ROI size, the better pixel statistics obtain. Relative SD was then estimated as SD in images with AEC activated compared with AEC non-activated.

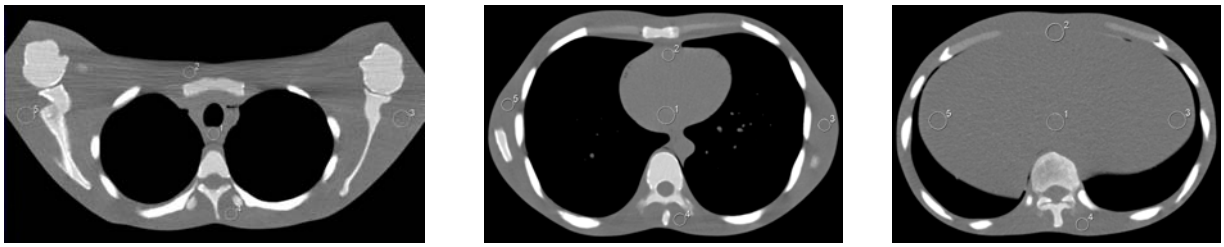

Figure 16. Examples of ROI position in the shoulder-, thorax- and abdomen region.

SD measurements were also performed in an ROI of 0.5 cm^2 large area placed in the spine throughout the thorax phantom (Fig. 17). This location was chosen since the region is rather uniform and available all over the phantom. There were also only minor changes in CT-number in this region. The results are presented as graphs were SD has been plotted against the image slice. The mean SD was calculated for the thorax phantom and also the SD of the measured SD values (image noise). Then, coefficient of variation (c_v) was estimated as the ratio of the SD (σ) to the mean value (μ) (Eq. 8). The coefficient of variation makes it possible to evaluate if the image noise becomes more consistent when the AEC systems are activated compared to non-activated.

$$c_v = \frac{\sigma}{\mu} \cdot 100\% \qquad \text{(Eq. 8)}$$

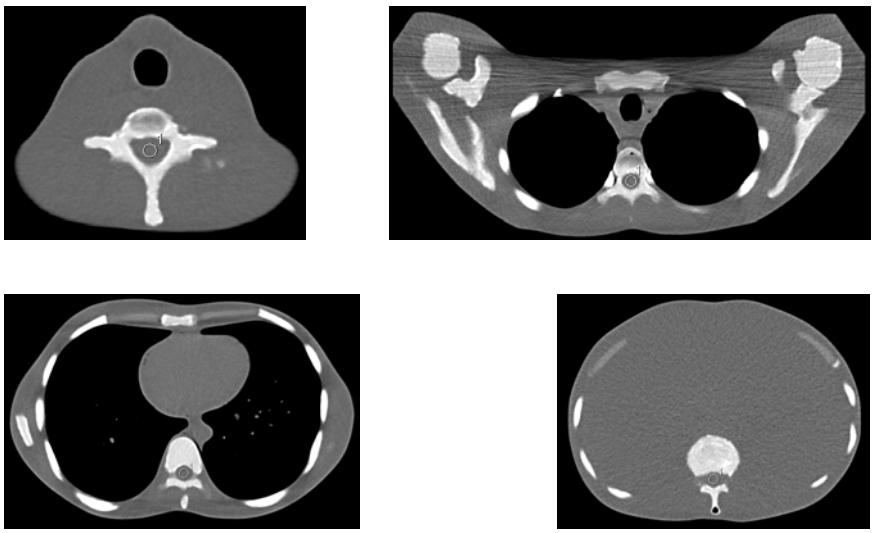

Figure 17. Examples of ROI position in slice 10, 25, 50 and 75.

For AEC systems with possibility to separate the element of rotational modulation from longitudinal modulation (Philips, GE and Toshiba), image noise were evaluated in rather uniform slices of the thorax phantom. SD was measured in 1 cm^2 large ROIs, placed in the center and periphery (north, east, south and west) of each image slice (Fig. 18). The intention was to study the effect of rotational AEC techniques separately; if the noise becomes more uniform across the image.

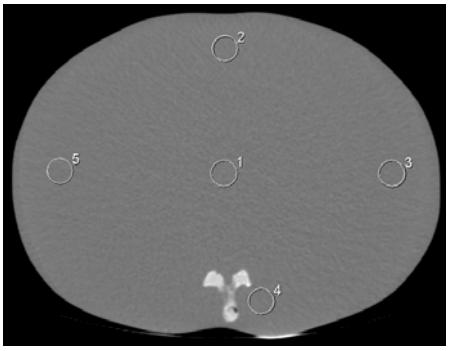

Figure 18. Examples of ROI position in a rather uniform slice.

3.5.2 Head phantom

For the anthropomorphic head phantom it was not possible to evaluate the image quality. The phantom contains a lot of bones and no heterogeneous regions. In the material that resembles the density of human tissue it was a lot of air bubbles that annihilate the possibility to insert ROIs in uniform areas.

3.5.3 Uncertainties

As a measure of the image noise was SD used. This process assumes that the pixel values are normally distributed. By study histograms for some of the inserted ROIs it was possible to establish that the pixel values are approximately normally distributed.

Since the ROIs were inserted manually in the images, it was interesting to evaluate how this affects the result. Some of the results were reproduced to estimate the uncertainty in ROI position.

The thorax phantom is anthropomorphic and consequently it contains no completely homogenous regions. In different slices this was investigated by moving ROIs in a small area around the primarily location of the ROI and receive a measure of the variation in SD value.

4. Results

4.1 Siemens

Unless otherwise stated, all of the presented results were acquired with scanning parameters from table 6 and 7. Siemens AEC system, CARE Dose 4D, is based upon the user selected quality reference mAs. For the thorax examinations a quality reference mAs value of 100 was used, which is standard for an adult routine thorax protocol. The thorax phantom was scanned with the head first.

There is a difference in the beam filtration for head modes between Somatom Sensation 16 and Somatom Sensation 64. This resulted for Somatom Sensation 16 that a quality reference mAs value of 320 was used and for Somatom Sensation 64 a quality reference mAs value of 380 was used. These values are standard for respective routine head examination. The head phantom was scanned with feet first. For adult head protocols is the tube current only modified to the variation along the patients scanning direction (longitudinal modulation) and consequently no angular modulation is performed.

CARE Dose 4D offer 9 different modulation strength settings that can be selected in the "Examination Configuration" under the section "Scanner options". Each setting was investigated for the thorax and head phantom. The setting weak/strong means that we will have a weak decrease in tube current for slim regions and a strong increase in tube current for obese regions. In the corresponding way we will have a strong decrease in tube current for slim regions and a weak increase in tube current for obese regions for the setting strong/weak. The setting average/average is the case in middle of the extreme cases.

4.1.1 Determination of dose reduction and dynamic of the AEC system for the thorax phantom

Figure 19 and figure 20 show how the mean effective mAs value per slice change along the length of the thorax phantom for different modulation strength settings.

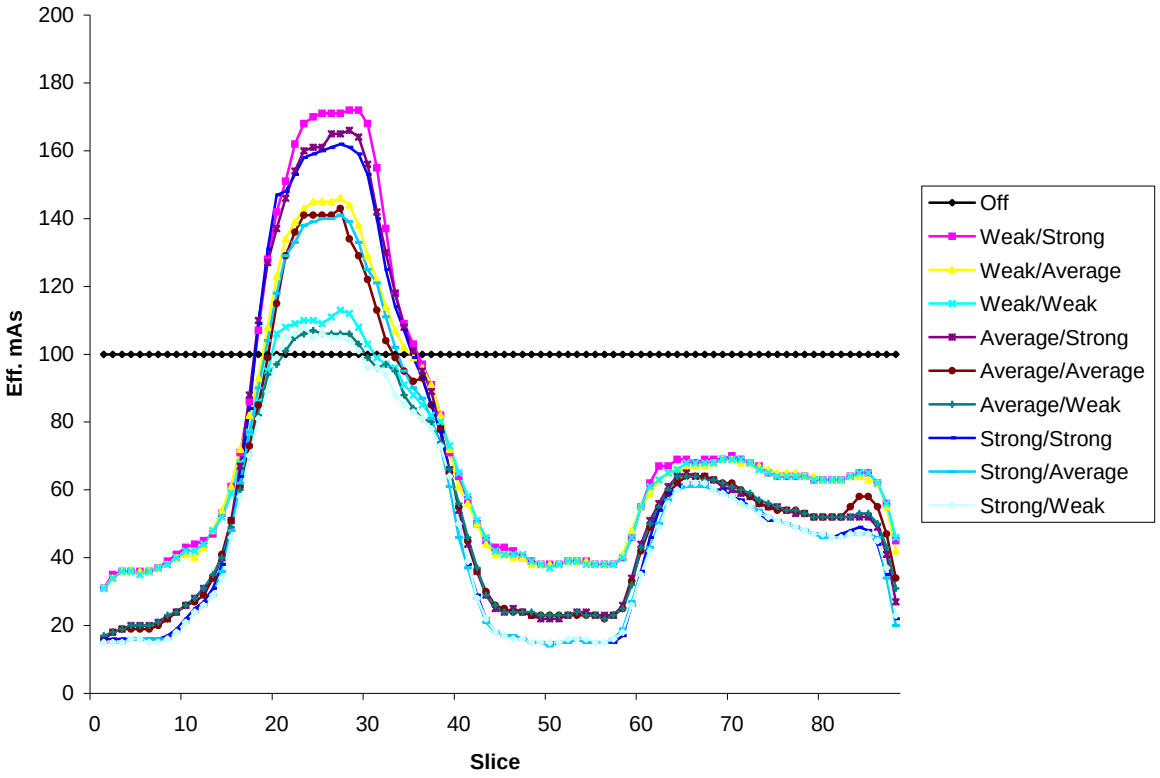

Figure 19. Mean effective mAs along the thorax phantom on Siemens SOMATOM Sensation 16.

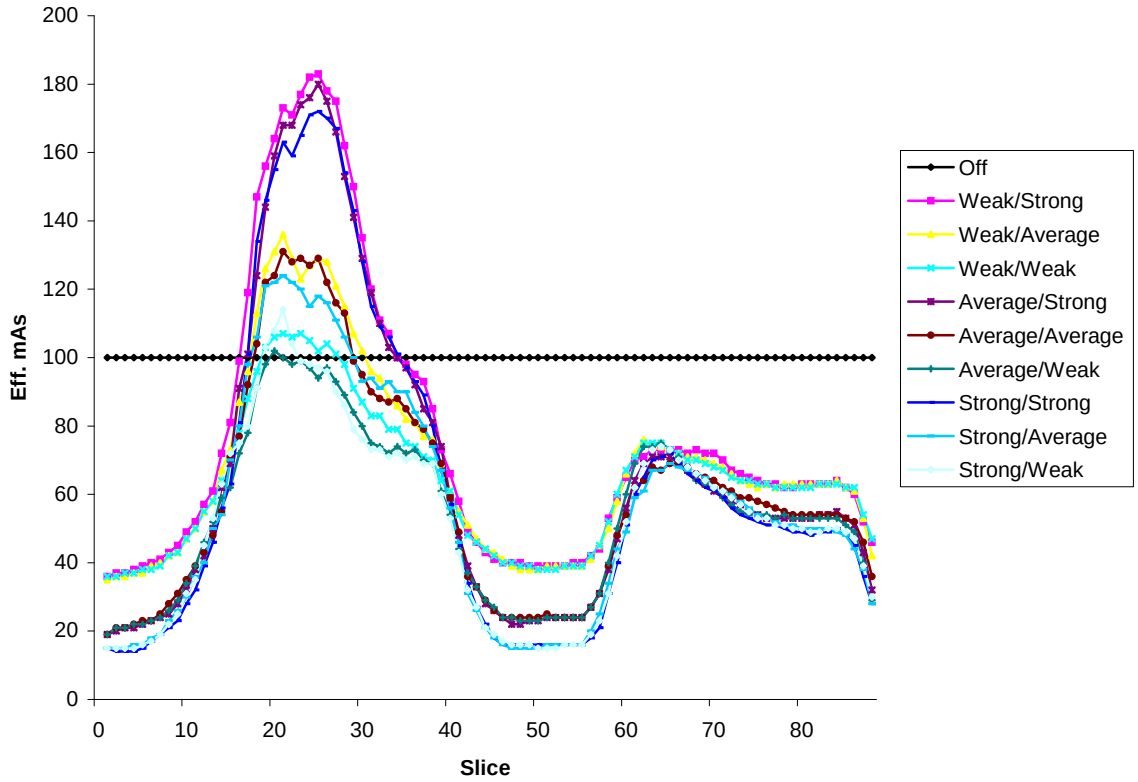

Figure 20. Mean effective mAs along the thorax phantom on Siemens SOMATOM Sensation 64.

Table 9 shows percentage dose reduction (DR) for different modulation strength settings achieved with SOMATOM Sensation 16 and 64 for a quality reference mAs of 100.

Table 9. Estimated dose reduction for thorax phantom on Siemens SOMATOM Sensation 16 and Siemens SOMATOM Sensation 64 for a quality reference mAs of 100.

	Siemens SOMATOM Sensation 16				Siemens SOMATOM Sensation 64			
Setting	Mean eff. mAs	Mean $CTDI_{vol}$ [mGy]	DLP [mGy*cm]	DR [%]	Mean eff. mAs	Mean $CTDI_{vol}$ [mGy]	DLP [mGy*cm]	DR [%]
Off	100	7.80	366	-	100	7.66	358	-
Weak/Strong	72	5.66	265	27.6	73	5.59	261	27.1
Weak/Average	68	5.30	248	32.2	64	4.94	230	35.8
Weak/Weak	63	4.91	230	37.2	61	4.71	220	38.5
Average/Strong	60	4.68	219	40.2	63	4.83	225	37.2
Average/Average	56	4.37	205	44.0	57	4.37	204	43.0
Average/Weak	51	4.02	188	48.6	53	4.06	189	47.2
Strong/Strong	57	4.49	209	42.9	59	4.56	213	40.5
Strong/Average	51	4.02	188	48.6	54	4.14	193	46.1
Strong/Weak	47	3.71	173	52.7	48	3.72	173	51.7

Figure 21 shows how the mean effective mAs value per slice change along the thorax phantom for the same settings as in figure 20**,** but in this examination was 80 kV used instead of 120 kV. Table 10 shows percentage dose reduction for different modulation strength settings.

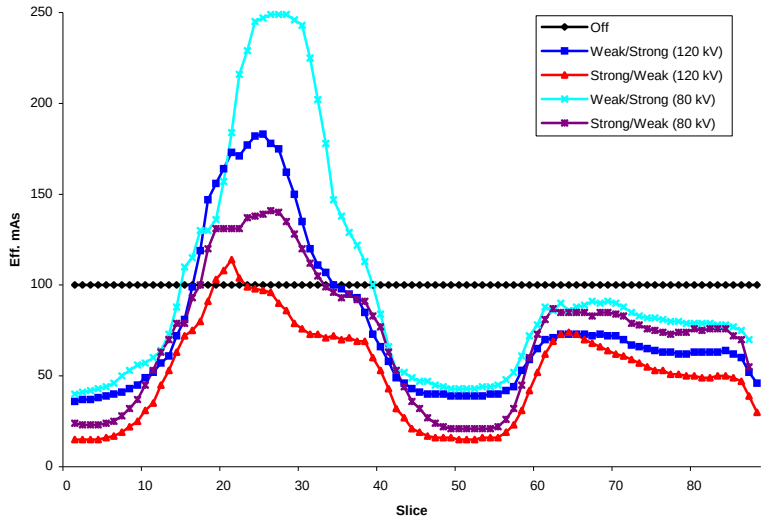

Figure 21. Mean effective mAs along the thorax phantom on Siemens SOMATOM Sensation 64 for 80 kV.

Table 10. Estimated dose reduction for thorax phantom on Siemens SOMATOM Sensation 64 for quality reference mAs of 100 and tube voltage of 80 kV.

Setting	Mean eff. mAs	Mean $CTDI_{vol}$ [mGy]	DLP [mGy*cm]	Dose reduction [%]
Off	100	2.03	95	-
Weak/Strong	95	1.93	90	5.3
Average/Average	80	1.62	76	20.0
Strong/Weak	67	1.37	64	32.6

4.1.2 Determination of dose reduction and dynamic of the AEC system for the head phantom

Figure 22 shows how the mean effective mAs value per slice change along the length of the head phantom for different modulation strength settings on SOMATOM Sensation 16 and 64.

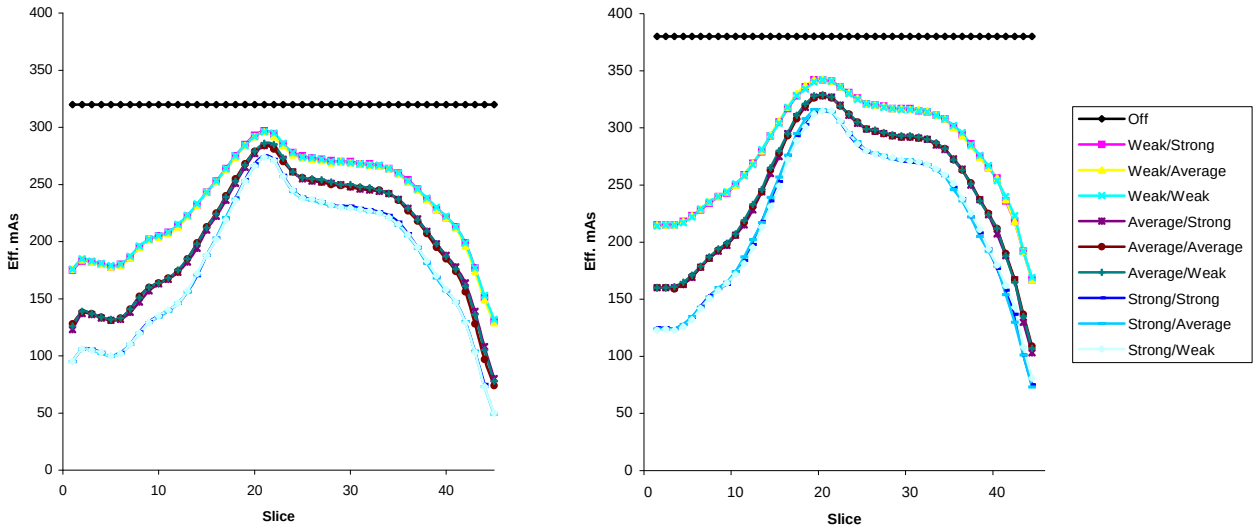

Figure 22. Mean effective mAs along the head phantom on Siemens SOMATOM Sensation 16 (left diagram) and Siemens SOMATOM Sensation 64 (right diagram).

Table 11 shows percentage dose reduction for different modulation strength settings achieved with SOMATOM Sensation 16 and 64.

Table 11. Estimated dose reduction for head phantom on Siemens SOMATOM Sensation 16 for quality reference mAs of 320 and on Siemens SOMATOM Sensation 64 for quality reference mAs of 380.

	Siemens SOMATOM Sensation 16				Siemens SOMATOM Sensation 64			
Setting	**Mean eff. mAs**	**Mean $CTDI_{vol}$ [mGy]**	**DLP [mGy*cm]**	**DR [%]**	**Mean eff. mAs**	**Mean $CTDI_{vol}$ [mGy]**	**DLP [mGy*cm]**	**DR [%]**
Off	320	67.52	1702	-	380	59.58	1484	0.0
Weak/Strong	227	47.9	1207	29.1	269	42.18	1044	29.6
Weak/Average	226	47.69	1197	29.7	269	42.18	1050	29.2
Weak/Weak	226	47.69	1206	29.1	269	42.18	1046	29.5
Average/Strong	192	40.51	1021	40.0	231	36.22	893	39.8
Average/Average	192	40.51	1023	39.9	231	36.22	898	39.5
Average/Weak	193	40.72	1030	39.5	232	36.38	902	39.2
Strong/Strong	169	35.66	891	47.6	203	31.83	789	46.8
Strong/Average	169	35.66	899	47.2	204	31.99	796	46.4
Strong/Weak	169	35.66	895	47.4	203	31.83	793	46.6

4.1.3 Evaluation of image quality for the thorax phantom

Table 12 shows mean SD values from five ROIs placed at centre and peripheral positions in three slices represented shoulder-, thorax and abdomen region on SOMATOM Sensation 16 and 64. Relative SD shows the ratio of the image noise for different settings in CARE Dose 4D activated compared to non-activated.

Table 12. Measured mean SD for 5 ROIs in different slices off the thorax phantom on Siemens SOMATOM Sensation 16 and Siemens SOMATOM Sensation 64.

Siemens SOMATOM Sensation 16					Siemens SOMATOM Sensation 64				
Slice	**Setting**	**Eff. mAs**	**Mean SD**	**Relative SD**	**Slice**	**Setting**	**Eff. mAs**	**Mean SD**	**Relative SD**
27	Off	100	8.40	1.00	27	Off	100	11.62	1.00
	Weak/Strong	171	6.84	0.81		Weak/Strong	175	8.14	0.70
	Average/Average	143	7.36	0.88		Average/Average	116	9.62	0.83
	Strong/Weak	105	8.34	0.99		Strong/Weak	90	11.12	0.96
50	Off	100	4.90	1.00	50	Off	100	6.16	1.00
	Weak/Strong	38	7.00	1.43		Weak/Strong	39	8.84	1.44
	Average/Average	23	9.08	1.85		Average/Average	24	11.16	1.81
	Strong/Weak	15	11.18	2.28		Strong/Weak	15	14.84	2.41
65	Off	100	7.72	1.00	65	Off	100	10.38	1.00
	Weak/Strong	69	9.32	1.21		Weak/Strong	73	11.72	1.13
	Average/Average	64	9.62	1.25		Average/Average	69	11.76	1.13
	Strong/Weak	62	10.08	1.31		Strong/Weak	73	11.68	1.13

Figure 23 shows measured SD in the spine throughout the thorax phantom on SOMATOM Sensation 16 and 64. The measurements were performed with 0.5 cm^2 large ROIs. Table 13 shows estimated mean SD100 and estimated coefficient of variations for respective CT scanner.

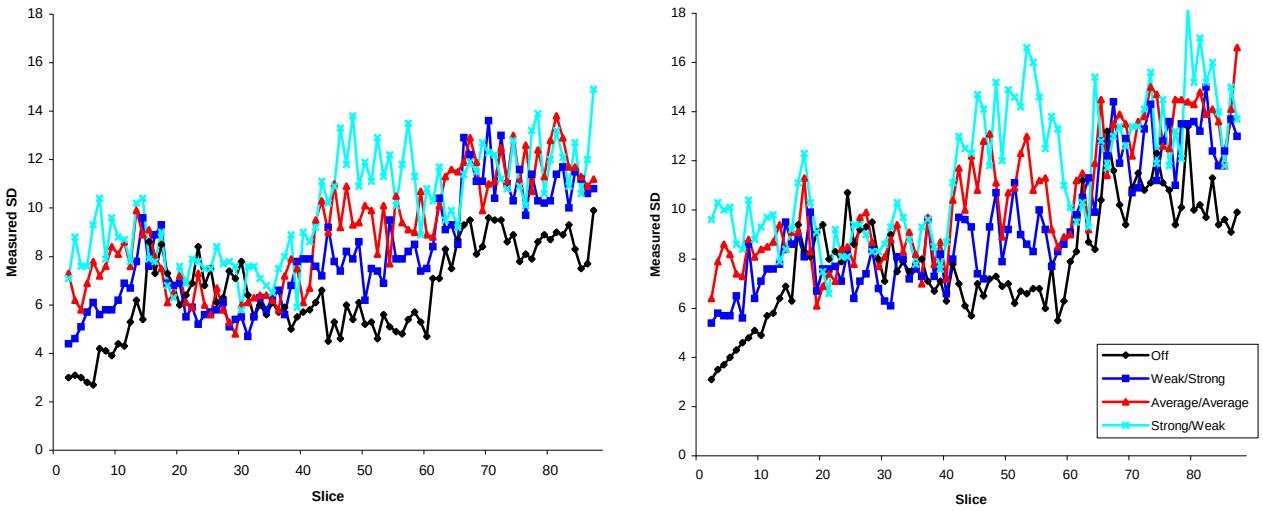

Figure 23. Measured SD in the spinal throughout the thorax phantom on Siemens SOMATOM Sensation 16 (left diagram) and Siemens SOMATOM Sensation 64 (right diagram).

Table 13. Estimated coefficient of variation for different modulation strength settings on Siemens SOMATOM Sensation 16 and Siemens SOMATOM Sensation 64.

	Siemens SOMATOM Sensation 16			Siemens SOMATOM Sensation 64		
Setting	**Mean SD**	**SD**	**Coefficient of variation [%]**	**Mean SD**	**SD**	**Coefficient of variation [%]**
Off	6.54	1.82	27.8	8.05	2.22	27.6
Weak/Strong	8.08	2.26	28.0	9.33	2.49	26.7
Average/Average	8.98	2.31	25.8	10.05	2.55	24.3
Strong/Weak	9.88	2.19	22.1	11.49	2.70	23.5

4.2 Philips

Unless otherwise stated, Philips DoseRight system was tested with scanning parameters from table 6 and 7. DoseRight consist of three elements and each element was investigated. Until today have Philips no currently available three-dimensional AEC system. It was possible to examined ACS by oneself and together with D-DOM or Z-DOM.

For a routine thorax protocol is 200 mAs/slice standard and ACS using this value as a starting point when it propose specific mAs value. For the thorax examinations were 200 mAs/slice and 100 mAs/slice selected and scanning type was set to chest. The thorax phantom was scanned with the feet first. Observe that mAs/slice is actually calculated as mAs/pitch.

It is not possible to use DoseRight for head mode. To elude this an own protocol was generated and scanning type was set to body. The drawback with this is that no head reconstruction filter could be selected and instead was a standard kernel for abdomen selected (standard B). For the head examinations were the mAs/slice selected to 350, which is standard for a routine head protocol. The head phantom was scanned with the feet first.

4.2.1 Determination of dose reduction and dynamic of the AEC system for the thorax phantom

Figure 24 and figure 25 show how the mean mAs value per slice change along the length of the thorax phantom on Brilliance CT 16 and 64 for 200 mAs/slice respective 100 mAs/slice.

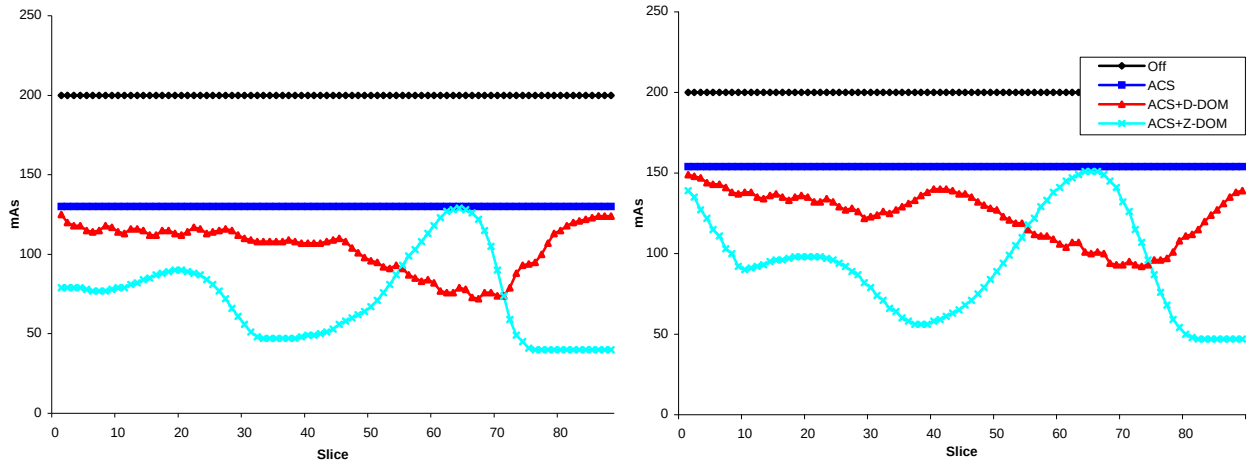

Figure 24. Mean mAs along the thorax phantom for planned mAs/slice of 200 on Philips Brilliance CT 16 (left diagram) and Philips Brilliance CT 64 (right diagram).

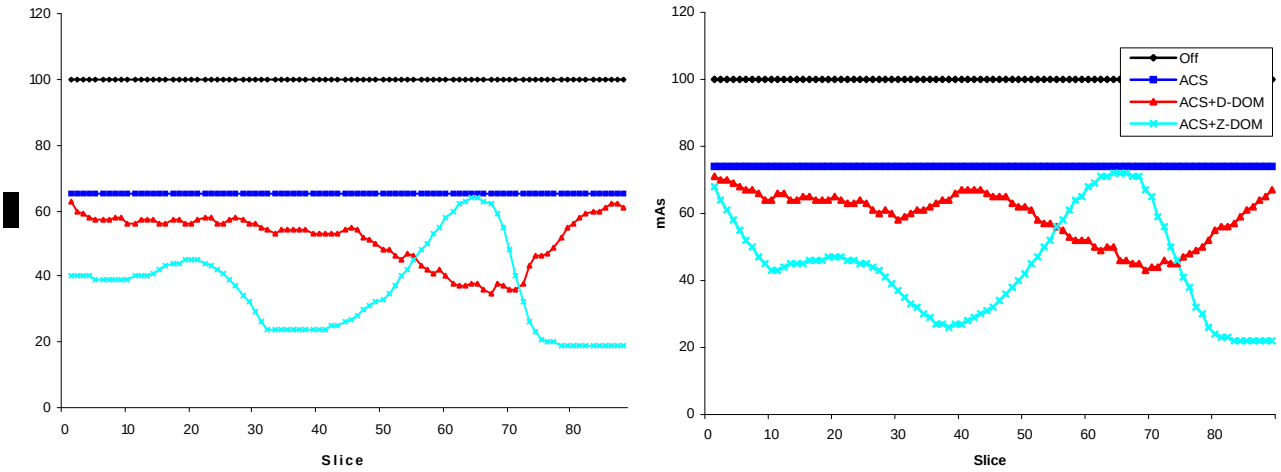

Figure 25. Mean mAs along the thorax phantom for planned mAs/slice of 100 on Philips Brilliance CT 16 (left diagram) and Philips Brilliance CT 64 (right diagram).

Table 14 and table 15 show percentage dose reduction for different elements in DoseRight achieved with Brilliance CT 16 and 64 for planned mAs/slice of 200 respective 100.

Table 14. Estimated dose reduction for thorax phantom on Philips Brilliance CT 16 and Philips Brilliance CT 64 for planned mAs/slice of 200.

	Philips Brilliance CT 16				Philips Brilliance CT 64			
Setting	Mean mAs	Plan $CTDI_{vol}$ [mGy]	DLP [mGy*cm]	DR [%]	Mean mAs	Plan $CTDI_{vol}$ [mGy]	DLP [mGy*cm]	DR [%]
Off	200	15.5	706.9	-	200	11.8	605.1	-
ACS	130	10.1	460.1	34.9	154	9.1	466.0	23.0
ACS+D-DOM	104	10.1	373.2	47.2	123	9.1	393.4	35.0
ACS+Z-DOM	72	10.1	256.1	63.8	93	9.1	296.7	51.0

Table 15. Estimated dose reduction for thorax phantom on Philips Brilliance CT 16 and Philips Brilliance CT 64 for planned mAs/slice of 100.

	Philips Brilliance CT 16				Philips Brilliance CT 64			
Setting	Mean mAs	Plan $CTDI_{vol}$ [mGy]	DLP [mGy*cm]	DR [%]	Mean mAs	Plan $CTDI_{vol}$ [mGy]	DLP [mGy*cm]	DR [%]
Off	100	7.8	354.6	-	100	5.9	302.6	-
ACS	65	5.0	228.7	35.5	74	4.4	223.9	26.0
ACS+D-DOM	52	5.0	183.9	48.1	59	4.4	190.8	36.9
ACS+Z-DOM	36	5.0	127.6	64.0	44	4.4	142.5	52.9

Figure 26 shows how the mean mAs value per slice change along the thorax phantom for the same settings as in figure 24 (left diagram), but in this examination was a lateral surview used for the ACS instead of a planar surview. Table 16 shows percentage dose reduction for different elements in DoseRight.

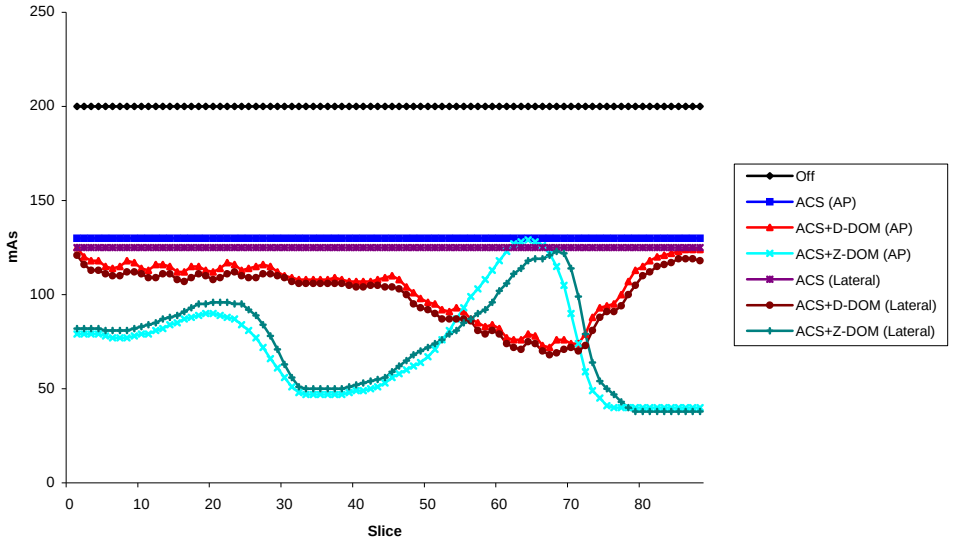

Figure 26. Mean mAs along the thorax phantom on Philips Brilliance CT 16 for planned mAs/slice of 200 and lateral surview.

Table 16. Estimated dose reduction for thorax phantom on Philips Brilliance CT 16 for planned mAs/slice of 200 and lateral surview.

Setting	Mean mAs	Plan $CTDI_{vol}$ [mGy]	DLP [mGy*cm]	Dose reduction [%]
Off	200	15.5	707.1	-
ACS	125	9.7	443.2	37.3
ACS+D-DOM	100	9.7	356.8	49.5
ACS+Z-DOM	75	9.7	265.1	62.5

Figure 27 shows how the mean mAs value per slice change along the thorax phantom for the same settings as in figure 24**,** but in this examination was 90 kV used instead of 120 kV. Table 17 shows percentage dose reduction for different elements in DoseRight.

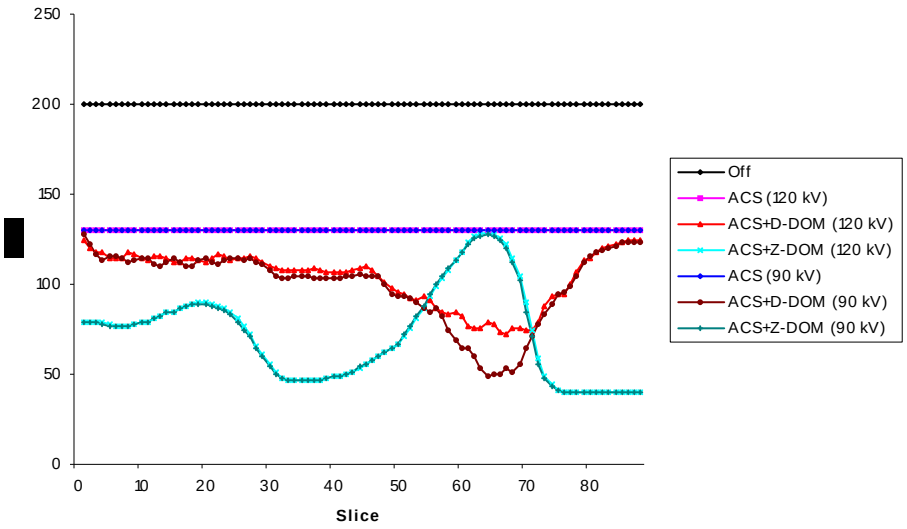

Figure 27. Mean mAs along the thorax phantom on Philips Brilliance CT 16 for planned mAs/slice of 200 and 90 kV.

Table 17. . Estimated dose reduction for thorax phantom on Philips Brilliance CT 16 for planned mAs/slice of 200 and 90 kV.

Setting	Mean mAs	Plan $CTDI_{vol}$ [mGy]	DLP [mGy*cm]	Dose reduction d D
Off	200	6.7	305.6	-
ACS	130	4.4	199.2	34.8
ACS+D-DOM	99	4.4	156.0	49.0
ACS+Z-DOM	72	4.4	111.6	63.5

4.2.2 Determination of dose reduction and dynamic of the AEC system for the head phantom

Figure 28 shows how the mean mAs value per slice change along the length of the head phantom for three different settings in DoseRight on Brilliance CT 16 respective 64.

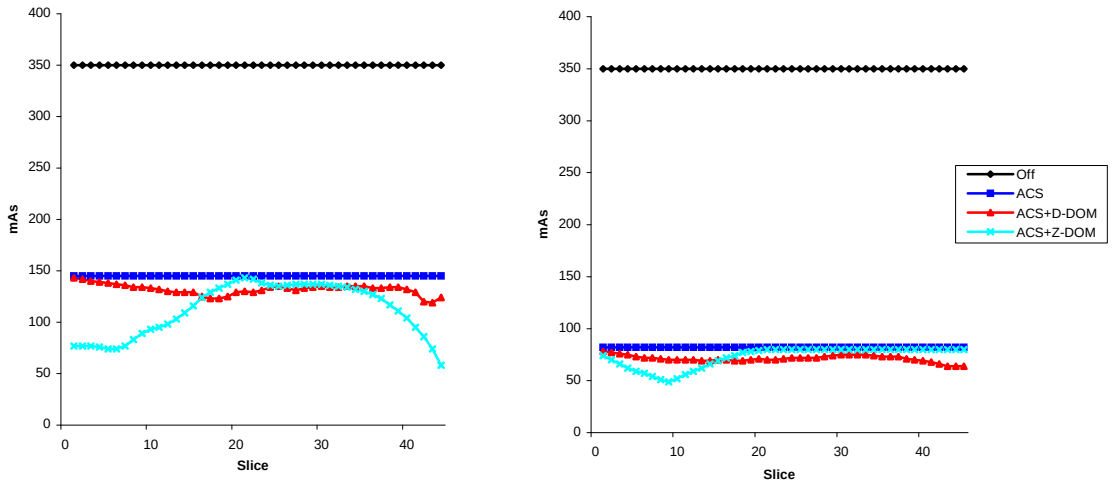

Figure 28. Mean mAs along the head phantom on Philips Brilliance CT 16 (left diagram) and Philips Brilliance CT 64 (right diagram) for planned mAs/slice of 350.

Table 18 shows percentage dose reduction for different elements in DoseRight achieved with Brilliance 16 and 64 for planned mAs/slice of 350.

Table 18. Estimated dose reduction for head phantom on Philips Brilliance CT 16 and Philips Brilliance CT 64 for planned mAs/slice of 350. Note that the planed $CTDI_{vol}$ and DLP is in real twice as high due to scanning mode was set to body and not to head.

	Philips Brilliance CT 16				Philips Brilliance CT 64			
Setting	Mean mAs	Plan $CTDI_{vol}$ [mGy]	DLP [mGy*cm]	DR [%]	Mean mAs	Plan $CTDI_{vol}$ [mGy]	DLP [mGy*cm]	DR [%]
Off	350	27.1	641.4	-	350	20.6	606.2	-
ACS	145	11.2	265.8	58.6	82	4.8	142.0	76.6
ACS+D-DOM	132	11.2	245.0	61.8	71	4.8	127.7	78.9
ACS+Z-DOM	112	11.2	199.7	68.9	73	4.8	132.5	78.1

4.2.3 Evaluation of image quality for the thorax phantom

Table 19 show mean SD values from five ROIs placed at centre and peripheral positions in three slices represented abdomen-, thorax- and shoulder region when planned mAs/slice was set to 200 on Brilliance CT 16 and 64. Relative SD shows the ratio of the image noise for different elements in DoseRight activated compared to DoseRight non-activated.

Table 19. Measured mean SD for 5 ROIs in different slices off the thorax phantom on Philips Brilliance CT 16 and Philips Brilliance CT 64.

Philips Brilliance CT 16					Philips Brilliance CT 64				
Slice	Setting	Mean mAs	Mean SD	Relative SD	Slice	Setting	Mean mAs	Mean SD	Relative SD
20	Off	200	5.88	1.00	20	Off	200	5.88	1.00
	ACS	130	6.80	1.16		ACS	154	6.32	1.07
	ACS+D-DOM	112	7.64	1.30		ACS+D-DOM	135	7.06	1.20
	ACS+Z-DOM	90	8.36	1.42		ACS+Z-DOM	98	7.78	1.32
38	Off	200	4.08	1.00	38	Off	200	5.02	1.00
	ACS	130	4.70	1.15		ACS	154	5.54	1.10
	ACS+D-DOM	108	5.02	1.23		ACS+D-DOM	138	5.24	1.04
	ACS+Z-DOM	47	6.80	1.67		ACS+Z-DOM	56	7.32	1.46
66	Off	200	7.12	1.00	66	Off	200	6.20	1.00
	ACS	130	7.52	1.06		ACS	154	7.74	1.25
	ACS+D-DOM	73	9.64	1.35		ACS+D-DOM	101	8.18	1.32
	ACS+Z-DOM	126	7.38	1.04		ACS+Z-DOM	151	7.14	1.15

Figure 29 shows measured SD in the spine throughout the thorax phantom when planned mAs/slice was set to 200 on Brilliance CT 16 and 64. The measurements were performed with 0.5 cm^2 large ROIs. Table 20 shows estimated mean SD and estimated coefficient of variations for respective CT scanner.

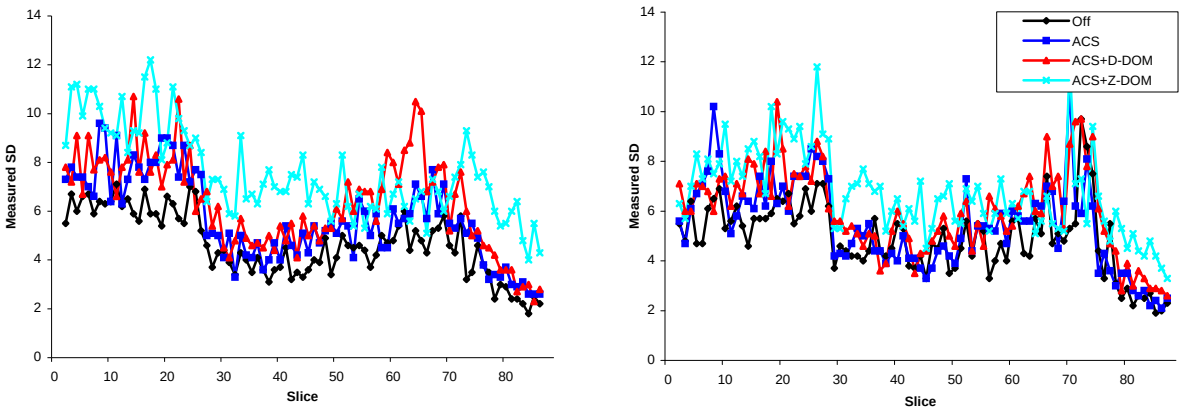

Figure 29. Measured SD in the spinal throughout the thorax phantom on Philips Brilliance CT 16 (left diagram) and Philips Brilliance CT 64 (right diagram).

Table 20. Estimated coefficient of variation for different modulation settings on Philips Brilliance CT 16 and Philips Brilliance CT 64.

	Philips Brilliance CT 16			Philips Brilliance CT 64		
Setting	**Mean SD**	**SD**	**Coefficient of variation [%]**	**Mean SD**	**SD**	**Coefficient of variation [%]**
Off	4.64	1.32	28.4	4.99	1.45	29.2
ACS	5.70	1.77	31.1	5.51	1.78	32.2
ACS+D-DOM	6.34	1.91	30.1	6.05	1.74	28.7
ACS+Z-DOM	7.57	1.83	24.1	6.83	1.69	24.7

Table 21 is intending to show the effect of D-DOM (angular modulation) when planned mAs/slice was set to 200. Relative SD is estimated as SD with D-DOM on to off. Table 22 shows tube load values for respective slice and CT scanner.

Table 21. Measured SD in ROIs for different positions on Philips Brilliance CT 16 and Philips Brilliance CT 64.

		Philips Brilliance CT 16			Philips Brilliance CT 64		
Slice	**Position**	**SD (ACS)**	**SD (ACS+D-DOM)**	**Relative SD**	**SD (ACS)**	**SD (ACS+D-DOM)**	**Relative SD**
5	Centre	8.5	8.9	1.05	7.6	8.1	1.07
	North	5.5	5.8	1.05	5.1	5.3	1.04
	East	6.8	6.8	1.00	5.6	5.4	0.96
	South	6.7	6.8	1.01	5.9	5.4	0.92
	West	6.3	6	0.95	5.1	5.5	1.08
15	Centre	8.7	9.2	1.06	7.6	7.9	1.04
	North	6.2	7.5	1.21	5.8	6.1	1.05
	East	6.7	6.7	1.00	5.6	5.8	1.04
	South	5.8	6.6	1.14	5.9	6.9	1.17
	West	6.6	6.6	1.00	5.5	6.7	1.22

Table 22. Mean tube load values for slice 5 and 15 on Philips Brilliance CT 16 and Philips Brilliance CT 64.

	Philips Brilliance CT 16		Philips Brilliance CT 64	
Slice	**Mean mAs (ACS)**	**Mean mAs (ACS+D-DOM)**	**Mean mAs (ACS)**	**Mean mAs (ACS+D-DOM)**
5	130	115	154	143
15	130	112	154	137

4.3 GE

Unless otherwise stated, all of the presented results were acquired with scanning parameters from table 6 and 7. The measurements were unless otherwise stated performed in plus mode, which is used by routine. GEs AEC system, AutomA 3D is based upon the user selected noise index and minimum and maximum limits of the tube current. The system consists of two elements; AutomA witch provides longitudinal AEC and SmartmA witch provides rotation AEC. It was possible to investigate AutomA individual and together with SmartmA.

GE LightSpeed VCT has better data acquisition then GE LightSpeed[16] and consequently were higher noise index values chosen. For a routine thorax examination in Halmstad (LightSpeed VCT) was a noise index of 38 typical and minimum and maximum mA limits set to 100 respective 750. For corresponding examination in Simrishamn (LightSpeed[16]) was a noise index of 12 standard and minimum and maximum mA limits set to 10 and 440. The thorax phantom was scanned with the head first.

The head phantom was scanned with head first and standard settings for a routine head examination. For LightSpeed[16] were noise index set to 2.8 and minimum and maximum mA limits set to 100 respective 440. For LightSpeed VCT was instead noise index set to 6 and minimum and maximum mA limits set to 50 respective 335.

4.3.1 Determination of dose reduction and dynamic of the AEC system for the thorax phantom

Figure 30-32 show how the mean mAs value per slice change along the length of the thorax phantom for a noise index of 12 and different tube current limits for LightSpeed[16]. The figures show the important meaning of choosing appropriate tube current boundaries. When AutomA 3D was turned off, a fixed tube current of 200 mA was used. To evaluate the effect of plus mode, one scan was performed on LightSpeed[16] in full mode with standard settings (NI=12, min=10 mA, max=440 mA). Figure 33 shows the result.

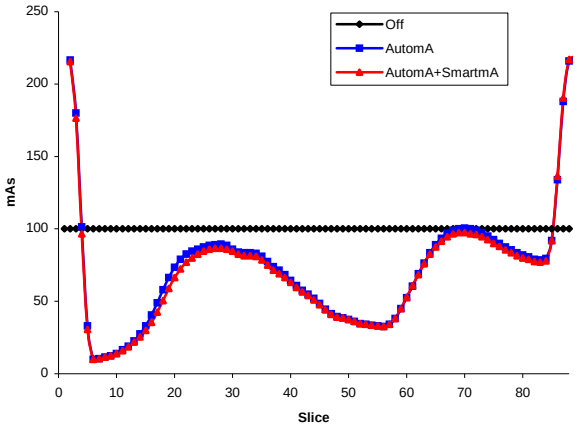

Figure 30. Mean mAs along the thorax phantom on GE LightSpeed[16] for a noise index of 12 and minimum and maximum limits set to 10 mA respective 440 mA (standard settings).

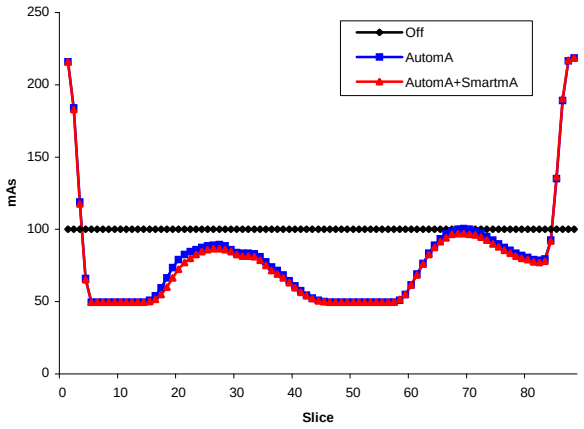

Figure 31. Mean mAs along the thorax phantom on GE LightSpeed[16] for a noise index of 12 and minimum and maximum limits set to 100 mA respective 440 mA.

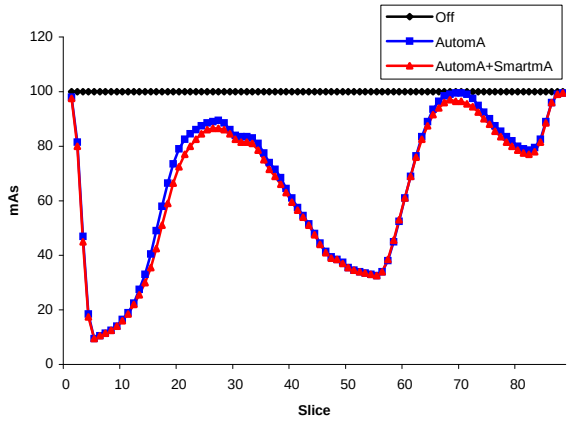

Figure 32. Mean mAs along the thorax phantom on GE LightSpeed[16] for a noise index of 12 and minimum and maximum limits set to 10 mA respective 200 mA.

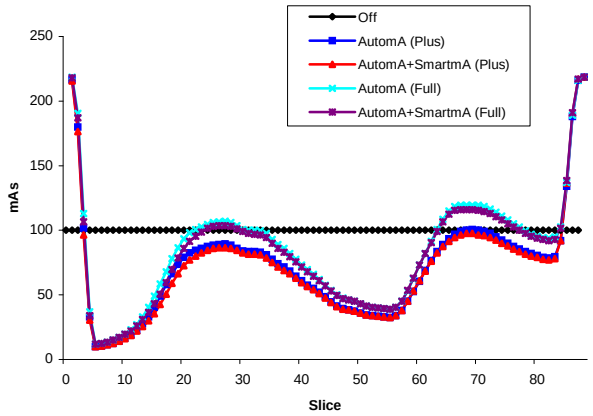

Figure 33. Mean mAs along the thorax phantom on GE LightSpeed[16] for same settings in figure 30 but scanned performed in full mode.

Figure 34 and figure 35 show how the mean mAs value per slice change along the thorax phantom for a noise index of 38 and different tube current limits for LightSpeed VCT. When AutomA 3D was turned off, a fixed tube current of 105 mA was used.

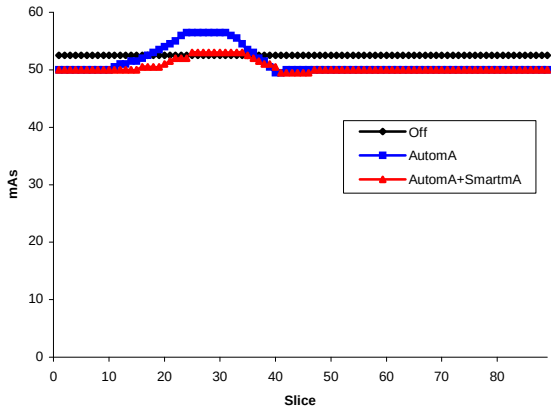

Figure 34. Mean mAs along the thorax phantom on GE LightSpeed VCT for a noise index of 38 and minimum and maximum limits set to 100 mA respective 750 mA.

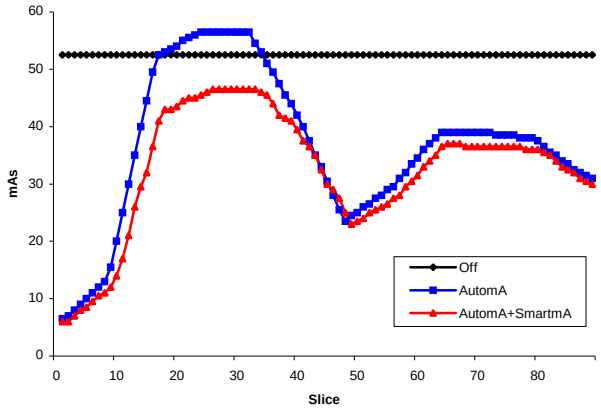

Figure 35. Mean mAs along the thorax phantom on GE LightSpeed VCT for same settings as in figure 34 but minimum tube current was changed to 10 mA.

Table 23-25 show percentage dose reduction for different AEC settings in AutomA 3D, achieved with LightSpeed[16] and LightSpeed VCT.

Table 23. Estimated dose reduction for thorax phantom on GE LightSpeed[16] for NI=12, min=10 mA and max=440 mA for plus and full mode.

	Plus mode				Full mode			
Setting	Mean mAs	Mean $CTDI_{vol}$ [mGy]	DLP [mGy*cm]	DR [%]	Mean mAs	Mean $CTDI_{vol}$ [mGy]	DLP [mGy*cm]	DR [%]
Off	100	11.2	508.3	-	100	11.2	506.9	-
Auto mA	73	9.6	437.9	13.9	85	11.0	498.4	1.7
Auto mA + Smart mA	71	9.4	429.3	15.5	83	10.7	488.3	3.7

Table 24. Estimated dose reduction for thorax phantom on GE LightSpeed[16] for different tube current limits.

	NI=12, min=100 mA and max=440 mA				NI=12, min=10 mA and max=200 mA			
Setting	Mean mAs	Mean $CTDI_{vol}$ [mGy]	DLP [mGy*cm]	DR [%]	Mean mAs	Mean $CTDI_{vol}$ [mGy]	DLP [mGy*cm]	DR [%]
Off	100	11.2	508.3	-	100	11.2	508.3	-
Auto mA	79	10.4	474.3	6.7	64	7.5	340.2	33.1
Auto mA + Smart mA	78	10.2	466.5	8.2	62	7.3	331.9	34.7

Table 25. Estimated dose reduction for thorax phantom on GE LightSpeed VCT for different tube current limits.

	NI=38, min=100 mA and max=750 mA				NI=38, min=10 mA and max=750 mA			
Setting	Mean mAs	Mean $CTDI_{vol}$ [mGy]	DLP [mGy*cm]	DR [%]	Mean mAs	Mean $CTDI_{vol}$ [mGy]	DLP [mGy*cm]	DR [%]
Off	53	4.4	214.5	-	53	4.4	214.5	-
Auto mA	51	4.3	209.2	2.5	37	3.0	144.8	32.5
Auto mA + Smart mA	51	4.2	206.5	3.7	33	2.6	128.7	40.0

4.3.2 Determination of dose reduction and dynamic of the AEC system for the head phantom

Figure 36 shows how the mean mAs value per slice change along the length of the head phantom for a noise index of 2.8 and minimum and maximum mA of 100 respective 440 on LightSpeed[16]. When AutomA 3D was turned off, a fixed tube current of 310 mA was used.

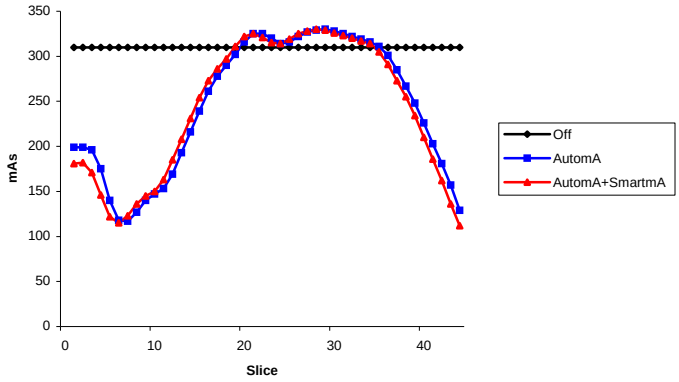

Figure 36. Mean mAs along the head phantom on GE LightSpeed[16].

Figure 37 shows how the mean mAs value per slice change along the length of the head phantom for a noise index of 6 and minimum and maximum mA limits of 50 respective 335 on LightSpeed VCT. When AutomA 3D was turned off, a fixed tube current of 315 mA was used (left diagram). The right diagram shows the result when the head phantom was positioned like a standard clinical situation. For this case when AutomA 3D was turned off, a fixed tube current of 335 mA was used.

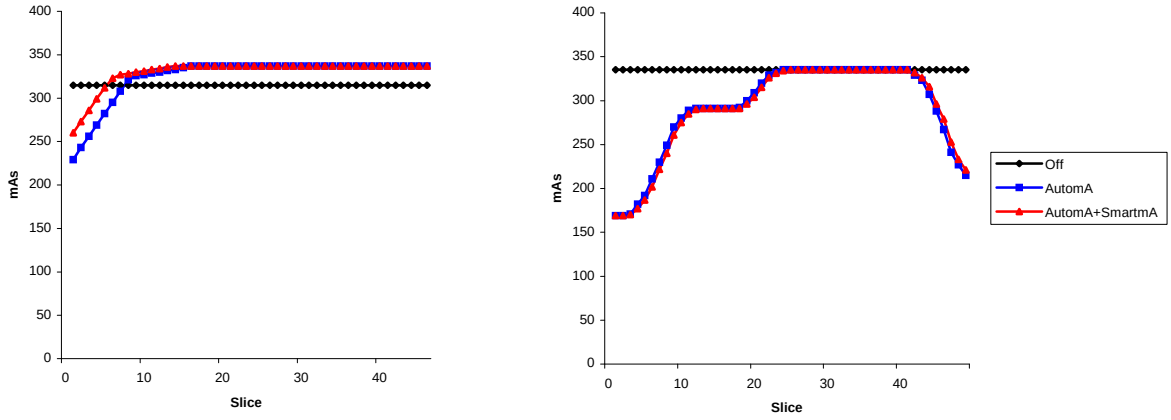

Figure 37. Mean mAs along the head phantom on GE LightSpeed VCT for a noise index of 6 and minimum and maximum limits of 50 mA respective 335 mA (left diagram). The right diagram shows the result when the head phantom was positioned like a standard clinical situation.

Table 26 and table 27 show percentage dose reduction for different AEC settings in AutomA 3D, achieved with LightSpeed[16] and LightSpeed VCT.

Tabell 26. Estimated dose reduction for head phantom on GE LightSpeed[16] for NI=2.8, min=100 mA and max=440 mA.

Setting	Mean mAs	Mean $CTDI_{vol}$ [mGy]	DLP [mGy*cm]	Dose reduction [%]
Off	310	75.4	1778.1	-
Auto mA	245	58.6	1380.9	22.3
Auto mA + Smart mA	243	57.7	1360.6	23.5

Table 27. Estimated dose reduction for head phantom on GE LightSpeed VCT for NI=6, min=50 mA and max=335 mA for general position and standard clinical position.

	General position				Clinical position			
Setting	Mean mAs	Mean $CTDI_{vol}$ [mGy]	DLP [mGy*cm]	DR [%]	Mean mAs	Mean $CTDI_{vol}$ [mGy]	DLP [mGy*cm]	DR [%]
Off	315	60.95	1651.6	-	335	63.7	1687.1	-
Auto mA	325	61.3	1660.4	-0.5	295	54.0	1429.9	15.2
Auto mA + Smart mA	330	62.2	1685.1	-2.0	294	54.0	1430.2	15.2

4.3.3 Evaluation of image quality for the thorax phantom

The evaluation of the image quality was performed on images acquired with LightSpeed[16] with a noise index of 12 and minimum and maximum limits of 10 mA respective 200 mA. For LightSpeed VCT was the images acquired with a noise index of 38 and minimum and maximum limits of 10 mA respective 750 mA.

Table 28 shows mean SD values from five ROIs placed at centre and peripheral positions in three slices represented shoulder-, thorax- and abdomen region on LightSpeed[16] and LightSpeed VCT. Relative SD shows the ratio of the image noise for different settings in AutomA 3D activated compared to non-activated.

Table 28. Measured mean SD for 5 ROIs in different slices off the thorax phantom on LightSpeed[16] and LightSpeed VCT.

GE LightSpeed[16]					GE LightSpeed VCT				
Slice	Setting	Mean mAs	Mean SD	Relative SD	Slice	Setting	Mean mAs	Mean SD	Relative SD
27	Off	100	10.36	1.00	28	Off	53	15.60	1.00
	AutomA	90	11.66	1.13		AutomA	57	15.66	1.00
	AutomA+SmartmA	87	11.48	1.11		AutomA+SmartmA	47	14.74	0.94
55	Off	100	5.26	1.00	49	Off	53	8.78	1.00
	AutomA	33	8.50	1.62		AutomA	25	11.36	1.29
	AutomA+SmartmA	33	7.92	1.51		AutomA+SmartmA	23	11.68	1.33
70	Off	100	9.28	1.00	70	Off	53	13.86	1.00
	AutomA	100	9.38	1.01		AutomA	39	16.78	1.21
	AutomA+SmartmA	97	9.46	1.02		AutomA+SmartmA	37	18.24	1.32

Figure 38 shows measured SD in the spine throughout the thorax phantom for LightSpeed[16] and LightSpeed VCT. The measurements were performed with 0.5 cm^2 large ROIs. Table 29 shows estimated mean SD and estimated coefficient of variations for respective CT scanner.

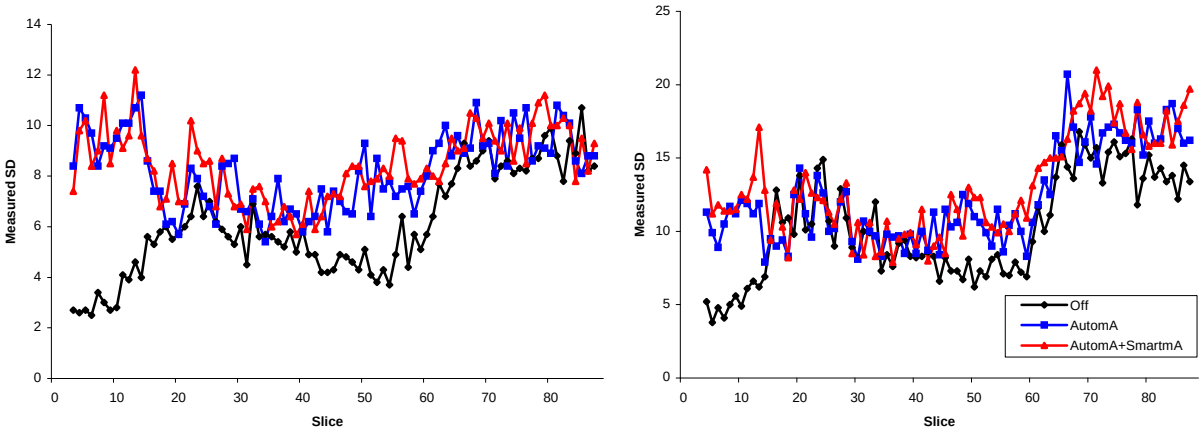

Figure 38. Measured SD in the spinal throughout the thorax phantom on GE LightSpeed[16] (left diagram) and GE LightSpeed VCT (right diagram).

Table 29. Estimated coefficient of variation for different modulation settings on GE LightSpeed[16] and GE LightSpeed VCT.

	GE LightSpeed[16]			GE LightSpeed VCT		
Setting	**Mean SD**	**SD**	**Coefficient of variation [%]**	**Mean SD**	**SD**	**Coefficient of variation [%]**
Off	6.14	2.02	32.9	8.73	3.22	36.9
AutomA	8.30	1.49	18.0	12.29	3.21	26.1
AutomA+SmartmA	8.55	1.41	16.5	13.07	3.44	26.3

Table 30 are intending to show the effect of SmartmA (angular modulation) on LightSpeed[16] and LightSpeed VCT. Relative SD is estimated as SD in images with SmartmA on compared with SmartmA off.

Table 30. Measured SD in ROIs for different positions in slice 70 (AutomA: 199 mA, AutomA+SmartmA: 193 mA) on GE LightSpeed[16] and in slice 75 (AutomA: 77 mA, AutomA+SmartmA: 73 mA) on GE LightSpeed VCT.

	GE LightSpeed[16]			GE LightSpeed VCT		
Position	**SD (AutomA)**	**SD (AutomA+SmartmA)**	**Relative SD**	**SD (AutomA)**	**SD (AutomA+SmartmA)**	**Relative SD**
Centre	11.1	10.2	0.92	22.8	21.8	0.96
North	8	8.3	1.04	13.6	14.1	1.04
East	10.9	10.6	0.97	16.9	17.3	1.02
South	8.1	7.9	0.98	13.7	13.4	0.98
West	10.3	9.3	0.90	18.5	17.8	0.96

4.4 Toshiba

Unless otherwise stated, all of the presented results were acquired with scanning parameters from table 6 and 7. Toshibas AEC system, SureExposure 3D, is based upon the user selected SD and minimum and maximum limits of the tube current. The system consists of longitudinal and rotational modulation and it was possible to investigate longitudinal modulation individual and together with rotational modulation. Unless otherwise stated, all examinations were performed with QDS and Boost 3D activated.

For the thorax examinations a SD of 10 and 15 was investigated, which is typical values for an adult routine thorax protocol. The range of tube current values were set as big as possible, minimum to 10 mA and maximum to 500 mA. The thorax phantom was scanned with the head first.

The head phantom was scanned with head first for typical values of a routine head examination. Two values of SD were investigated, 2 and 2.5, and the range of tube current values was set as big as possible, minimum to 10 mA and maximum to 500 mA.

4.4.1 Determination of dose reduction and dynamic of the AEC system for the thorax phantom

Figure 39 and 40 show how the mean mAs value per slice change along the length of the thorax phantom for a SD of 10 respective 15 and tube current limits of 10 mA and 500 mA for Aquilion 16 and Aquilion 64. When SureExposure 3D was turned off, a fixed tube current of 200 mA was used.

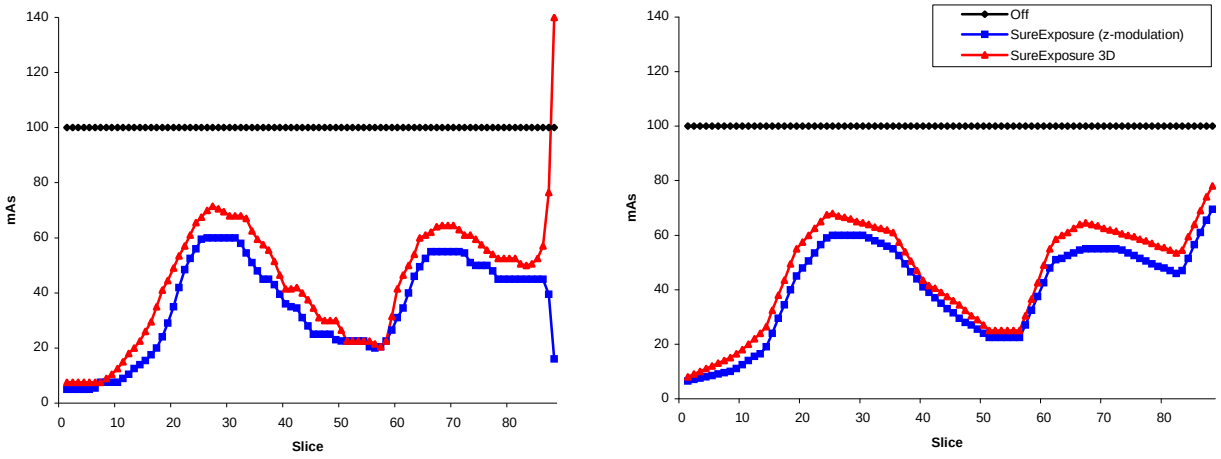

Figure 39. Mean mAs along the thorax phantom on Toshiba Aquilion 16 (left diagram) and Toshiba Aquilion 64 (right diagram) for SD of 10 and minimum and maximum limits of 10 mA respective 500 mA.

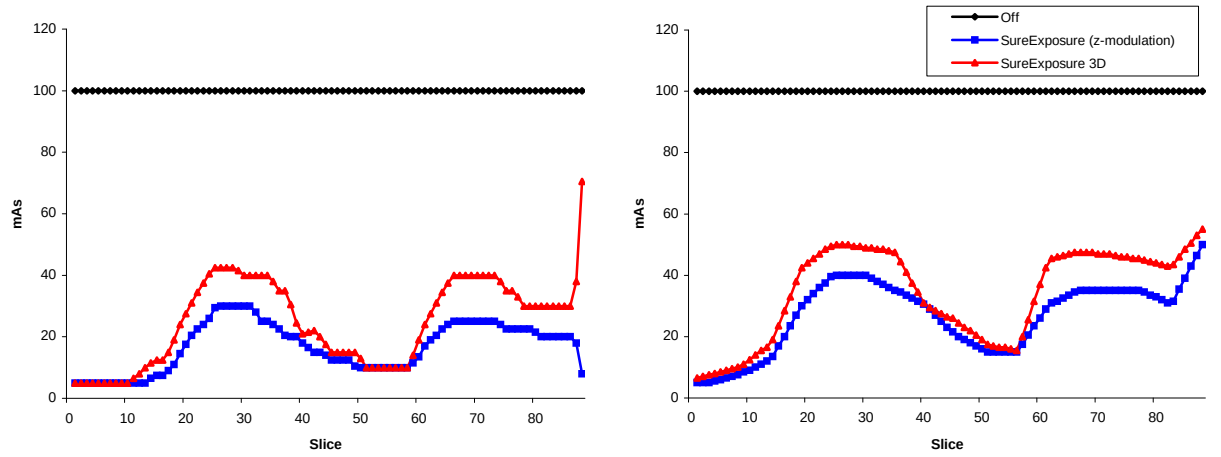

Figure 40. Mean mAs along the thorax phantom on Toshiba Aquilion 16 (left diagram) and Toshiba Aquilion 64 (right diagram) for SD of 15 and minimum and maximum limits of 10 mA respective 500 mA.

Table 31 and table 32 show percentage dose reduction for different AEC settings in SureExposure 3D, achieved with Aquilion 16 and 64.

Table 31. Estimated dose reduction for thorax phantom on Toshiba Aquilion 16 and Toshiba Aquilion 64 for SD=10, min=10 mA and max=500 mA.

	Toshiba Aquilion 16				Toshiba Aquilion 64			
Setting	Mean mAs	Max $CTDI_{vol}$ [mGy]	DLP [mGy*cm]	DR [%]	Mean mAs	Max $CTDI_{vol}$ [mGy]	DLP [mGy*cm]	DR [%]
Off	100	16.9	769.3	-	100	14.6	720.4	-
SureExposure (z-mod.)	35	10.1	263.2	65.8	40	10.2	272.2	62.2
SureExposure 3D	44	26.3	333.1	56.7	46	11.5	293.8	59.2

Table 32. Estimated dose reduction for thorax phantom on Toshiba Aquilion 16 and Toshiba Aquilion 64 for SD=15, min=10 mA and max=500 mA.

	Toshiba Aquilion 16				Toshiba Aquilion 64			
Setting	Mean mAs	Max $CTDI_{vol}$ [mGy]	DLP [mGy*cm]	DR [%]	Mean mAs	Max $CTDI_{vol}$ [mGy]	DLP [mGy*cm]	DR [%]
Off	100	16.9	769.3	-	100	14.6	720.4	-
SureExposure (z-mod.)	17	5.1	126.2	83.6	27	7.3	183.2	74.6
SureExposure 3D	25	13.3	185.4	75.9	35	8.1	218.1	69.7

Figure 41 shows the effect of SureExposure 3D when the QDS was non-activated and table 33 shows the percentage dose reduction for different AEC settings in SureExposure 3D.

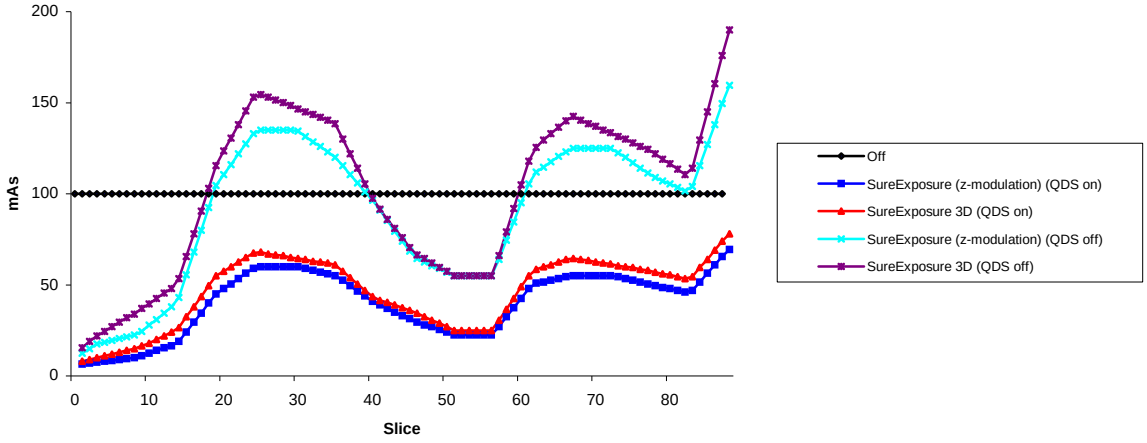

Figure 41. Mean mAs along the thorax phantom on Toshiba Aquilion 64 for SD of 10 and minimum and maximum limits set to 10 mA respective 500 mA when QDS was turned on and off.

Table 33. Estimated dose reduction for thorax phantom on Toshiba Aquilion 64 for SD=10, min=10 mA and max=500 mA when QDS was turned off.

Setting	Mean mAs	Max $CTDI_{vol}$ [mGy]	DLP [mGy*cm]	Dose reduction [%]
Off	100	14.6	720.4	-
SureExposure (z-mod.)	91	24.3	644.7	10.5
SureExposure 3D	101	29.0	685.0	4.9

4.4.2 Determination of dose reduction and dynamic of the AEC system for the head phantom

Figure 42 and figure 43 show how the mean mAs value per slice change along the length of the head phantom for a SD of 2 respective 2.5 and the tube current limits of 10 mA and 500 mA for Aquilion 16 and Aquilion 64. When SureExposure 3D was turned off, a fixed tube current of 300 mA was used.

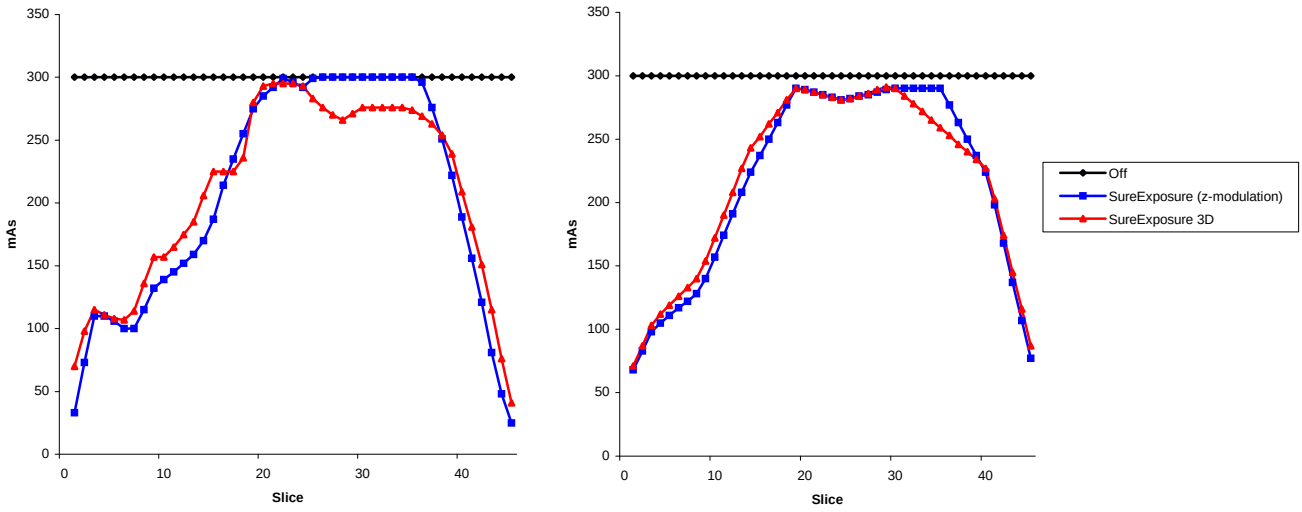

Figure 42. Mean mAs along the head phantom on Toshiba Aquilion 16 (left diagram) and on Toshiba Aquilion 64 (right diagram) for SD of 2 and minimum and maximum limits of 10 mA respective 500 mA.

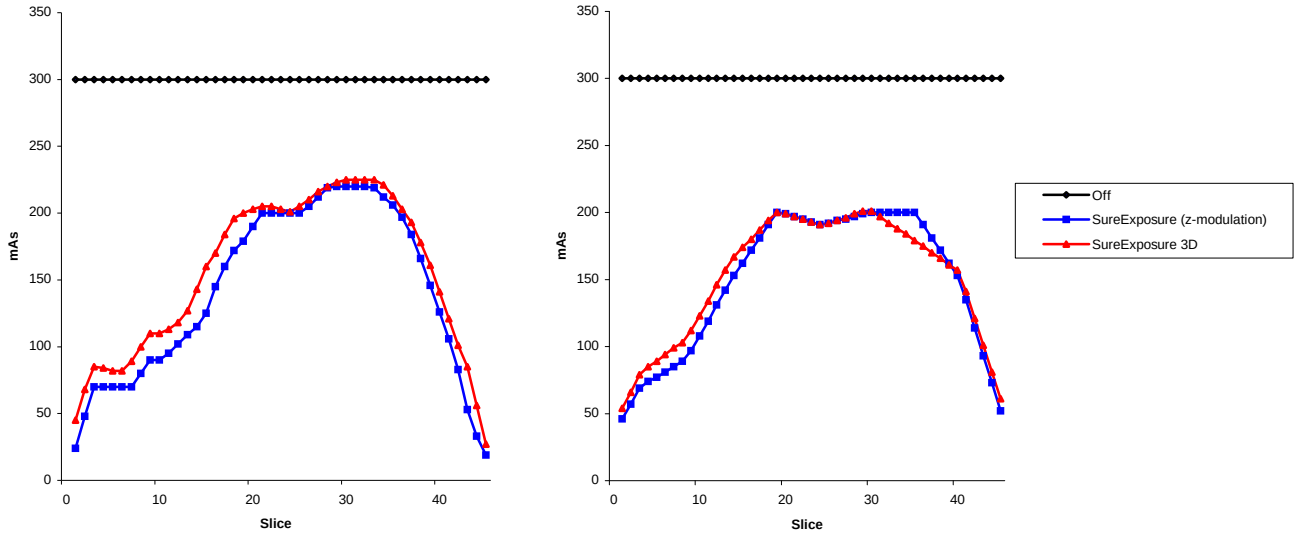

Figure 43. Mean mAs along the head phantom on Toshiba Aquilion 16 (left diagram) and on Toshiba Aquilion 64 (right diagram) for SD of 2.5 and minimum and maximum limits of 10 mA respective 500 mA.

Table 34 and table 35 show percentage dose reduction for different AEC settings in SureExposure 3D, achieved with Aquilion 16 and 64.

Table 34. Estimated dose reduction for head phantom on Toshiba Aquilion 16 and Toshiba Aquilion 64 for SD=2, min=10 mA and max=500 mA.

	Toshiba Aquilion 16				Toshiba Aquilion 64			
Setting	Mean mAs	Max $CTDI_{vol}$ [mGy]	DLP [mGy*cm]	DR [%]	Mean mAs	Max $CTDI_{vol}$ [mGy]	DLP [mGy*cm]	DR [%]
Off	300	89.8	2160	-	300	74.3	2060	-
SureExposure (z-mod.)	205	89.8	1390	35.6	217	71.8	1250	39.3
SureExposure 3D	209	88.5	1350	37.5	219	75.3	1160	43.7

Table 35. Estimated dose reduction for head phantom on Toshiba Aquilion 16 and Toshiba Aquilion 64 for SD=2.5, min=10 mA and max=500 mA.

	Toshiba Aquilion 16				Toshiba Aquilion 64			
Setting	Mean mAs	Max $CTDI_{vol}$ [mGy]	DLP [mGy*cm]	DR [%]	Mean mAs	Max $CTDI_{vol}$ [mGy]	DLP [mGy*cm]	DR [%]
Off	300	89.8	2160	-	300	74.3	2060	-
SureExposure (z-mod.)	141	65.9	953.5	55.9	149	49.5	855.5	58.5
SureExposure 3D	155	67.4	997.7	53.8	153	50.1	772.4	62.5

4.4.3 Evaluation of image quality for the thorax phantom

The evaluation of the image quality was performed on images acquired with a SD of 10 and minimum and maximum limits of 10 mA respective 500 mA for both Aquilion 16 and Aquilion 64.

Table 36 shows mean SD values from five ROIs placed at centre and peripheral positions in three slices represented shoulder-, thorax- and abdomen region on Aquilion 16 and 64. Relative SD shows the ratio of the image noise for different settings in SureExposure3D activated compared to non-activated. Table 37 shows the effect on image noise when QDS was non-activated.

Table 36. Measured mean SD for 5 ROIs in different slices off the thorax phantom on Toshiba Aquilion 16 and Toshiba Aquilion 64.

Toshiba Aquilion 16					Toshiba Aquilion 64				
Slice	**Setting**	**Mean mAs**	**Mean SD**	**Rel. SD**	**Slice**	**Setting**	**Mean mAs**	**Mean SD**	**Rel. SD**
27	Off	100	7.24	1.00	25	Off	100	7.69	1.00
	SureExposure (z-mod.)	60	8.44	1.17		SureExposure (z-mod.)	60	9.90	1.29
	SureExposure 3D	72	8.30	1.15		SureExposure 3D	68	8.49	1.10
55	Off	100	5.02	1.00	54	Off	100	4.07	1.00
	SureExposure (z-mod.)	21	8.16	1.62		SureExposure (z-mod.)	23	8.17	2.01
	SureExposure 3D	21	7.79	1.55		SureExposure 3D	25	7.15	1.76
70	Off	100	7.00	1.00	68	Off	100	6.84	1.00
	SureExposure (z-mod.)	55	10.08	1.44		SureExposure (z-mod.)	55	9.76	1.43
	SureExposure 3D	65	8.99	1.28		SureExposure 3D	63	8.79	1.29

Table 37. Measured mean SD for 5 ROIs in different slices of the thorax phantom on Toshiba Aquilion 64 when QDS was non-activated.

Slice	Setting	Mean mAs	Mean SD	Relative SD
25	Off	100	10.10	1.00
	SureExposure (z-mod.)	135	9.44	0.93
	SureExposure 3D	155	8.33	0.82
54	Off	100	6.26	1.00
	SureExposure (z-mod.)	55	7.80	1.25
	SureExposure 3D	55	7.90	1.26
68	Off	100	10.34	1.00
	SureExposure (z-mod.)	125	9.31	0.90
	SureExposure 3D	141	8.52	0.82

Figure 44 shows measured SD in the spine throughout the thorax phantom for Aquilion 16 and 64. The measurements were performed with 0.5 cm^2 large ROIs. Table 38 shows estimated mean SD and estimated coefficient of variations for respective CT scanner.

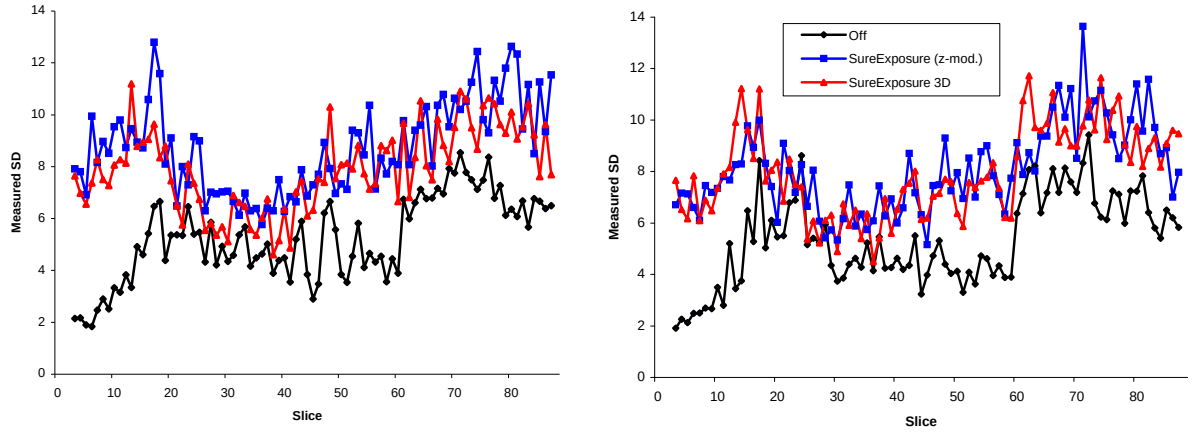

Figure 44. Measured SD in the spinal throughout the thorax phantom on Toshiba Aquilion 16 (left diagram) and Toshiba Aquilion 64 (right diagram).

Table 38. Estimated coefficient of variation for different modulation settings on Toshiba Aquilion 16 and Toshiba Aquilion 64.

	Toshiba Aquilion 16			Toshiba Aquilion 64		
Setting	**Mean SD**	**SD**	**Coefficient of variation [%]**	**Mean SD**	**SD**	**Coefficient of variation [%]**
Off	4.43	1.37	30.9	4.47	1.54	34.3
SureExposure (z-mod.)	8.74	1.76	20.2	8.08	1.68	20.8
SureExposure 3D	7.92	1.59	20.1	7.95	1.72	21.6

Table 39 is intending to show the effect of angular modulation in SureExposure 3D. Relative SD is estimated as SD in images with angular modulation on compared with off.

Table 39. Measured SD in ROIs in slice 82 on Toshiba Aquilion 16 (z-mod: 45 mAs, xyz-mod: 50.5 mAs) and Toshiba Aquilion 64 (z-mod: 46 mAs, xyz-mod: 53.5 mAs).

	Toshiba Aquilion 16			Toshiba Aquilion 64		
Position	**SD (z-mod.)**	**SD (xyz-mod.)**	**Relative SD**	**SD (z-mod.)**	**SD (xyz-mod.)**	**Relative SD**
Centre	11.06	9.68	0.88	10.62	9.97	0.94
North	8.21	7.76	0.95	7.85	7.94	1.01
East	9.86	10.15	1.03	10.15	8.61	0.85
South	9.4	8.88	0.94	8.75	8.16	0.93
West	8.55	8.26	0.97	8.91	8.18	0.92

4.5 Uncertainties in ROI position

One of the evaluations, where five ROIs were placed in different slices, has been reproduced. The result shows that the estimated relative SD deviates with less than 5%. To investigate the variation in SD, ROIs were also inserted in a small area around the primary ROI location. This was performed for one of the thorax examinations in slice 27. Table 40 shows the results where the maximum derivation has been estimated.

Table 40. Maximum deviation has been estimated by inserting ROIs in a small area around the primary ROI position.

ROI	SD	Min SD	Max SD	Max deviation [%]
1	7.2	7.0	7.5	4.2
2	14.7	13.7	15.1	6.8
3	8.0	7.8	8.3	3.8
4	5.8	5.7	6.4	10.3
5	7.9	7.8	8.4	6.3

A further evaluation, where ROIs were inserted in the spine throughout the thorax phantom, was also reproduced. The outcome shows that in 87% of the slices was the deviation between the results less than 5%. Could also add that the deviation was never bigger than 8%. To investigate how stable the SD is in the spine, measurements were performed in some slices by inserting 0.5 cm^2 large ROIs in an area of 1 cm^2. Table 41 shows the result where the maximum derivation has been estimated.

Table 41. Maximum deviation has been estimated by inserting ROIs in a 1 cm^2 large area.

Slice	SD	Min SD	Max SD	Max deviation [%]
15	8.6	7.8	9.0	9.3
30	7.8	7.3	8.0	6.4
45	5.3	4.8	5.6	9.4
60	4.7	4.5	5.3	12.8
75	7.8	7.3	8.0	6.4

One of the evaluations, where the effect of angular modulation was investigated, has also been reproduced. The result shows that the estimated relative SD deviates with up to 10%.

4.6 Summary of the results

To be able to summarize the AEC systems, the result for each manufacturer has been plotted together. It is however important to remember that the result for each AEC system depends on the selected image quality parameters, which determines the image quality and the radiation dose reduction. The AEC systems also have different implementations; consequently it is not possible

to make direct comparisons between the manufacturers. Since the thorax examinations for Philips was scanned with feet first, this values have been reversed to correspond to the other manufacturers results.

4.6.1 Thorax phantom

Figure 45 shows measured SD in the spine throughout the thorax phantom for respective manufacturer, when the AEC systems were not in use, i.e. for a constant tube current value. The results refer to measurements performed on each manufacturer's 16-slice CT scanner. For Siemens, GE and Toshiba a fix mAs value of 100 was used. For Philips the planned mAs/slice value was set to 200.

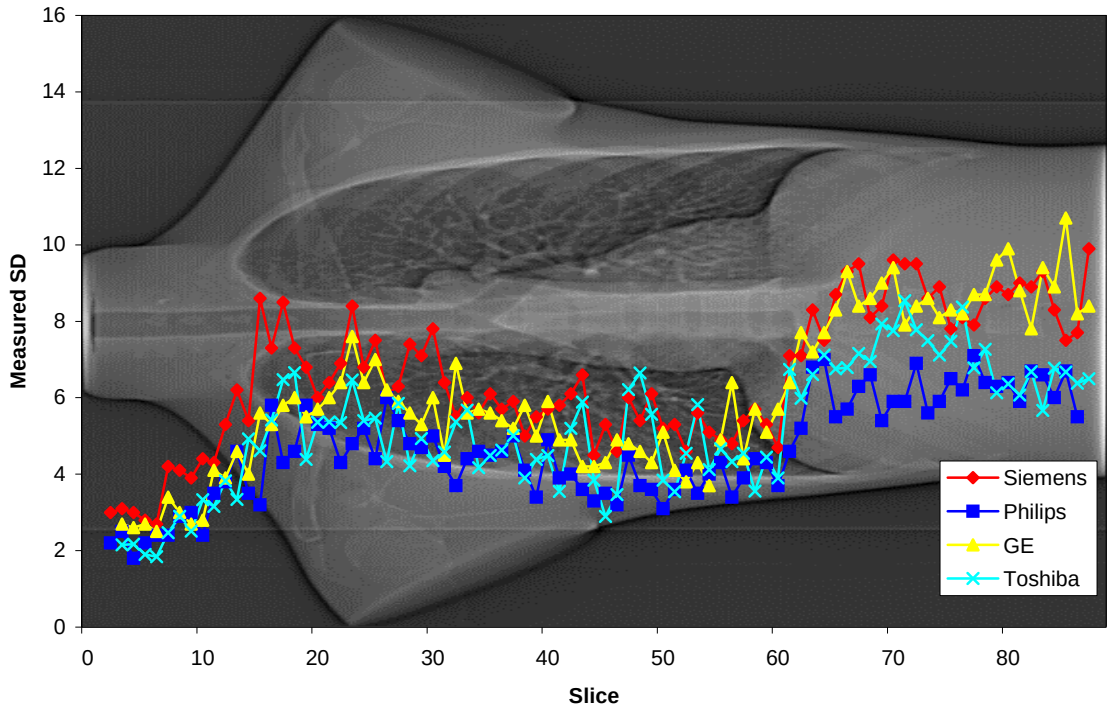

Figure 45. Measured SD in the thorax phantom for each manufacturer for a fix tube current on respective 16-slice CT scanner.

Figure 46 shows how the mean mAs value per slice change along the length of the thorax phantom for each manufacturers AEC system on respective 16-slice CT scanner. CARE Dose 4D with the modulation strength setting average/average was used for Siemens. The reference effective mAs value was set to 100. The result for Philips refers to measurements performed with DoseRight, ACS together with Z-DOM. As a starting point, 200 mAs/slice was selected. For GEs AEC system AutomA 3D, a noise index of 12 and minimum and maximum tube current limits of 10 mA respective 200 mA was used. For Toshibas AEC system SureExposure 3D, the SD was set to 10 and minimum and maximum tube current limits were set to 10 mA respective 500 mA. Figure 47 shows measured SD for each AEC system in the spine throughout the thorax phantom for mentioned settings above.

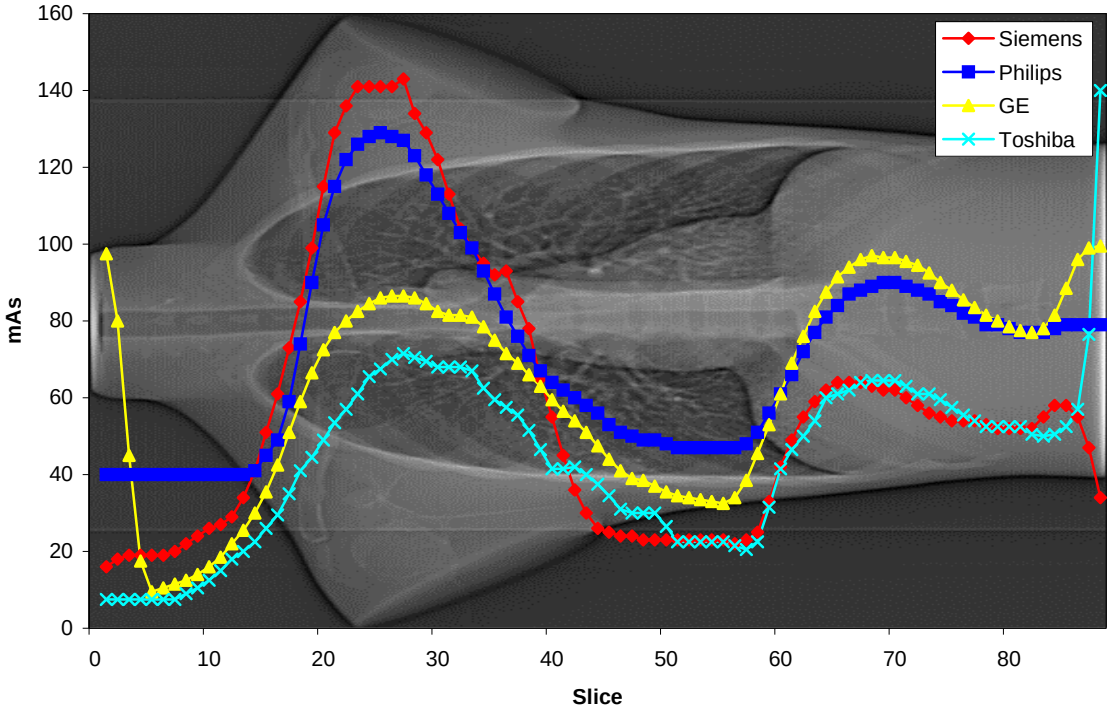

Figure 46. Mean mAs along the thorax phantom for each manufacturer on respective 16-slice CT scanner.

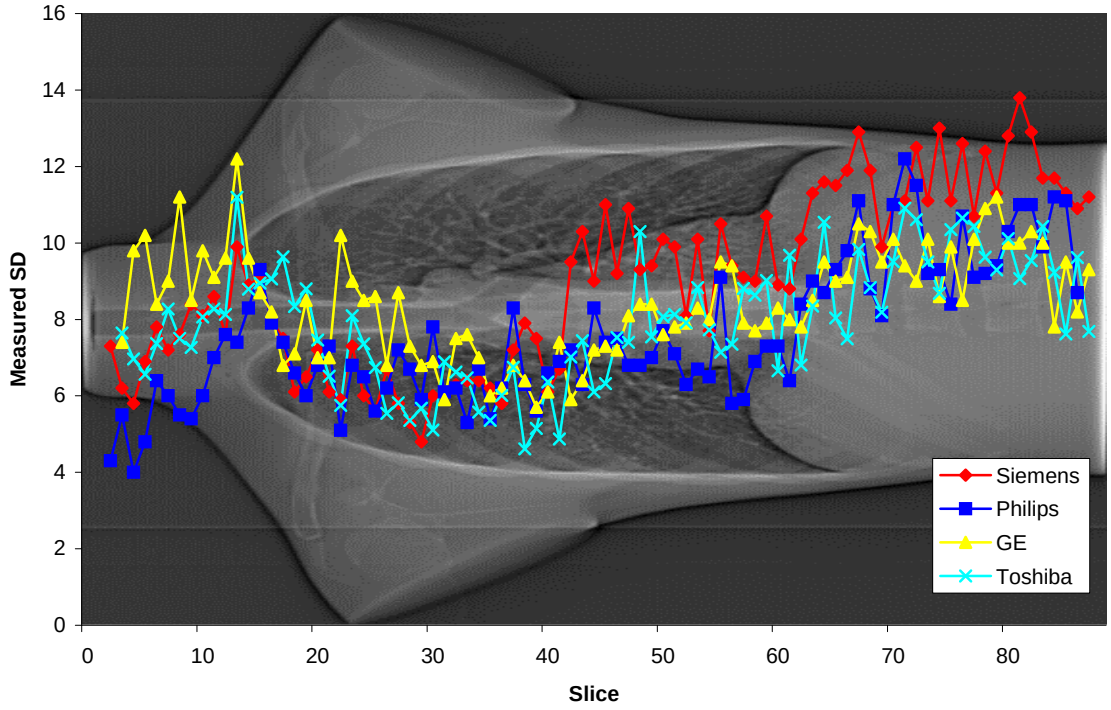

Figure 47. Measured SD in the thorax phantom for each manufacturers AEC system on respective 16-slice CT scanner.

Figure 48 shows measured SD in the spine throughout the thorax phantom for respective manufacturer, when the AEC systems were not in use, i.e. for a constant tube current value. The results refer to measurements performed on each manufacturers 64-slice CT scanner. For Siemens and Toshiba was a fix mAs value of 100 used. For Philips was instead the planned mAs/slice value set to 200. For GE was a fix mAs value of 53 used.

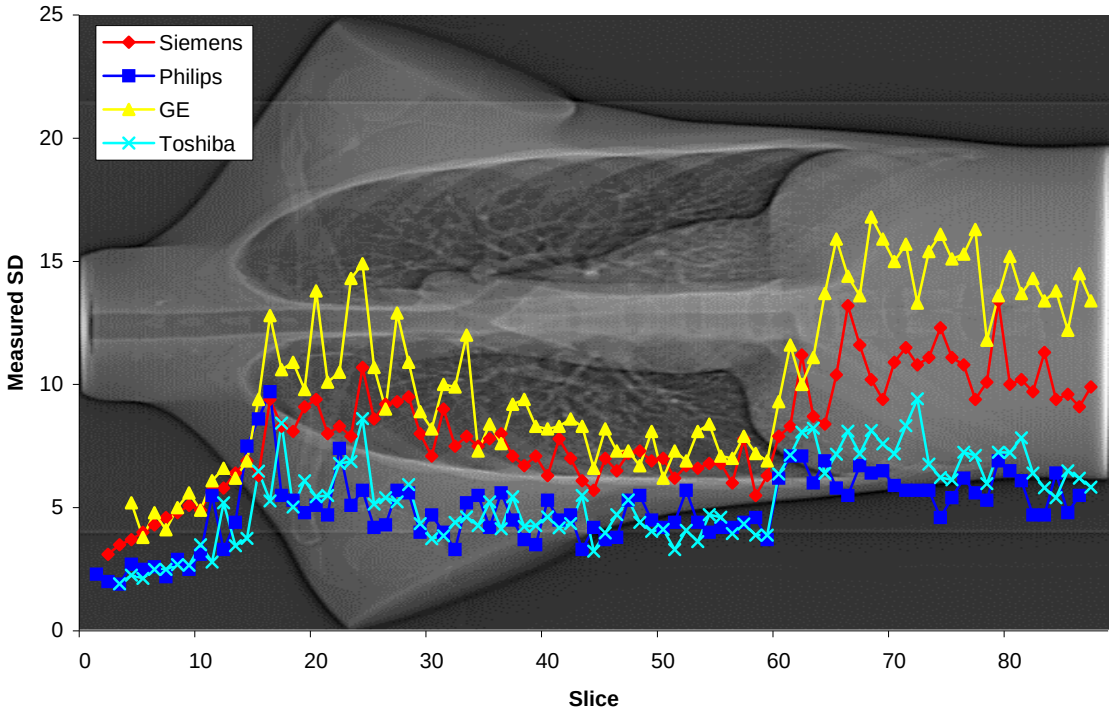

Figure 48. Measured SD in the thorax phantom for each manufacturer for a fix tube current on respective 64-slice CT scanner.

Figure 49 shows how the mean mAs value per slice change along the length of the thorax phantom for each manufacturers AEC system on respective 64-slice CT scanner. CARE Dose 4D with the modulation strength setting average/average was used for Siemens. The reference effective mAs value was set to 100. The result for Philips refers to measurements performed with DoseRight, ACS together with Z-DOM. As a starting point, 200 mAs/slice was selected. For GEs AEC system AutomA 3D, a noise index of 38 and minimum and maximum tube current limits of 10 mA respective 750 mA was used. For Toshibas AEC system SureExposure 3D, the SD was set to 10 and minimum and maximum tube current limits were set to 10 mA respective 500 mA. Figure 50 shows measured SD for each AEC system in the spine throughout the thorax phantom for mentioned settings above.

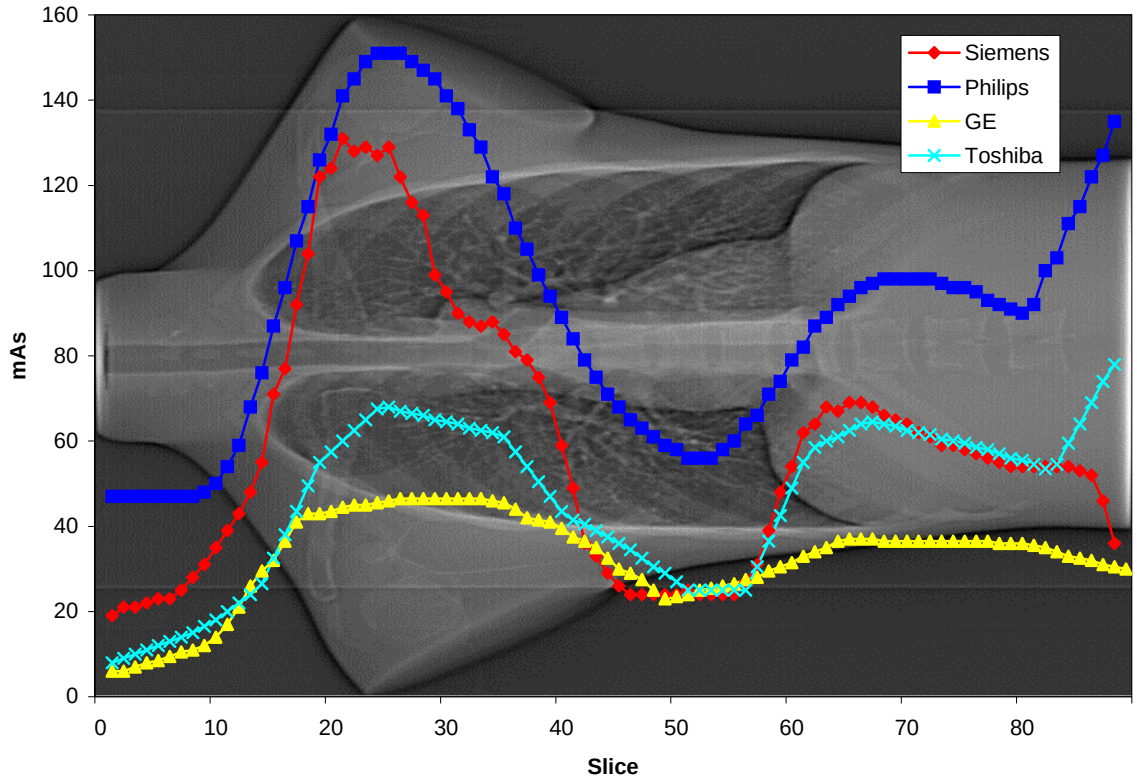

Figure 49. Mean mAs along the thorax phantom for each manufacturer on respective 64-slice CT scanner.

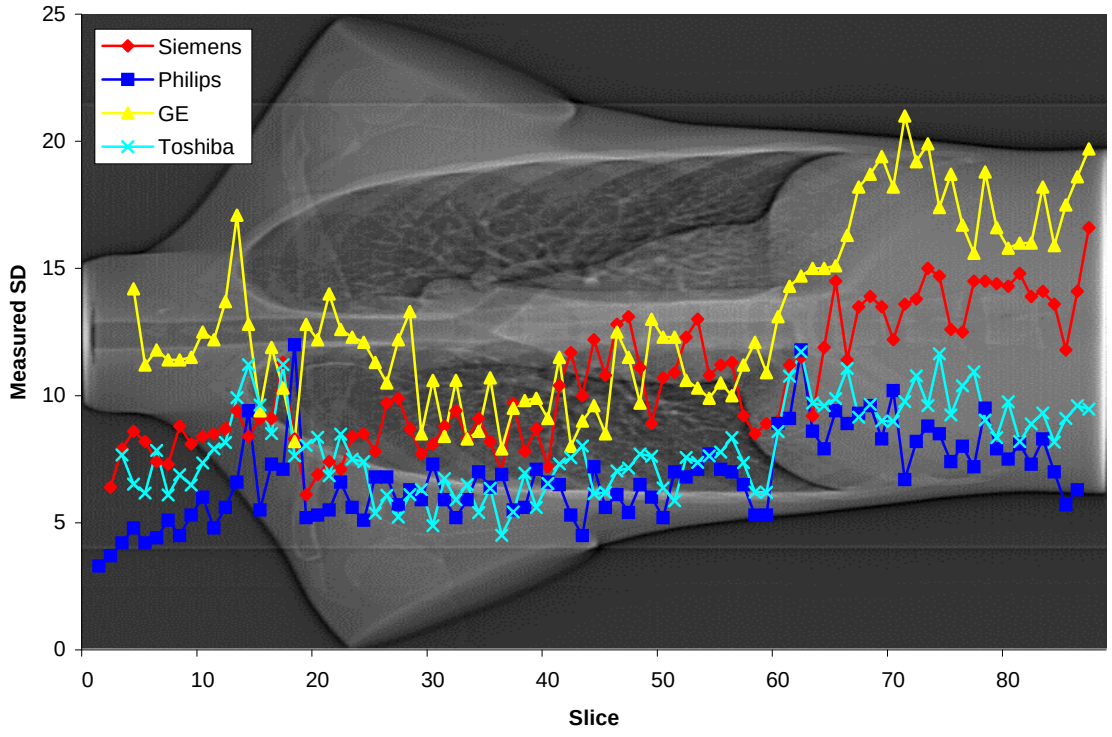

Figure 50. Measured SD in the thorax phantom for each manufacturers AEC system on respective 64-slice CT scanner.

4.6.2 Head phantom

Figure 51 shows how the mean mAs value per slice changes along the length of the head phantom for each manufacturers AEC system on respective 16-slice CT scanner. For Siemens, CARE Dose 4D with the modulation strength setting average/average was used. The reference effective mAs value was set to 320. The result for Philips refers to measurements performed with DoseRight, ACS together with Z-DOM. As a starting point 350 mAs/slice was selected. For GEs AEC system AutomA 3D, a noise index of 2.8 and minimum and maximum tube current limits of 10 mA respective 440 mA was used. For Toshibas AEC system SureExposure 3D, the SD was set to 2 and minimum and maximum tube current limits were set to 10 mA respective 500 mA.

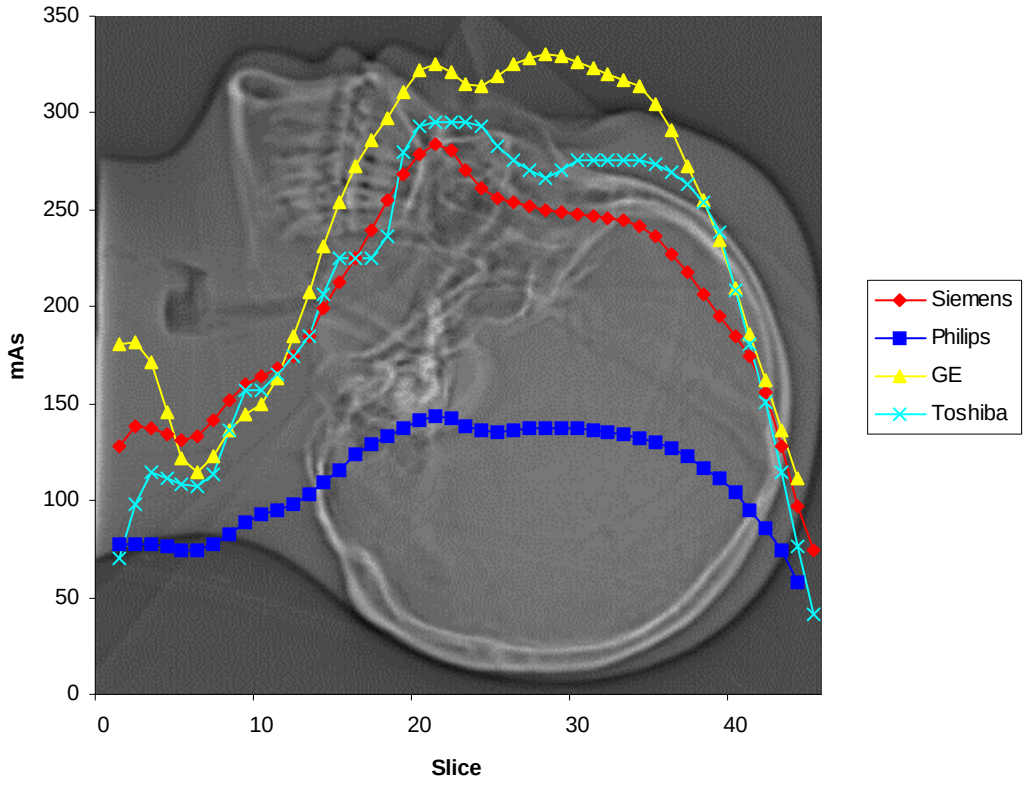

Figure 51. Mean mAs along the head phantom for each manufacturer on respective 16-slice CT scanner.

Figure 52 shows how the mean mAs value per slice changes along the length of the head phantom for each manufacturers AEC system on respective 64-slice CT scanner. For Siemens, CARE Dose 4D with the modulation strength setting average/average was used. The reference effective mAs value was set to 380. The result for Philips refers to measurements performed with DoseRight, ACS together with Z-DOM. As a starting point 350 mAs/slice was selected. For GEs AEC system AutomA 3D, a noise index of 6 and minimum and maximum tube current limits of 50 mA respective 335 mA was used. For Toshibas AEC system SureExposure 3D, the SD was set to 2 and minimum and maximum tube current limits were set to 10 mA respective 500 mA.

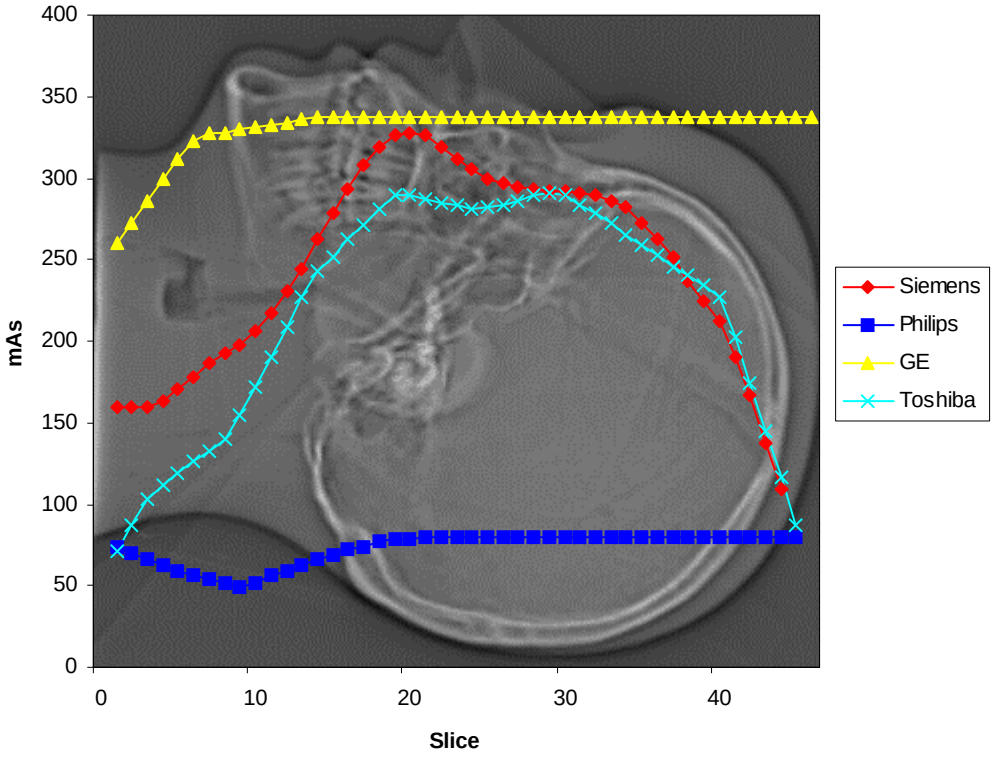

Figure 52. Mean mAs along the head phantom for each manufacturer on respective 64-slice CT scanner.

5. Discussion

5.1 Siemens

The dynamic of the tube current modulation for SOMATOM Sensation 16 and SOMATOM Sensation 64 in the thorax phantom was much of the same shape (Fig. 19 and Fig. 20). The diversity of X-ray tube and different detector configuration could explain parts of the difference in dynamic. The X-ray tube Akron (SOMATOM Sensation 16) is somewhat slower in the tube current modulation than the smaller and faster X-ray tube Straton (SOMATOM Sensation 64) that works a bit more efficient. The possibility of dose reduction was rather like for the two CT scanners (Tab. 9).

Figure 19 and figure 20 verify the different modulation strength settings; e.g. weak/strong, average/average and strong/weak. For the setting weak/strong we obtained a weak decrease in the tube current for the thorax region (slim region) and a strong increase in the tube current for the shoulder region (obese region). In the corresponding way for the setting strong/weak we obtained a strong decrease in the tube current for the thorax region (slim region) and a weak increase in the tube current for the shoulder region (obese region). For the setting average/average, the tube current is modulated in middle of the two extreme cases.

The degree of dose reduction achieved with CARE Dose 4D depends on which modulation strength setting is used. CARE Dose 4D could be a hazardous AEC system if the user not is conscious of the big difference between the modulation strength settings. Table 9 shows about 20% difference in dose reduction between strong/weak and weak/strong, which result in different image quality. Figure 23 shows that the image noise generally increases over the whole

thorax phantom, especially in the lung region. Table 13 shows that the image noise became more consistent when CARE Dose 4D was used. Which modulation strength setting that is preferable is up to the clinically requirements. A drawback with CARE Dose 4D is that it is not possible to set an upper limit of the tube output and in this way restricts excessive radiation doses.

Figure 21 and table 10 show that the tube current adjustment depends upon the tube voltage. The result is on the contrary to the result from ImPACT (4). This is explained by the version of CARE Dose 4D have been updated. When 80 kV was used instead of 120 kV, the image noise increases and consequently requires higher tube load to maintain the image quality. Therefore receives lower dose reduction for 80 kV.

Conclusion from figure 22 is that CARE Dose 4D makes no modulation for obese regions in the head phantom (the effective mAs value never adapts higher than the selected quality reference mAs value). The system always considers the head phantom smaller than the reference patient. The dynamic of the tube current modulation in the head phantom for SOMATOM Sensation 16 and SOMATOM Sensation 64 was principally equivalent. The possibility to receive a dose reduction was also the same for both CT scanners (Tab. 11). It should be noticed that the principally dose reduction were achieved in the neck region and in the top of the phantom. A clinically performed head examination will consequently not obtain such dose reduction.

A specific source of error for the Siemens examinations is that the different modulation strength settings were not based on same topogram. Because of the start and end point for each scan is manually set from the topogram, the image slices are not corresponding exactly.

5.2 Philips

Figure 24 and figure 25 show the dynamic of the tube current modulation for Brilliance 16 and Brilliance 64 in the thorax phantom. The dynamic for the three elements in DoseRight was quite similar between the two CT scanners. For Brilliance 16, the ACS proposed a lower tube load compared to the 64-slices scanner. ACS proposed a mAs value based upon a previously stored reference image and the users dose preferences. Consequently was this different for respective CT scanner. Philips claims that the suggested mAs values are in order to achieve a constant image noise level. Since the requirements for various body regions are different, each protocol has its own settings. In this study the scanning type was set to chest. Since the thorax phantom covers various regions we didn't obtained a constant noise level (Fig. 29). But table 20 shows that the image noise became more consistent when ACS+Z-DOM was used.

For D-DOM, which provides angular modulation, the mean mAs decreased in the shoulder region (Fig. 24 and Fig. 25). Since there are large variations in attenuation between anterior-posterior direction compared to lateral direction, the system could reduce the tube current in the anterior-posterior direction. Abdomen and thorax is more symmetric regions and consequently was the mean mAs more constant there. The dynamic for Z-DOM, which provides longitudinal modulation, resembles the dynamic for the other manufacturers combined AEC system. Z-DOM showed a much broader dynamic range in tube current modulation than D-DOM and is better adapted for a thorax examination. With ACS used together with Z-DOM obtains the largest dose reduction but also the largest increase in image noise (Fig. 29). The right diagram in figure 24 (Brilliance 64) shows that the ACS+Z-DOM starts with a high mAs value and then strongly decreases in the first 5 centimetres. This could be explained by the whole phantom length not was covered on the surview image and consequently the AEC system has no data to perform tube current modulation there.

Since the planned mAs/slice for a routine thorax examination is twice as high for Philips compared to the other manufacturers, also 100 mAs/slice was investigated. Figure 24 and figure 25 show that the dynamic of the tube current modulation did not changed; everything was roughly scaled down by a factor 2. Table 14 and table 15 show that the dose reduction was about the same independent of chosen planned mAs/slice of 200 or 100.

Figure 26 shows the effect of planning a scan by using an a.p. versus lateral surview. The result shows that the dynamic of tube current modulation was not considerable changed but generally a higher tube load was used throughout the phantom when the a.p. surview was used. This was not expected since the a.p. view goes through the thinnest cross section of the thorax phantom.

Figure 27 shows the effect of using 90 kV instead of 120 kV. The result shows that it was only the dynamic for the ACS+D-DOM that changed. In the shoulder region the tube load decreased further when 90 kV was used. This result was not expected; it should be on the contrary. A lower tube voltage causes increase in the image noise, consequently requires higher tube load to maintain the image quality.

The thorax phantom was scanned with the feet first. How this affects the dynamic of tube current modulation has not been investigated in this study.

Philips doesn't allow the user to use DoseRight for head examinations. To elude this, the scanning type was set to body mode. Figure 28 shows large dose reduction for the head phantom. This large dose reduction could be explained by the scanning type was set to body mode and not to head mode. Consequently the ACS suggests a mAs/slice based on a body examination, which is entirely to low for a head examination. The dynamic of the tube current modulation for ACS+Z-DOM (Brilliance 16) reminds the dynamic for the other manufacturers combined AEC system (Fig. 51). But the tube load is much lower then the other AEC systems due to that the ACS have reduced the tube load so greatly.

5.3 GE

Figures 30-32 show different possibilities to affect the dynamic of the tube current modulation by changing the range of where the modulation is desired, i.e. change maximum and minimum tube current boundaries. Largest dose reduction was received when maximum mA was set equal with the fix tube current and minimum mA was set as lowest possible. The dynamic of the tube current modulation for the thorax phantom for both LightSpeed[16] and LightSpeed VCT reminds the other manufacturers AEC system (Fig. 46 and Fig 49). However there are differences between the two scanners. The 64-slice scanner does not increase the tube load in the abdomen as much as the 16-slice, in comparison with the increase in the shoulder region (Fig. 32 and Fig 35). In the shoulder region we also found a larger difference between AutomA used individual and together with SmartmA for LightSpeed VCT.

For either the thorax phantom or the head phantom we found any larger differences when angular modulation was used together with longitudinal modulation compared to only longitudinal modulation. This result is remarkably when it should be a larger difference, especially in the shoulder region where it is large asymmetries. SmartmA works in a different way compared to Siemens, Philips and Toshibas angular modulation systems. GEs angular modulation system is based on the scout image unlike to use feedback from previous rotations.

In the beginning and end of each thorax scan, performed with LightSpeed[16], large mAs values can be seen. This could be explained by the whole phantom length not was covered on the scout

image and consequently the AEC system has no data to perform tube current modulation there. The extra radiation dose this brings could be avoided by set the maximum tube current lower, as in figure 32. This shows how important it is to use an optimum maximum tube current boundary.

The effect of using plus mode compared to full mode is presented in figure 33. The result shows that plus mode reduced the dose compared to full mode with about 10%. This result is confirmed by *Gutierrez et al.* (11), which found a difference of 6.6%. The reason for the additional dose reduction is that when plus mode is in use, the algorithm use the same amount of data as in full mode plus 45° additional rotational data for the image reconstructions. This has the effect that the image will be less noisy and thus allow the AEC system to reduce the dose further.

GE claim that's their AutomA 3D system aims to achieve the same level of noise in each image (Fig. 12). Table 29 shows that the image noise generally has increased, but the level of image noise has became more consistent when AutomA 3D was used. Figure 38 shows that the measured SD values were always lower than the selected noise indices. These differences are explained in section 2.6.3 General Electric - AutomA 3D.

The dynamic of the tube current modulation in the head phantom for LightSpeed[16] reminds the result for the other manufacturers (Fig. 51). LightSpeed VCT shows a strange dynamic, the tube load is almost constant (Fig. 52). Unexpectedly the result shows an increase in radiation dose to the head phantom compared to a fix tube current. Again this is an example of how important it is to set an optimum maximum tube current boundary. When the phantom was positioned like in a typical clinical situation, a totally other dynamic was obtained (Fig. 37). We have no explanation for these results.

5.4 Toshiba

Compared to the other manufacturers AEC system, the thorax examinations performed on Toshibas CT-scanners, show rather similar dynamic for the tube current modulation, especially AutomA 3D (Fig. 46 and Fig. 49). For both Aquilion 16 and Aquilion 64 two different SD values were investigated. The dynamic was similar independent of chosen SD value (Fig. 39 and Fig. 40). When a higher SD is used, i.e. one allows more noise in the images and consequently obtains more dose reduction. Table 38 verifies that the image noise became more consistent through the thorax phantom when the AEC system was activated. Figure 44 shows that the measured SD values generally were increased when SureExposure 3D was used, compared to a fix tube current. The measured SD values were slightly lower then the selected SD values. These differences reflect the differences between the anthropomorphic thorax phantom and the water phantom that SureExposure 3D is based on.

The measurements performed on the thorax phantom show divergent measures at the end of the scan (Fig. 39 and Fig. 40). This could be explained by the whole phantom length not was covered on the scanogram and consequently the AEC system has no data to perform tube current modulation there.

The comparison of the two AEC techniques shows that SureExposure 3D gives higher doses than only longitudinal modulation (Tab. 31 and Tab. 32). This result is on the contrary to the result from GEs AEC system. Toshiba claims that SureExposure 3D (angular modulation) compensates for beam hardening artefacts and consequently the tube current was increased in the lateral direction for regions with large asymmetries. The gist of this, a total increase in the tube load in mentioned image slices.

The effect of using QDS is presented in figure 41. The result shows that QDS reduces the radiation dose with about 50%, compared to non-active. The dynamic of the tube current modulation did not change when QDS was inactivated. SureExposure 3D calculates the tube load based on the expected noise reduction from QDS and consequently allows the AEC system to reduce the radiation dose. Table 36 compared to table 37 shows that the measured image noise is lower when QDS is activated despite of the greater tube load reduction.

Table 39 shows the effect of angular modulation; the noise became more uniform across the image. This result is very uncertain because there are large uncertainties in ROI position (10%).

The dynamic of the tube current modulation in the head phantom reminds the result for the other AEC systems (Fig. 51 and Fig 52). The principally dose reduction achieves in the neck region and in the top of the phantom.

Table 31 and table 32 show that Aquilion 16 resulted in higher DLP values compared to Aquilion 64 when the AEC system was turned off. This due to that the penumbra effect is higher for Aquilion 16 then for Aquilion 64. But in the other way the effect off overscan is higher for a 64-slice CT scanner, but this effect is not large since the scanning length is far. It can also be seen from the tables that the dose reduction is about the same for Aquilion 16 and Aquilion 64 for both the thorax and the head examination.

SureExposure 3D includes a very favourable tool that makes it possible for the user to see how the tube current is modulated for present scanning parameters before the CT scan is performed. This is a very pedagogic way for the operator to understand how different scanning parameters affect SureExposure 3D and it makes it easier to determine the optimal image quality for a specific diagnostic task.

5.5 General discussion

A clinically performed CT examination often covers different anatomic regions that have variable attenuation values. When an AEC system is not in use, the tube current is regularly set to high since the tube current is based on regions with high attenuation (e.g. shoulder and pelvis) or on the region that require highest image quality. Another reason is that standard protocols is usually planned to generate images of good quality for all patient sizes. Without an AEC system, smaller patients will be exposed for unnecessary high patient radiation dose.

AEC systems are intended to modulate the tube current to the patient's size, shape and attenuation. There are a number of benefits with AEC system, first of all the potential for dose reduction, which have been verified in this study. The manufacturers AEC system has different purposes; some are expected to increase the consistency of image quality between different anatomic regions in the same patient. Philips, GE and Toshiba claim this and it has also been verified by estimating the coefficient of variation. The estimation assumes that the measured SD values are normally distributed through the thorax phantom. We are conscious of that it is not completely fulfilled. For instance, table 29 shows that the estimated SD of the measured SD values is bigger when SureExposure 3D is activated but the coefficient of variation is smaller. This means that there are larger differences in the image noise, but relative to the mean value the image noise is more steady when SureExposure 3D is activated.

It is very complex to make a direct comparison between the manufactures since their AEC system have differences in the implementation. All systems have different solutions of defining the image quality level. Siemens uses a reference mAs value and Philips uses a reference image

concept. GEs and Toshibas AEC system are more similar. Both systems are based on the user selected SD on an image-by-image basis and minimum and maximum mA limits. There could also be differences between each scanner model since they may be equipped with different X-ray tube, software and detector configuration. Likewise scanning geometry and beam filtration will affect the AEC efficacy.

The dynamic of the tube current modulation for the thorax phantom is quite similar between the manufactures for both 16- and 64-slice CT scanners (Fig. 46 and Fig. 49). Common for the AEC systems is that the tube load increases for the shoulder region and then be lower through the thorax region that is less attenuating due to the presence of the air filled lungs. Through abdomen that is denser, the mean tube load increases again. How broad dynamic range the modulation cover is dependent on the image quality settings. It is essential to remember that the image quality parameters affect the dynamic of tube current modulation and consequently the image quality. In this study, the focus was not to study the variation in radiation dose and image quality for different circumstances.

The dynamic of the tube current modulation for the head phantom is rather similar between the manufacturers for both 16- and 64-slice CT scanners (Fig. 51 and Fig. 52). The dynamic is strongly dependent on selected image quality parameters, but common for the AEC systems are that the tube load is low in the neck region and higher and more constant through the cranium, which is more attenuating. This is because of the head is more or less circular and homogenous in the cranium, consequently it is not much potential to obtain dose reduction for a clinical routine head examination.

In this study, the potential for dose reduction when an AEC system is in use has been compared with a fixed tube current value. The manually tube current values were always set so it could be clinically representative. Due to manufacturer and AEC setting, as big as 80% dose reduction have been determined for the thorax phantom. For the head phantom, up to 60% dose reduction have been determined, dependent on manufacturer and AEC setting. The percentage dose reduction values were estimated based on the DLP values and accordingly was no account of the radiosensitivity of the irradiated tissues taken. Effective dose is a good risk indicator that can be used to estimate radiation risk. This was out of the scope for this study.

It is complex to compare the estimated dose reduction values with values presented in the literature. The results are strongly dependent on the selected scanning parameters, CT scanner/model and specified image quality for the AEC system. Result from a study performed by *Papadakis et al.* (44) shows a percent dose reduction of 13.9% (only angular modulation) for thorax and abdomen region, achieved with an adult anthropomorphic phantom. Our study and results by *Mulkens et al.* (10) and *Rizzo et al.* (9) verify that the combination of angular with longitudinal AEC makes it possible to obtain much higher dose reductions.

The received DLP values from the DICOM information were compared with national diagnostic reference levels (Tab. 8). For all manufacturers, when scanning with a fix tube current value, the DRL was exceeded for the head examinations. This due to the whole head phantom was scanned (including the neck region) and DRL only includes scanning the brain. Also for some of the thorax examinations the DRL was exceeded. This due to that the used scanning lengths were longer then clinically used for a routine thorax examination. The reason for this is that the purpose was to study the dynamic of the tube current modulation for all regions in the two anthropomorphic phantoms. The reader must have this in mind when considering the estimated percentage dose reduction values. The values are not valid for a clinical thorax respective head examination. For example, figure 36 that shows how the mean mAs value per slice change along

the length of the head phantom, the great dose reduction is in the neck region and not in the cranium where the head is more symmetric and homogenous.

There are a lot of performed studies on AEC system where the AEC performance and image quality is evaluated by use of uniform phantoms (4, 12, 45). Some studies have also performed clinical evaluations where radiologists assess the image quality (9, 10, 25, 46). In this study anthropomorphic phantoms was used instead, which is more appropriate to assess the capabilities and limitations of an AEC system in a rather like clinical situation. It was accordingly possible to investigate the response for each AEC technique: angular-, longitudinal- and combined tube current modulation. With use of a uniform phantom the performance of the AEC systems may have been different. Likewise to do noise measurements in a homogeneous phantom are not analogous to noise in a human body. The drawback with the anthropomorphic phantoms is the restricted possibilities to quantitative evaluate the image quality. The phantoms contain air, bones and other structures that resemble the human body. This makes it difficult to insert ROIs in a uniform area. Consideration to starvation artefacts in the shoulder region must also been taken. The lack of heterogeneous areas in the head phantom made it impossible to evaluate the image quality.

It is very complex to determine optimal image quality for a clinical diagnose, since both quantitative measurements and the observer's perception are involved. In this study the quantum noise has been used to assess the image quality. Image noise is the parameter that is direct influenced by a tube current modulation. An increase in the image noise may have potential to impair the low contrast resolution and affect the diagnostic information. Image noise is affected by differences in phantom position and a lot of scanning parameters (Tab. 1). Therefore were the phantoms positioned in same position and as many as possible of the scanning parameters were set equal for the manufacturers. Furthermore, the image noise depends also on the reconstruction process, e.g. reconstruction filter. These parameters differ between the manufacturers but they were set as standardize as possible for a routine thorax respective head examination.

A common result for all manufacturers is that the image noise increases when the AEC system was in use, compared to the scan with a fix tube current. This could especially been seen in regions where the tube current was greatly decreased e.g. in lung region (Siemens Fig. 23, Philips Fig. 29, GEs Fig. 38, Toshiba Fig. 44). Figure 45 and figure 48 show that different regions in the thorax phantom obtain large variations of image quality when a fix tube current is used. Despite use of tube current modulation, different anatomical regions obtained different levels of image noise (Fig. 47 and Fig. 50). But the figures also show that the image quality was more consistent throughout the thorax phantom, compared to a fix tube current. This might be acceptable since the image requirements differ from organ to organ. The national diagnostic reference levels (Tab. 8) also show a lower $CTDI_{vol}$ for thorax compared to abdomen. In the abdominal region it is very important to detect low contrast lesions and therefore is lower noise desirable. It is essential that radiologists and physicist be aware of how the dynamic changes in tube current affect the image quality so that the acceptable threshold of image quality with the minimum possible radiation exposure to the patient, in agreement with the ALARA principle, could be established.

An assessment between the manufactures (Fig. 46 respective Fig. 49) shows that generally lowest mAs is used for Toshiba, even though (Fig. 47 respective Fig. 50) the measured image noise is almost lowest for Toshiba. But, when one looks at the DLP values, Toshiba was responsible for highest values. A possible explanation is the differences in beam filtration between the manufacturers.

The final question is, if the diagnostic information were affected of the increase in image noise. A limitation of the study is that image noise was the only parameter used for the image quality evaluation. E.g. contrast-to-noise ratio could have been a good complement as a measure of the image quality. It was not clinically relevant to do this, as the phantoms contain no pathology. But a future good complement to the quantitative image quality study would be a subjective image quality analysis by using the software tool ViewDEX (47). Radiologists could in a blinded fashion assess the image noise, diagnostic acceptability, presence of streak artefacts and visibility of small structures. A clinical evaluation performed by *Rizzo et al.* (9) shows that the image noise was significantly higher in examinations performed with combined modulation (CARE Dose 4D) compared to a fix tube current. But the study also concludes that the diagnostic acceptability was acceptable.

There are some sources of errors that could explain differences in the results. First of all is the anthropomorphic thorax phantom not completely homogenous where the ROIs were inserted. The ROIs were also inserted manually and this affects the accuracy of the measurements. Results show that the SD deviates with about 5-10% due to region in the phantom. Due to the inherent nature of quantum statistics, SD measurements in a uniform phantom would also have resulted in variability of the measured results (22).

The investigation where the intention was to individually study the effect of rotational AEC techniques is not applicable (Tab. 21, 30 and 39). The difference between the estimated relative SD for respective ROI position is about 10%. One of the tests was reproduced and shows a deviation with up to 10%, consequently it is not possible to establish if the noise becomes more uniform across the image. This high deviation due to that only a small variation in SD considerable affects the result, since it is only a small difference between the SD when the angular modulation is on compared to non-activated. The investigated slices were in abdomen and consequently have good symmetry. It would have been better to do the measurements in a more asymmetric region, e.g. in the shoulder region. But the anthropomorphic thorax phantom is not homogenous in the shoulder region and consequently not suitable to do measurements there.

In this study we have assumed that used CT scanners were correct calibrated, e.g. the laser system used for positioned the phantoms was correct aligned. We ourselves have not measured the radiation dose, but assumed that the received $CTDI_{vol}$ and DLP values from the CT console were correct.

6. Conclusions

This study has established that there are large potential to attain large dose reductions by using AEC systems. For the anthropomorphic thorax phantom it was possible to reduce the radiation dose by about 50%. The principal dose reduction for the head phantom was in the neck region and not in the investigated area for a clinically routine head examination.

The dynamic off the AEC systems were rather similar. A common result was that the image noise generally increased when the AEC systems were activated. The result for all manufacturers also showed that the image noise became more consistent throughout the thorax phantom by adapting the tube current to the anatomy.

It is essential that radiologists and physicist are aware of the performance of their AEC system and how the image quality is affected. This study have not evaluated whether the diagnostic accuracy is influenced and further studies are required to evaluate this subject.

It is fascinating to imagine about what an ideal AEC system should be able to perform in the future. Today, the AEC systems control the tube current, future development should be modulation of tube voltage and rotation time. The adjustment should be according to each anatomic region since the diagnostic image quality requirements differ from organ to organ.

7. Acknowledgements

First of all I would like to thank my supervisor Mikael Gunnarsson for given me the great opportunity to study this interesting subject and for your excellent support, help and knowledge during the project. I would also like to thank Mats Nilsson for helpful discussions and Sigrid Leide Svegborn for comments of my report.

Furthermore I would like to thank the manufacturers for providing me information; in particular:

- Lars Karlsson (Siemens), for providing information and answering questions,
- Kristina Norrgren (Philips), for help with doing the measurements and answering questions,
- Magdalena Bäckström (GE), for providing information and answering questions,
- Mårten Svensson (Mediel), for the connection with Toshiba,
- Steen Olesen (Mediel), for a pleasant travel to Zoetermeer, Netherlands,
- Kor Valkenier (Toshiba), for the possibility to do measurements in Zoetermeer, Netherlands,
- Roy Irwan (Toshiba), for answering questions and comments of my work.

In addition I would like to acknowledge physicists and radiographers that have helped me doing the measurements; in particular:

- Jimmy Börjesson, for the possibility to do measurements at Halmstad county hospital,
- Willy Van Pinxteren (GE), for valuable discussions and help with doing the measurements,
- Bo Olsson, for a kindly visit at Simrishamn hospital and help with doing the measurements,
- Arie Munne (Toshiba), for useful discussions and help with doing the measurements.

Finally I would like to forward a special thank to my girlfriend, Sofie Alriksson, she has been a tremendous support during these months.

8. References

1. United Nations Scientific Committee on the Effects of Atomic Radiation. 2000 report to the General Assembly, Annex D: Medical radiation exposure. New York, NY: United Nations; 2000.
2. Leitz W, Jönsson H. Statens strålskyddsinstitut (Swedish Radiation Protection Authority), 2001:01 Patientdoser från röntgenundersökningar i Sverige - sammanställning av resultaten från sjukvårdens rapportering 1999.
3. Kalra MK, Maher MM, Rizzo S, Saini S. Radiation exposure and projected risks with multidetector-row computed tomography scanning: clinical strategies and technologic developments for dose reduction. J Comput Assist Tomogr 2004; 28 Suppl 1:S46-49.
4. Nicholas K. MHRA Report 05016 CT scanner automatic exposure control systems. 2005.

5. McCollough CH, Bruesewitz MR, Kofler JM, Jr. CT dose reduction and dose management tools: overview of available options. Radiographics 2006; 26:503-512.

6. Kalra MK, Naz N, Rizzo SM, Blake MA. Computed tomography radiation dose optimization: scanning protocols and clinical applications of automatic exposure control. Curr Probl Diagn Radiol 2005; 34:171-181.

7. 87 IP. Managing Patient Dose in Multi-Detector Computed Tomography (MDCT). 32/219/06 Dec vers.

8. McCollough CH. Automatic exposure control in CT: are we done yet? Radiology 2005; 237:755-756.

9. Rizzo S, Kalra M, Schmidt B, et al. Comparison of angular and combined automatic tube current modulation techniques with constant tube current CT of the abdomen and pelvis. AJR Am J Roentgenol 2006; 186:673-679.

10. Mulkens TH, Bellinck P, Baeyaert M, et al. Use of an automatic exposure control mechanism for dose optimization in multi-detector row CT examinations: clinical evaluation. Radiology 2005; 237:213-223.

11. Gutierrez D, Schmidt S, Denys A, Schnyder P, Bochud FO, Verdun FR. CT-automatic exposure control devices: What are their performances? Nuclear Instruments and Methods in Physics Research Section A: Accelerators, Spectrometers, Detectors and Associated Equipment 2007; 580:990-995.

12. Goo HW, Suh DS. The influences of tube voltage and scan direction on combined tube current modulation: a phantom study. Pediatr Radiol 2006; 36:833-840.

13. Kalender WA. Computed Tomography: Fundamentals, System Technology, Image Quality, Applications, 2005 by Publics Corporate Publishing, Erlangen.

14. Hägglund P, Johansson R, Wickman G. Utvärdering av datortomografers doseffektivitet Slutrapport. Statens strålskyddsinstitut Projekt P1069.98 Umeå 2004.

15. McNitt-Gray MF. AAPM/RSNA Physics Tutorial for Residents: Topics in CT. Radiation dose in CT. Radiographics 2002; 22:1541-1553.

16. Brochure: LightSpeed 7.X. General Electric Company, 2006.

17. Aweda MA, Arogundade RA. Patient dose reduction methods in computerized tomography procedures: A review. International Journal of Physical Sciences 2007; 2 (1):001-009.

18. Brochure: Dose in Computed Tomography: Basics, Challenges and Solutions. GE Medical Systems 1098-BE, France 2001.

19. Leitz W, Axelsson B, Szendrö G. Computed Tomography Dose Assessment - A Practical Approach. Radiation ProtectionDosimetry 1995; 57:377-380.

20. Verdun FR, Gutierrez D, Schnyder P, Aroua A, Bochud F, Gudinchet F. CT dose optimization when changing to CT multi-detector row technology. Curr Probl Diagn Radiol 2007; 36:176-184.

21. American Association of Physicists in Medicine (AAPM) Report 96. The Measurement, Reporting, and Management of Radiation Dose in CT. New York: AAPM, 2008.

22. Goldman LW. Principles of CT: Radiation Dose and Image Quality. J Nucl Med Technol 2007; 35:213-225.

23. Kalra MK, Maher MM, Toth TL, et al. Strategies for CT radiation dose optimization. Radiology 2004; 230:619-628.

24. Brenner D, Elliston C, Hall E, Berdon W. Estimated risks of radiation-induced fatal cancer from pediatric CT. AJR Am J Roentgenol 2001; 176:289-296.

25. Namasivayam S, Kalra MK, Pottala KM, Waldrop SM, Hudgins PA. Optimization of Z-axis automatic exposure control for multidetector row CT evaluation of neck and comparison with fixed tube current technique for image quality and radiation dose. AJNR Am J Neuroradiol 2006; 27:2221-2225.

26. Nyman U, Leitz W, Kristiansson M, Påhlstorp P-Å. Stråldosreglering vid kroppsdatortomografi - bakgrund till dosregleringsprogrammet OmnimAs. SSI Rapport 2004:12.

27. Brochure: More precision Better confidence GE Healthcare Solutions for Dose Reduction. GE Healthcare 7222-BE, 2007.

28. Kalra MK, Rizzo SM, Novelline RA. Reducing radiation dose in emergency computed tomography with automatic exposure control techniques. Emerg Radiol 2005; 11:267-274.

29. Kalra MK, Maher MM, Toth TL, et al. Techniques and applications of automatic tube current modulation for CT. Radiology 2004; 233:649-657.

30. Kalender W. Dose management in multi--slice spiral computed tomography. European Radiology Supplements 2004; 14:40-49.

31. Wilting JE, Zwartkruis A, van Leeuwen MS, Timmer J, Kamphuis AG, Feldberg M. A rational approach to dose reduction in CT: individualized scan protocols. Eur Radiol 2001; 11:2627-2632.

32. SIEMENS. SOMATOM Sensation 64 Application Guide. Siemens AG Medical Solutions, 2004.

33. Philips. Brilliance Workspace 2.0 Scanner Upgrade.

34. Brochure: Brillance CT - Volume 1. Philips Medical Systems 4535 673 86351.

35. Brochure: LightSpeed Serien 2369740-142. General Electric Company, 2004.

36. Blobel J, Mews J, de Vries H, Juran R, Rogalla P. Optimization and Reduction of CT Radiation Exposure using SureExposure control, illustrated by a thorax protocol. Toshiba Medical Systems, Charité Berlin, Campus Mitte, Germany.

37. Blobel J, Okumura M, Kazama M, Tsukagoshi T. SureExposure 3D Image Quality Optimization by Three-Demensional Tube Current Control TOSHIBA Medical Systems Corporation. Computed Tomography Visions:1-4.

38. Powerpoint presentation: Aquilion SUREExposure V.2.0. Toshiba Medical Systems Europe

39. Brochure: Volume CT a GE Healthcare publication. General Electric Company, July 2004.

40. Blobel J, Okumura M, Ota T, Tsukagoshi S. Advanced Quantum Denoising System - QDS. TOSHIBA Medical Systems Corporation. Visions Computed Tomography:2-3.

41. Brochure: Chest phantom PBU-X-21. Kyoto Kagaku CO., LTD.

42. Brochure: Sectional Brochure. The Phantom Laboratory.

43. Statens strålskyddsinstitut (Swedish Radiation Protection Authority). Föreskrifter och allmänna råd om diagnostiska standarddoser och referensnivåer inom medicinsk röntgendiagnostik. 2002:2.

44. Papadakis AE, Perisinakis K, Damilakis J. Angular on-line tube current modulation in multidetector CT examinations of children and adults: the influence of different scanning parameters on dose reduction. Med Phys 2007; 34:2864-2874.

45. Brisse HJ, Madec L, Gaboriaud G, et al. Automatic exposure control in multichannel CT with tube current modulation to achieve a constant level of image noise: experimental assessment on pediatric phantoms. Med Phys 2007; 34:3018-3033.

46. Kalra MK, Maher MM, Toth TL, Kamath RS, Halpern EF, Saini S. Comparison of Z-axis automatic tube current modulation technique with fixed tube current CT scanning of abdomen and pelvis. Radiology 2004; 232:347-353.

47. Borjesson S, Hakansson M, Bath M, et al. A software tool for increased efficiency in observer performance studies in radiology. Radiat Prot Dosimetry 2005; 114:45-52.